

Investigating the Secretion of HtpB, the Multifunctional Chaperonin of *Legionella pneumophila*

by

Peter Robertson

Submitted in partial fulfilment of the requirements
for the degree of Master of Science

at

Dalhousie University
Halifax, Nova Scotia
August 2016

© Copyright by Peter Robertson, 2016

Table of Contents

List of Tables	v
List of Figures	vi
Abstract	ix
List of Abbreviations and Symbols Used	x
Acknowledgements	xii
1. Introduction	1
1.1 <i>Legionella pneumophila</i> : An Overview	1
1.1.1 <i>Legionella pneumophila</i> : History and Pathogenesis	1
1.1.2 A Brief Account of the Known Virulence Factors of <i>L. pneumophila</i>	8
1.2 Chaperonins.....	12
1.2.1 The GroEL model of chaperonin function	12
1.2.2 <i>L. pneumophila</i> HtpB is a Multifunctional Protein	18
1.3 Translocation and Secretion	26
1.3.1 Secretion is a Key Aspect of Pathogenesis in <i>L. pneumophila</i>	26
1.3.2 Outline of Known Secretion Mechanisms in <i>L. pneumophila</i>	28
1.4 Hypotheses and Intent	38
2. Materials and Methods	39
2.1 General Techniques.....	39
2.1.1 Growth of Bacterial Strains	39
2.1.2 Growth of Eukaryotic Cell Lines.....	39
2.1.3 PCR with <i>Taq</i>	41
2.1.4 PCR with <i>Pfx</i>	43
2.1.5 Restriction Digestion	43
2.1.6 Ligation.....	44

2.1.7	Generating Electrocompetent Cells	44
2.1.8	Plasmid Extraction, Purification and Transformation	44
2.1.9	SDS-PAGE	45
2.1.10	Total Protein Quantification	48
2.2	Generation of Bacterial Strains	50
2.2.1	Generation of a <i>dotA</i> deletion mutant in <i>L. pneumophila</i> strain JR32	50
2.2.2	Genetic Complementation of the <i>dotA</i> Deletion Mutant.....	51
2.2.3	Generation of JR32 Strains Carrying the GSK Reporter Construct	51
2.2.4	Generation of JR32 Strains Carrying the IcdH-HtpB C-terminal Fusion	52
2.2.5	Generation of a JR32 Strain Carrying a 6 x His-Tailed <i>htpB</i> Gene Construct.	52
2.3	Other Techniques Used in This Study.....	52
2.3.1	Infection of Mammalian Cells.....	53
2.3.2	Osmotic Shock of <i>L. pneumophila</i> and Fractionation of Soluble and Membrane-associated Proteins	53
2.3.3	Densitometry and Statistical Analysis	55
2.3.4	Immunogold Electron-Microscopy.....	55
2.3.5	Resistance-to-salt Testing.....	60
2.3.6	Testing for AP Activity	61
3.	Results.....	62
	Part I: Translocation of HtpB to the cytoplasm of <i>L. pneumophila</i> -infected cells relies on a functional Dot/Icm system	62
3.1	HtpB has some, but not all, markers of a Dot/Icm effector	62
3.1.1	HtpB does not have the hydrophobicity index of a Dot/Icm effector	62
3.1.2	HtpB does not possess amino acid enrichments characteristic of a Dot/Icm effector.....	62
3.1.3	HtpB has a degenerate E-block motif.....	62

.....	65
3.2 HtpB has sequence similarity to several known Cell Penetrating Peptides (CPPs)	63
3.3 Translocation of a GSK tagged HtpB	63
3.3.1 A <i>dotA</i> deletion mutant was created and complemented <i>in-trans</i>	63
3.3.2 HtpB and appropriate controls were tagged with GSK	81
3.3.3 GSK tagged HtpB is not phosphorylated in a Dot/Icm mutant	81
Part II: The C-terminus of HtpB is involved in its translocation across the inner membrane of <i>L. pneumophila</i>	88
3.4 Adding the C-terminus of HtpB to a non-secreted form of PhoA does not restore its translocation to the periplasm	88
3.5 Post-osmotic shock fractionation of soluble and insoluble proteins indicates that the HtpB C-terminus associates with the <i>L. pneumophila</i> envelope.....	95
3.6 Immunogold microscopy indicates that the C-terminus of HtpB is involved in determining the sub-cellular localization of HtpB	95
3.6.1 Blocking the C-terminus results in a Cytoplasmic build-up of HtpB.....	95
3.6.2 Adding the C-terminus of HtpB to Icd causes an increase in translocation ...	102
4. Discussion	113
4.1 A new Method for Assessing Chaperonin Secretion in <i>L. pneumophila</i> was Validated	113
4.2 The C-terminus of HtpB is essential but not sufficient for translocation.....	118
4.3 The translocation of HtpB is explained by non-canonical, Dot/Icm dependent secretion	126
4.4 Final Thoughts.....	134
References	136
Appendices.....	151
Appendix A: Rights and Permissions.....	151
Appendix B: Media Recipes	157

List of Tables

Table 1: Strains used in this study.....	40
Table 2: Primers used in this study.....	42
Table 3: Plasmids used in this study.....	46
Table 4: Antibodies used in this study.....	49

List of Figures

Figure 1: A diagram depicting the life cycle and differentiation network in <i>L. pneumophila</i>	5
Figure 2: Chaperonins function to prevent protein misfolding.....	14
Figure 3: The current model of the Dot/Icm secretion system.....	33
Figure 4: Quality of fractionation was confirmed by western blotting and enzymatically.....	56
Figure 5: A graphical representation of the formula used to determine the TSR values from densitometric western blotting.....	58
Figure 6: HtpB does not possess most amino acid characteristics of a typical Dot/Icm effector.....	64
Figure 7: HtpB displays sequence homology to several known Cell-Penetrating Peptides.....	66
Figure 8: Diagram showing the sequential steps followed to construct the knockout vector used to create the $\Delta dotA$ mutant.....	68
Figure 9: Agarose gels of a PCR for <i>dotA</i> and a control gene in parent strain JR32 and two $\Delta dotA$ mutants.....	70
Figure 10: Pictures of BCYE plates showing the growth patterns of the <i>L. pneumophila</i> parent strain JR32 and its $\Delta dotA$ derived mutant in the presence or absence of sodium chloride.....	73
Figure 11: Pictures of BCYE plates showing the growth patterns of the <i>L. pneumophila</i> $\Delta dotA$ mutant complemented in trans with pMMB:: <i>dotA</i> and a vector control consisting of $\Delta dotA$ containing empty pMMB in the presence or absence of sodium chloride.....	75
Figure 12: Light micrographs of <i>A. castellanii</i> following sixteen hours of infection with parent strain, <i>dotA</i> deletion mutant, and <i>dotA</i> complemented <i>L. pneumophila</i>	77
Figure 13: Growth curves of parent strain, <i>dotA</i> deletion mutant, and <i>dotA</i> complemented <i>L. pneumophila</i>	79

Figure 14: Diagram describing the cloning procedures to generate GSK fusion proteins.....	82
Figure 15: Immunoblots of lysed JR32 strains carrying <i>gsk</i> constructs reveal that the GSK tag is not phosphorylated by <i>L. pneumophila</i>	84
Figure 16: A western blot of lysates recovered following an infection of L929 cells by parent strain JR32 and the $\Delta dotA$ mutant expressing HtpB-GSK, LegC6-GSK and Mdh-GSK.....	86
Figure 17: A western blot of lysates recovered following an infection of L929 cells by parent strain JR32 and the $\Delta dotA$ mutant expressing HtpB-GSK, LegC6-GSK and Mdh-GSK.....	89
Figure 18: A western blot of lysates recovered following an infection of U937 cells by parent strain JR32 and the $\Delta dotA$ mutant expressing HtpB-GSK, LegC6-GSK and Mdh-GSK.....	91
Figure 19: Images of BL21, and <i>phoA</i> KO <i>E.coli</i> carrying recombinant <i>phoA</i> with an HtpB ‘tail’, incubated on agar containing a chromogenic substrate which assays alkaline phosphatase activity.....	93
Figure 20: Recombinant <i>icdH</i> with an <i>htpB</i> ‘tail’ is expressed at the protein level in JR32.....	96
Figure 21: western blots of osmotic shockate samples for Icd-H50 and Icd-H100 and the densitometric analysis of these blots for sub-cellular localization.....	98
Figure 22: A graphical plot of the ratio relating the amount of recombinant Icd found in the membrane and periplasmic fractions after osmotic shock that cannot be explained by cell lysis.....	100
Figure 23: Diagram describing the cloning procedures to generate a 6xHis tagged version of HtpB.....	103
Figure 24: Transmission electron micrographs of JR32 expressing a recombinant HtpB with a C-terminal 6xHis tag.....	105
Figure 25: Graphs representing the sub-cellular distribution of HtpB-6xHis seen in immunogold micrographs.....	107
Figure 26: Transmission electron micrographs of JR32 expressing a recombinant Icd tagged with the last 50 amino acids of HtpB.....	109

Figure 27: Graphs representing the sub-cellular distribution of Icd seen in immunogold micrographs.....	111
Figure 28: An alignment of the sequence encoding the LepA used in this study with the reference sequence of <i>L. pneumophila lepA</i> (NCBI, Gene ID:19833438).....	116
Figure 29: Immunoblot of fractionated lysate dilutions intended to ensure linearity-of-scale during densitometry analysis.....	122
Figure 30: A diagram depicting elements of the putative new model for Dot/Icm secretion.....	130

Abstract

Legionella pneumophila is a ubiquitous freshwater pathogen of unicellular eukaryotes, namely several species of amoeba. Following inhalation of *Legionella*-contaminated aerosols, susceptible human populations may also develop an atypical, pneumonia-like illness, as *L. pneumophila* opportunistically infects alveolar macrophages. One of the many virulence factors possessed by *L. pneumophila* is High Temperature Protein B (HtpB), a multifunctional chaperonin that has been found on the cell surface. Despite the several virulence-related roles that have been described for the surface-exposed or extracellularly released HtpB, no mechanism has yet been proposed for how this essential, typically cytoplasmic protein reaches extracytoplasmic compartments. In this work, we present evidence that Dot/Icm, a type IV secretion system of *L. pneumophila*, is responsible for the translocation of HtpB through a non-canonical secretion pathway. An infection model using *L. pneumophila* carrying a genetically tagged, recombinant HtpB demonstrated that HtpB does not reach the cytoplasm of *Legionella*-infected host cells without a functional Dot/Icm system. By fusing the C-terminus of HtpB to the cytoplasmic protein Icd and assaying its sub-cellular locale by western blotting, we demonstrate that the C-terminus of HtpB has affinity for the *Legionella* envelope membranes but is not sufficient to mediate secretion. These results, as well as prior data generated by other researchers/students in the Garduño Lab at Dalhousie University, led us to conclude that HtpB normally traffics through the periplasm of *L. pneumophila* and relies on the Dot/Icm system for escaping the periplasm, but crosses the inner membrane in an uncharacterized manner. This unknown mechanism by which HtpB seems to translocate across the cytoplasmic membrane may apply to other *Legionella* proteins and thus contribute to explain the unusual quantity and diversity of Dot/Icm effectors, therefore being of critical importance to the understanding of virulence in *L. pneumophila*.

List of Abbreviations and Symbols Used

ACS-Actual Cytoplasmic HtpB Seen

Amp- Ampicillin

AP- Alkaline Phosphatase

BCYE- Buffered Charcoal Yeast Extract (medium)

BCIP- 5-Bromo-4-Chloro-3-Indolyl Phosphate

BSA- Bovine Serum Albumin

BYE- Buffered Yeast Extract (medium)

Cm- Chloramphenicol

EPF- Exponential Phase Form

FBS- Fetal Bovine Serum

HPS- Hypothetical Periplasmic Secretion of HtpB

IDT- Integrated DNA Technologies

IPTG- Isopropyl β -D-1-thiogalactopyranoside

LB- Lysogeny Broth (medium)

LCV- Legionella Containing Vacuole

MEM- Minimum Essential Medium

Met- Metronidazole

MIF- Mature Infectious Form

NEB- New England Biolabs

NZT- Nitro Blue Tetrazolium Chloride

OD_#- Optical Density at #nm

PBS- Peptone Buffered Saline

PCR- Polymerase Chain Reaction

PMA- Phorbol Myristate Acetate

PYG- Peptone Yeast Glucose (medium)

RPF- Replication Phase Form

RPMI- Roswell Park Memorial Institute (medium)

SPF- Stationary Phase Form

Tris- Tris(hydroxymethyl)aminomethane

TBS- Tris Buffered Saline

TTBS- Tween-20 Tris-Buffered Saline

Acknowledgements

Without the people listed below, this thesis would never have reached completion. They have my eternal gratitude for their unwavering support.

Drs. Rafael Garduño and Jason LeBlanc, my supervisors

Drs. John Rohde and Song Lee, my committee members

Karla Valenzuela, Aaron Liu, and Wolim Lee, my lab-mates and friends,

And finally my family, who put up with me despite everything.

1. Introduction

1.1 *Legionella pneumophila*: An Overview

1.1.1 *Legionella pneumophila*: History and Pathogenesis

The genus *Legionella* consists of aerobic, Gram-negative bacteria that are found ubiquitously in the environment. The species most relevant to human health is *Legionella pneumophila*, an environmental pathogen capable of causing severe disease in humans (Fraser et al., 1977). *L. pneumophila* resides mainly in freshwater ecosystems both natural and manmade. In the natural environment *L. pneumophila* exists mainly in lakes and ponds, whereas environments more relevant to human health include water cooling towers, air-conditioners and residential water systems (Wadowsky, Yee, Mezmar, Wing, & Dowling 1982). In the natural environment *L. pneumophila* can exist as a free-living, environmentally resistant bacteria, but must act as an intracellular pathogen of freshwater protozoa in order to replicate (Barbaree, Fields, Feeley, Gorman & Martin, 1986). *L. pneumophila* is therefore faced with two distinct environments in which it must survive: the oligotrophic freshwater environment, and the intracellular vacuole of phagocytic protozoa. The former environment entails a lack of nutrients, a highly variable environment and ever-present osmotic stress (caused by the hypotonic conditions of oligotrophic water), while the latter requires some mechanism with which to overcome host defenses and prevent intracellular killing. While many bacteria have adaptations designed to assist survival in multiple environments, *L. pneumophila* has taken adaptation to the next step in that it possesses several differentiated forms designed to withstand

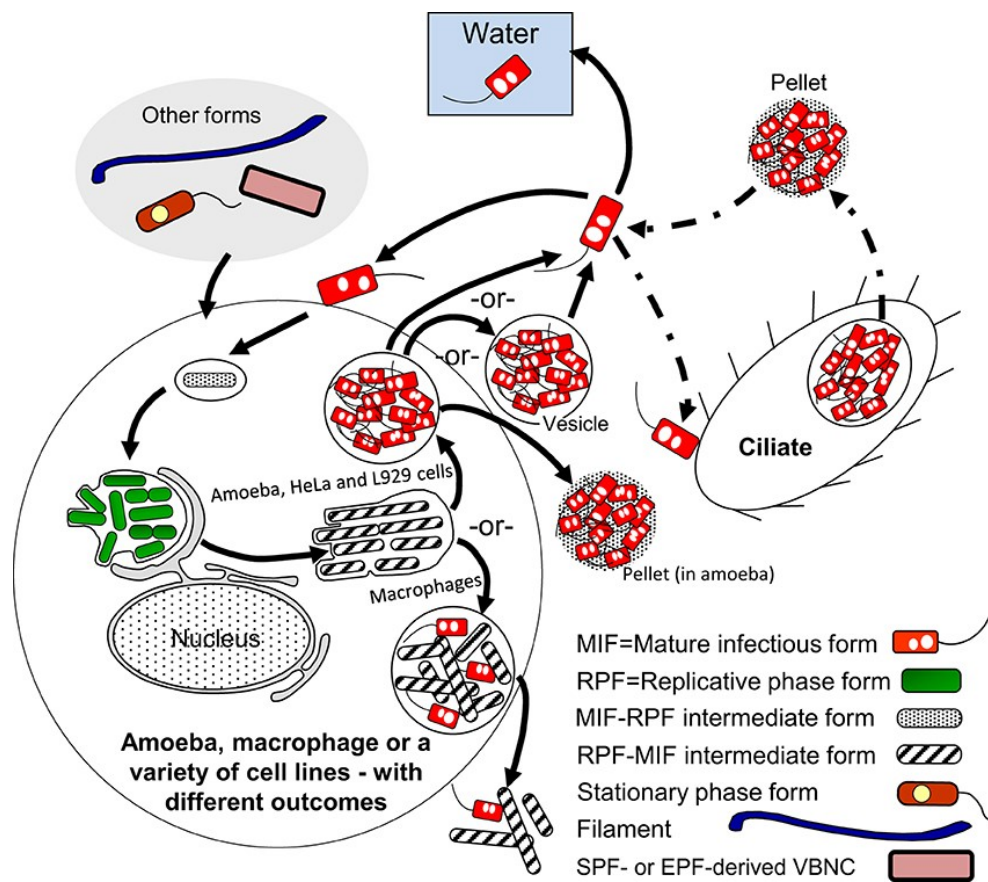
pressures in different environments. While the differentiation network of *L. pneumophila* is complicated, for the purposes of this work only four forms are important; two from the *in vitro* lifecycle of *L. pneumophila* and two from the *in vivo* lifecycle. *In vitro* the two forms are known as the Exponential Phase Form (EPF) and the Stationary Phase Form (SPF). The EPF occurs during exponential growth, and is the actively replicating form of *in vitro* *L. pneumophila*, whereas the SPF is more resistant to stress but non-replicative. These forms cycle, as the EPFs differentiate into the SPFs at high culture density, and the SPFs become EPFs when inoculated into new media. While many bacteria exhibit stress responses similar to this cycle, in *L. pneumophila* the two forms differ so much in morphology, staining patterns, genetic expression profiles and resistance to stress that they are considered distinct forms. These *in vitro* forms of *L. pneumophila* are considered to be incompletely differentiated versions of the two *in vivo* forms observed, the MIF (Mature Infectious Form, analogous to the SPF) and the RF (Replicative Form, analogous to the EPF). When extant as a free-living bacterium in freshwater, *L. pneumophila* is present as a MIF. The MIF possesses several distinct features, including a thick envelope with a difficult-to-resolve periplasm, membrane invaginations, cytoplasmic inclusions of β -hydroxybutyrate, and resistance to antibiotics and chemical stressors (Faulkner & Garduño, 2002; Garduño R., Garduño E., Hiltz & Hoffman, 2002). These adaptations, while not all fully studied, are simple to understand in the context of surviving the freshwater environment: a thick membrane and resistance to chemicals would help compensate for a variable environment and osmotic stress, and inclusions of β -hydroxybutyrate could act as a store of food in an environment low in nutrients. The MIF is therefore capable of long-term survival in a harsh environment,

allowing *L. pneumophila* to survive until it can encounter an appropriate protozoan host. Once a host is encountered and invaded, however, the MIF stage of differentiation is a liability as it cannot replicate. This multiplication defect presumably prevents *L. pneumophila* from replicating in the freshwater environment (where using energy to replicate would almost certainly be fatal), but once a host is encountered *L. pneumophila* must quickly differentiate into the replication-competent RPF (Replicative Form) in order to take advantage of the host environment (Faulkner & Garduño, 2002; Garduño *et al.*, 2002). This differentiation occurs intracellularly as a response to signals present in the host but absent from the environment. Upon entering into a host vacuole (in the MIF form), *L. pneumophila* delays phagosome-lysosome fusion and begins to recruit host organelles such as mitochondria and endoplasmic reticulum to establish the so-called *Legionella*-containing vacuole (LCV) where *Legionella* replication begins (Bozue & Johnson, 1996; Horwitz, 1983). The recruitment of host-cell organelles floods the LCV with nutrients, inducing a transcriptional change in *L. pneumophila* and resulting in differentiation to the RPF (reviewed in Robertson, Abdelhady & Garduño, 2014). When the levels of uncharged tRNAs in *L. pneumophila* go down (due to increasing nutrient levels), the ribosome bound protein RelA ceases to make ppGpp, the major signaling molecule of *L. pneumophila* differentiation (Hammer & Swanson, 1999). The bifunctional lipid metabolism protein SpoT may also begin to break down ppGpp in response to increased nutrient levels (Dalebroux, Edwards & Swanson, 2009). As ppGpp is capable of binding RNA polymerase in order to alter promoter preference (Artsimovich *et al.*, 2004), the sudden decrease in ppGpp is associated with systemic transcriptional changes in *L. pneumophila*. As a result, *L. pneumophila* begins to differentiate into the

RF (Hammer & Swanson, 1999). Taking advantage of host nutrients, the RF replicates to high number, until the *L. pneumophila* progeny drain the nutrients present in the LCV. When this happens, the lack of amino acids and perturbations to fatty acid biosynthesis cause RelA and SpoT to generate ppGpp, reversing the earlier differentiation and resulting in a transition from RPF to MIF. The MIFs are then released to the freshwater environment through host lysis (Baine, 1985; Kirby, Vogel, Andrews & Isberg, 1998). These new MIFs constitute infectious particles, and upon encountering a new host they can continue the infection cycle. Despite the presentation herein of *L. pneumophila*'s lifecycle as a series of unconnected cycles, in reality these cycles are a joined 'network' of differentiation (Figure 1). The *in vitro* and *in vivo* cycles, for example, are not independent: feeding SPFs to amoebae will result (post infection) in MIFs, and MIFs grown *in vitro* will replicate (as EPFs, before becoming SPFs). MIFs may also escape the host in different forms; they may be free living bacteria after lysis (as implied above) or packaged together in 'pellets', host-derived vesicular bodies that wrap *L. pneumophila* in several layers of membrane (Berk, Ting, Turner & Ashburn, 1998). Additionally, other types of stress can result in *L. pneumophila* assuming other differentiated forms (such as the filament or the VBNC, reviewed in Robertson *et al.*, 2014). A full discussion of the differentiation program of *L. pneumophila* lies beyond the scope of this work, but the point must be made that the organism's lifecycle is dictated by the external environment. Investigations into the virulence of *L. pneumophila* must take host context into account.

Most of the investigative work in *L. pneumophila* is performed in a few model host systems. In relation to natural hosts, these are usually species of the *Acanthamoeba*, *Naegleria* and *Tetrahymena* genera. Despite this, *L. pneumophila* has a broad host range

Figure 1: A diagram depicting the life cycle and differentiation network in *L. pneumophila*. Differentiation of *L. pneumophila* into its many forms is dictated by host and environmental factors. Entrance of *L. pneumophila* MIFs (red and white), filaments (blue), VBNCs (light red) or stationary phase forms (red and yellow) into host eukaryotes promotes differentiation into RPFs. Metabolic factors then influence RPFs to differentiate into MIFs (in natural host cells) or MIF-RPF intermediates (in human macrophages) prior to escape. Following release, *L. pneumophila* may exist freely in water, or be packaged into a pellet by ciliates. As a highly expressed surface protein, HtpB may play an important role in all of these interactions. Figure adapted with permission from Robertson *et al.*, 2014.



and is capable of infecting many organisms (reviewed in Taylor, Ross & Bentham, 2009). Most of these are freshwater protozoa, organisms that *L. pneumophila* is likely to encounter in its natural environment. Occasionally, however, *L. pneumophila* is capable of infecting and causing disease in an organism outside of its normal host range, as is the case with Legionellosis in humans. Legionellosis refers to diseases caused by infection with *Legionella*, including the atypical pneumonia known as Legionnaire's disease and the less severe cold-like illness known as Pontiac fever (McDade *et al.*, 1977; Kaufmann *et al.*, 1980). Legionnaire's disease is a result of bacterial replication and cell destruction in the lungs, as human alveolar macrophages are the preferred replication niche in human hosts. The disease tends to strike as large, but thankfully uncommon, outbreaks in vulnerable populations (such as hospital patients or nursing home residents) (Phin *et al.*, 2012). Mortality rates among *Legionella*-infected patients vary wildly depending on the health of the affected population and the healthcare resources available, but tend towards 5-30% (Benin, Benson & Besser, 2002). Despite the severity of the disease, it is considered an accidental infection on the part of *L. pneumophila*, as the bacterial infection is ultimately non-productive and is not a viable portion of the *L. pneumophila* life cycle. As well, the disease is only caused through environment-to-person transmission, and cannot be transmitted person-to-person, solidifying *L. pneumophila* as an environmental pathogen with an occasional accidental foray into human pathogenesis (Victor, Zuravleff, Gavlik & Magnussen, 1983). The most common method of transmission is from an infected water source (such as a shower head or air-cooling unit) to a vulnerable population via inhalation of infected aerosols. As such droplets are often of respirable size, *L. pneumophila* is then able to interact with lung epithelial cells and

alveolar macrophages. As an organism with a broad host range, it is doubtful that *L. pneumophila* can distinguish between phagocytosis by human alveolar macrophages and phagocytosis by a viable host, such as *Acanthamoeba castellanii*. *L. pneumophila* therefore enters the human macrophage and begins the infection cycle, much as it would in a freshwater protozoan. Human macrophages are apparently incapable of supporting the full differentiation process, however, as the product of infection in a human macrophage is a population of *L. pneumophila* progeny with fewer morphological features characteristic of a fully differentiated MIF (Abdelhady & Garduño, 2013). As well, these pseudo-MIF progenies lack the same genetic regulation in response to differentiation possessed by fully differentiated MIFs emerging from amoebae (Bruggemann *et al.*, 2006; Faucher, Mueller & Schuman, 2011). This indicates that host specific factors may play a role in inducing differentiation, which may be responsible for the lack of person-to-person transmission seen in Legionellosis. Despite this deficiency, the infection of freshwater protozoa and human macrophages is broadly similar, and presents broadly similar challenges to *L. pneumophila*. As with any pathogenic infection, prevention, treatment and diagnosis may all be improved by an in-depth understanding of the biology of the causative agent. Despite many years of work in understanding *L. pneumophila* virulence, significant gaps are still present in our understanding of the infection cycle.

1.1.2 A Brief Account of the Known Virulence Factors of *L. pneumophila*

While the current understanding of virulence in *L. pneumophila* is far from complete, many virulence factors have been identified and partially investigated. Below is a brief

description of known virulence factors in *L. pneumophila*, organized by their most characterized functions.

Motility and Attachment Factors: In order for *L. pneumophila* to infect host cells, it must first reach and bind them. Motility in *L. pneumophila* is achieved through the action of the flagellum. In *L. pneumophila*, nutrient scarcity causes production of a flagellum through the activation of the alternate sigma factors RpoN and FliA (reviewed in Heuner & Steinert, 2003). Inhibition of motility (via deletion of genes encoding either the flagellum itself or the ion channel that powers it) results in severely reduced adherence to, and an inability to lyse, bone-marrow derived macrophages (Molofsky, Sheton-Rama & Swanson, 2005). Deletion of *fliA* also results in increased destruction of *L. pneumophila* by lysosomes, although this is likely due to functions of *fliA* not related to motility (such as regulating other virulence genes) (Molofsky *et al.*, 2005). The adhesion factors of *L. pneumophila* are even more poorly worked out than the motility factors, and are likely host cell dependant. E-cadherin and β -1 Integrin have been previously implicated in the attachment of filamentous (but not coccoid) *L. pneumophila* to human lung epithelium (Prashar *et al.*, 2012). As well, pre-exposure of host cells to a variety of sugars (such as galactose), or pre-exposure of *L. pneumophila* to oligosaccharide receptor mimics (such as GalNAc β 1-4Gal) is known to reduce attachment of the bacteria to some protozoa but not others (Harb, Venkataraman, Haack, Gao & Abu Kwaik, 1998; Thomas & Brooks, 2004). Attachment of *L. pneumophila* has also been associated with protein synthesis and phosphorylation in host cells, but in a host dependent manner (Harb *et al.*, 1998). This indicates that *L. pneumophila* likely attaches to a broad spectrum of sugar

and protein residues rather than relying on one or two defined receptors, which may help to explain the diversity of its host range.

Internalization Factors: The mechanisms by which *L. pneumophila* invades cells are poorly studied. Phagocytosis (and, more rarely, coiling phagocytosis) have been reported (Horwitz, 1984; Cirillo *et al.*, 1999), however *L. pneumophila* is known to invade non-phagocytic cell lines (such as HeLa cells) (Daisy, Benson, McKittrick & Friedman, 1981; Horwitz, 1984). The process by which *L. pneumophila* becomes phagocytosed seems to vary by cell line, as different authors have reported different results on the necessity of PI3-K for phagocytosis. Tachado *et al.* and others have reported that inhibition of PI3-K inhibits phagocytosis of *L. pneumophila* in J774A.1 macrophages, whereas Harada *et al.* report that inhibition had no effect in U937 macrophages (Tachado, Samrakandi & Cirillo, 2008; Harada *et al.*, 2012). A process similar to pinocytosis has also been observed in mouse macrophages with a permissive *Lgn1* allele, however the relevance of this to general pathogenesis is uncertain (Watarai *et al.*, 2001). As with other virulence factors in *L. pneumophila*, mechanisms of internalization may be numerous and host-specific.

Intracellular Modification Factors: In order to survive intracellular conditions and modify host processes, *L. pneumophila* secretes an entire suite of effectors through its major virulence factor, the Dot/Icm type IV secretion system. Upon engulfment, *L. pneumophila* is entrapped in a host phagosome which would normally progress through degradative processes. To prevent phagosome acidification *L. pneumophila* secretes SidK, an effector which binds and inactivates the eukaryotic proton pump (Xu *et al.*, 2010). Although it is known that *L. pneumophila* delays and prevents phagosome-

lysosome fusion as well, the effectors which mediate this are understudied. Outer Membrane Vesicles (OMVs) (and LPS alone) are known to inhibit phagosome-lysosome fusion, although their effect seems to be temporary (Seeger *et al.*, 2010). There are also likely Dot/Icm effectors involved, however, as deletion of Dot/Icm secretion results in significantly early fusion of phagosomes with lysosomes, leading to bacterial killing (Roy, Berger & Isberg, 1998). It is known that LCVs do not recruit normal phagosomal markers such as LAMP-2 or cathepsin D, except in macrophages pre-stimulated with interferon γ (Santic, Molmeret & Abu Kwaik, 2005). It may then be theorized that *L. pneumophila* secretes effectors which interfere with host cell IFN signalling.

As well as evading degradation, *L. pneumophila* also remodels the cell to enhance nutrient uptake. The LCV anchored protein AnkB is known to promote degradation of host proteins into amino acids for bacterial consumption (Price *et al.*, 2009). *L. pneumophila* also requires several amino acid transporters to differentiate, including the threonine transporter PhtA (Faucher *et al.*, 2011; Sauer, Bachman & Swanson, 2005). As well, *L. pneumophila* is known to decorate the LCV with MavN, an iron transporter essential for efficient acquisition of iron (and therefore, essential for growth) during intracellular infection, and secretes a siderophore called legiobactin (Isaac, Laguna, Valtz & Isberg, 2015; Liles, Scheel & Cianotto, 2000). This may be critical for bacterial survival during an immune response, as human macrophages are known to sequester iron during infection with certain pathogens (reviewed in Collins, 2008). *L. pneumophila* is also known to recruit mitochondria and endoplasmic reticulum to the LCV, presumably as sources of energy and metabolites (Horwitz, 1983). While the recruitment factors are

unknown, the ATP transporter LncP is thought to be responsible for stealing ATP from host mitochondria (Dolezal *et al.*, 2012).

Factors of Bacterial Escape: Following exploitation of a host's resources, *L. pneumophila* must escape in order to infect new hosts. In infection of mouse macrophages, pore-formation is a result of the host cell's inflammasome reaction to bacterial flagellin (Silveira & Zamboni, 2010). *L. pneumophila* must possess multiple means of escape, however, as an escape strategy dependent on pyroptosis is unlikely to work in non-immune cells. In human cells, *L. pneumophila* escape is dependent on pore-formation in the host membrane followed by osmolysis (Kirby, Vogel, Andrews & Isberg, 1998).

Recent data have pointed to an important yet understudied virulence factor: the multifunctional chaperonin HtpB (Garduño, Chong, Nasrallah & Allan, 2011; Garduño & Chong, 2013; Valenzuela-Valderas, Riveroll, Robertson, Murray & Garduño, in press). As an essential protein, HtpB is present in high amounts throughout the entire infection lifecycle. Additionally, it is one of the two major surface-exposed proteins in *L. pneumophila* (along with the porin OmpS), meaning that HtpB could contribute significantly to the initial bacteria-host interaction. Over time, it has been discovered that HtpB possesses numerous functions relating to infection, making a study of HtpB critical to understanding the pathogenesis of *L. pneumophila*.

1.2 Chaperonins

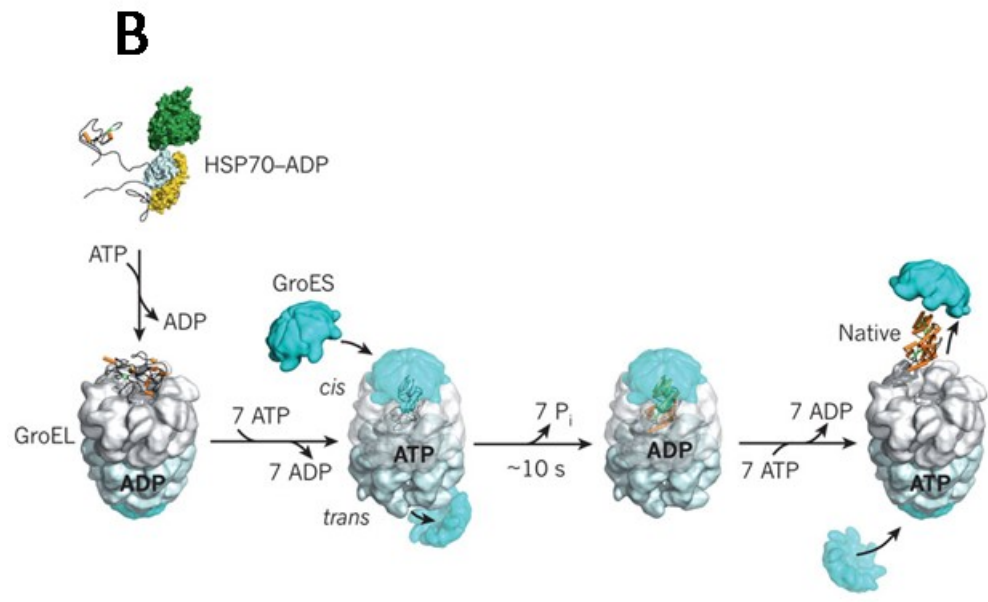
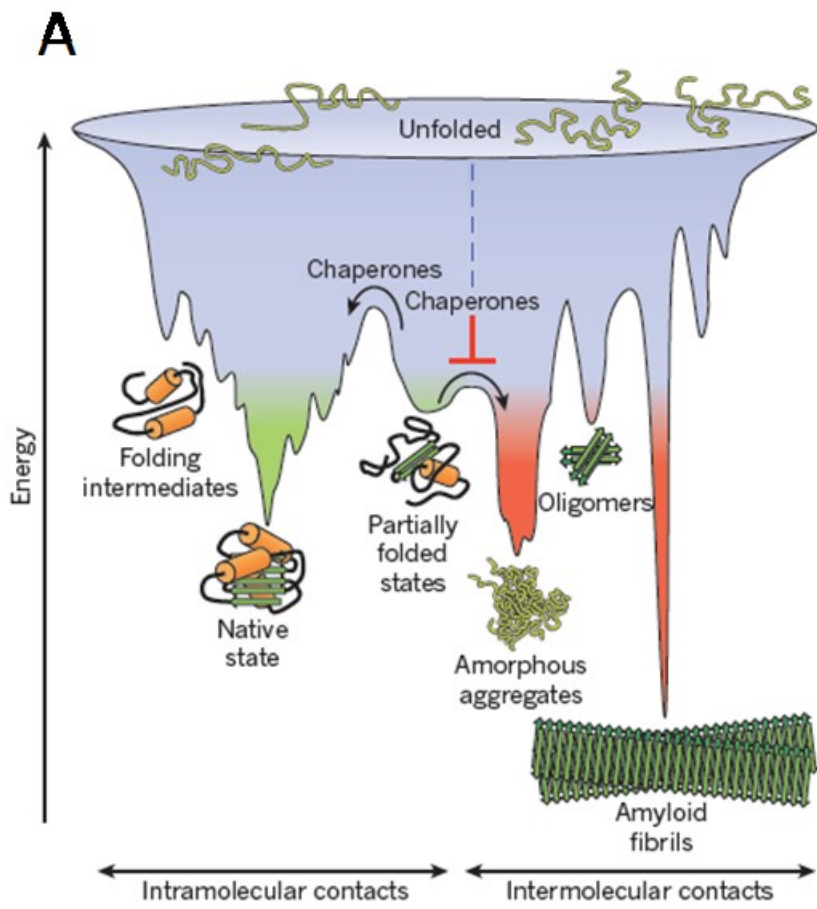
1.2.1 The GroEL model of chaperonin function

Chaperonins, also known as heat shock protein 60s (Hsp60s), are a family of proteins responsible for assisting other cytoplasmic proteins to fold and are present in all forms of

cellular life. They are separated into group I chaperonins, found in bacteria, mitochondria and plastids, and group II chaperonins, found in archaea and the cytoplasm of eukaryotes. These group I chaperonins, known variously as Hsp60, Cpn60, or Htp proteins, are β -barrel rich proteins which form a multimeric barrel structure in which protein folding occurs. They are also associated with co-chaperonins, ~ 10 kDa proteins which form a multimeric 'lid' to cap the chaperonin barrel. The most thoroughly studied bacterial chaperonin in relation to protein folding is the *E. coli* GroEL/GroES chaperonin/co-chaperonin complex. This complex consists of two homoheptameric barrels of 60kDa GroEL subunits stacked on top of one another, capped by a homoheptameric lid of 10kDa GroES subunits. Upon binding of an unfolded substrate to one of the GroEL barrels, complex conformation changes ensue such that ATP binding and association with a GroES lid is favoured. Association with the GroES lid causes the unfolded substrate to relocate to the inside of the GroEL barrel. This encapsulation provides a sheltered microenvironment in which the substrate can fold without interference from other proteins. Additionally, hydrolysis of ATP to ADP in the seven subunits of GroEL causes a torsional motion which may contribute to proper folding. The two barrels of GroEL are anti-cooperative for ATP, such that when all ATP is converted to ADP the empty barrel can now bind ATP. When this occurs, steric changes force the barrel containing the now-folded substrate to dissociate from the GroES lid and release the substrate to the cytoplasm (Figure 2) (reviewed in Hayer-Hartl, Bracher & Hartl, 2016).

Group II chaperonins are more poorly studied. Their structures and function are broadly similar to group I chaperonins, although there are significant differences: group II chaperonins possess rings composed of eight or nine chaperonin proteins (as opposed to

Figure 2: Chaperonins function to prevent protein misfolding. (A) Cartoon depicting the various energy states proteins may occupy. Without intervention, proteins will tend to fold into thermodynamically favoured (but non-functional) fibrils or clusters (red valleys). Chaperonins allow proteins to overcome energy barriers (curved arrows) and fold into their native (i.e. functional) state (green valley). (B) A diagram of the steps involved in GroEL mediated protein folding. GroEL (white) oligamerizes into a tetrakaidecamer double barrel complex (white and light blue) with the help of Hsp70 (yellow). This barrel encloses an unfolded substrate, and requires capping from a homoheptamer of GroES subunits (blue). Binding of this GroES lid results in conformational changes, forcing the dissociation of the trans GroES lid and initiating the folding process. This process is ATP-dependant and consists of a torsional motion, isolation of the substrate from the environment, and potentially interactions with the C-terminus of GroEL. Following dephosphorylation of 7 ATP molecules, the GroES lid disassociates from the barrel complex and allows the now-folded substrate to escape. Reprinted by permission from Macmillan Publishers Ltd: *Nature*, Hartl, Bracher, & Hayer-Hartl, 2011, copyright 2011.



seven in GroEL) and do not require a co-chaperonin for folding to occur (reviewed in Klumpp & Baumeister, 1998).

Molecular chaperone function is essential for most cytoplasmic proteins to enter and maintain their functional states. The most stable state of proteins is either globular agglutinations or amyloid fibrils, both of which prevent protein function. Chaperonins are known to interact with many essential proteins (GroEL being the only folding partner for thirteen in *E. coli*) (Kerner *et al.*, 2005), and are found in almost all forms of cellular life (the sole exceptions being some species of *Mycoplasma*, reviewed in Williams and Fares, 2010). Chaperonins are therefore considered essential proteins themselves, and their elimination leads to cell death (Fayet, Ziegelhoffer & Georgopoulos, 1988).

Accumulating deletions, insertions or non-silent substitutions in a chaperonin-encoding gene is a risky strategy, evolutionarily speaking, as a loss of chaperonin function is fatal. Despite this risk, chaperonins can be viewed as an ‘easy’ target for acquiring a useful adaptation; as the protein already has the ability to bind many other proteins (at least 250, according to Kerner *et al.*, 2005) and alter their shape, few substitutions would be required to acquire a vastly altered function. In light of this, many chaperonins with alternative functions do exist in nature, but are usually the product of gene duplication. In this process, an extra copy of the chaperonin gene is encoded stably on the chromosome (through a variety of methods; reviewed in Sandegren and Andersson, 2009) such that mutation in one copy will not result in a loss of chaperonin function. As an example, *Chlamydia trachomatis*, an intracellular pathogen with a developmental cycle, has three copies of its chaperonin. Only GroEL1 appears to react to heat shock in *C. trachomatis* and therefore likely possesses chaperonin function (Karunakaran *et al.*, 2003). GroEL2 is

seemingly involved in persistence of *Chlamydia* during iron starvation, and the function of GroEL3 has yet to be clearly determined (LaRue, Dill, Giles, Whittimore & Raulston, 2007). This evolutionary strategy is relatively safe, as mutations in GroEL2 or GroEL3 will not result in non-viable progeny, as the protein folding requirements of the cell are met by GroEL1. More rarely, a single chaperonin may possess multiple functions. For example, the chaperonin of *Enterobacter aerogenes*, a bacterium commonly found in the spit of the ant lion *Myrmeleon bore*, is a potent paralytic toxin to German cockroaches (*Blattella germanica*) (Yoshida *et al.*, 2001). Other chaperonins can function as proteases (*Mycobacterium leprae*; Portaro *et al.*, 2002), histidine kinases (*Buchnera aphidicola*; Morioka, Yamamoto & Ishikawa, 1994), biofilm formation factors (*Histophilus somni*; Zarankiewicz, Madej, Galli, Bajwert & Stefaniak, 2012) and strong modulators of the mammalian immune system (reviewed in Henderson, Fares & Lund, 2013). As with all multifunctional proteins, it is difficult to retrospectively resolve whether or not during their evolution chaperonins began possessing multiple functions and current lineages have simply lost primordial chaperonin traits through substitution mutations, or whether ancestral chaperonins possessed only their main protein folding ability and alternative functions were then gained through evolution. While neither possibility can be completely ruled out, several arguments favour the latter scenario over the former. Firstly, the sheer number of functions that chaperonin-like proteins are seen to perform makes it unlikely that any ancestral protein could perform so many functions, and raises the question of why the functions have partitioned along bacterial lineages the way they have. Secondly, the small number of substitutions in the chaperonin-encoding genes of organisms with alternative chaperonin functions (e.g. only four amino acid differences

are required to generate an insect toxin, with only three needed for protease activity) (Yoshida *et al.*, 2001; Portaro *et al.*, 2002) suggests that these modifications are recent and not ancient. Regardless of how chaperonins acquire alternative functions, it is known that many bacteria do encode for a single, essential chaperonin which has multiple functions. Special even amongst these oddities is High Temperature Protein B (HtpB) of *L. pneumophila*, a chaperonin with many additional functions.

1.2.2 *L. pneumophila* HtpB is a Multifunctional Protein

HtpB, a 60kDa protein, forms the cytoplasmic protein-folding complex of *L. pneumophila* along with the co-chaperonin HtpA. These two proteins are encoded by the *htpAB* operon on the chromosome of *L. pneumophila*, and constitute the only chaperonin/co-chaperonin complex present in this organism (D'Auria, Jimenez-Hernandez, Periss-Bondia, Moya & Letorre, 2010; Garduño *et al.*, 2011; Nasrallah, Gagnon, Orton & Garduño, 2011). The HtpAB complex is therefore inferred to have protein folding function, although this has only recently been confirmed (Lee, 2014). In addition to the essential function of protein folding, HtpB is known to possess many other functions, leading to the description of this protein as a “moonlighting” chaperonin (reviewed in Garduño & Chong, 2013). While multifunctional proteins are far from uncommon, the sheer number of functions HtpB is suspected to possess make this protein highly unusual. The known and suspected functions of HtpB are listed below.

HtpB as an adhesion and invasion factor: As a pathogen of freshwater protozoa, *L. pneumophila* possesses mechanisms which mediate its attachment to and ingestion by potential host cells. While freshwater protozoa are already capable of performing

phagocytosis, it has long been known that *L. pneumophila* enhances its own uptake (Hilbi, Segal & Schuman, 2001). As an organism that requires ingestion by eukaryotic cells in order to replicate, this function presumably ensures ingestion so that the bacteria can produce progeny. In addition, *L. pneumophila* persistence in commercial water systems may be abetted by the ability of *L. pneumophila* to ‘hide’ from disinfectants by internalizing into protozoa (Thomas *et al.*, 2004; Donlan *et al.*, 2005). In light of this, promoting its own phagocytosis may also provide a survival benefit to the organism, as it allows *L. pneumophila* to gain a reprieve from environmental stressors. In addition, ingestion of *L. pneumophila* by *Tetrahymena tropicalis* results in the ‘pelletting’ of these bacteria without significant loss of viability, and causes the *Legionella* to differentiate in the absence of replication (Berk *et al.*, 2008; Faulkner, Berk, Garduño, Ortiz-Jiménez & Garduño, 2008). Phagocytosis/ingestion can therefore confer a direct benefit to survival, as these pelleted bacteria are more resistant to certain forms of chemical and physical stressors (analogous to a mobile particulate biofilm) (Koubar, Rodier, Garduño & Frère, 2011).

Surface-expressed HtpB acts as an invasion factor in human HeLa cells. *L. pneumophila* is known to internalize into HeLa cells, despite the fact that this cell line is not naturally phagocytic. The internalization of *L. pneumophila* into HeLa cells is disrupted by the addition of anti-HtpB antibodies (but not OmpS antibodies) in a dose-dependent manner, indicating that free HtpB residues are needed for uptake (Garduño, Faulkner, Trevors, Vats & Hoffman, 1998). Furthermore, latex beads coated in purified HtpB were able to significantly out-compete beads coated with BSA for internalization into HeLa cells (Garduño *et al.*, 1998). Latex beads coated with HtpB were also able to compete with *L.*

pneumophila for HeLa cell internalization, whereas the BSA coated beads were not (Garduño *et al.*, 1998). Taken together, these data indicate that HtpB is able to act as an adhesin, and may be partially responsible for mediating the invasion of host cells. HeLa cells are epithelial in origin, however, and therefore lack many of the receptors that would be found on freshwater protozoa, or even on human macrophages. It is therefore likely that other receptor-ligand interactions are present in mediating the *in vivo* internalization of *L. pneumophila* into target cells: recent data has implicated E-cadherin and $\beta 1$ integrin in the adhesion to and invasion of lung epithelium by filamentous *L. pneumophila* (Prashar *et al.*, 2012), the gene product of *laiA* is necessary for adhesion to and invasion of murine epithelial cells (Chang, Kura, Amemura-Maekawa, Koizumi & Watanabe, 2005), and the collagen-like protein Lcl enhances adhesion to both human macrophage and human lung epithelial cell lines (Vandersmissen, de Buck, Saels, Coil & Anné, 2010). It is likely that additional surface proteins will be discovered to function in adhesion and invasion as *L. pneumophila* is further studied.

The ability of a chaperonin to act as an invasion factor is not limited to *L. pneumophila*. The pathogenic fungus *Histoplasma capsulatum* is known to use its Hsp60-like chaperonin to increase phagocytosis by human macrophages (in which this pathogen survives), and vaccines against this Hsp60 are known to promote clearance of *H. capsulatum* in mouse models (Long *et al.*, 2003; Deepe and Gibbons, 2002). The chaperonin Cpn60.1 of *Mycobacterium bovis* BCG (a pathogen of humans and commercial livestock) is able to bind DC-SIGN, a molecule present on macrophages and dendritic cells (Carroll *et al.*, 2010). Overall, at least 10 distinct species of bacteria have surface-expressed chaperonins with known ligands, and many more are suspected to

utilize their chaperonins in adhesion and invasion (reviewed in Henderson et al., 2013). Of these, the case of *Brucella abortus* (an intracellular pathogen of human and bovine gastric epithelium) is of interest due to the similarities between this pathogen and *L. pneumophila*. *B. abortus*, like *L. pneumophila*, is an intracellular pathogen which modifies its own replication niche inside cells and expresses its major virulence traits through type IV secretion. *B. abortus* possesses surface Hsp60, which serves as an attachment and internalization factor through its ability to bind cellular prion protein. This surface expression of Hsp60 is dependent on the type IV secretion system of *B. abortus* (Watarai et al., 2003). As *L. pneumophila* relies heavily on type IV secretion for virulence, the case of *B. abortus* serves as an example of the confluence of secretion, chaperonins, and a multifunctional protein in pathogenesis.

HtpB and Recruitment of Host Organelles: All bacteria require a source of nutrients in order to replicate and spread. For intracellular parasites such as *L. pneumophila*, the nutrients required to sustain the pathogen during its intracellular phase must be derived from the host itself. This is especially true for *L. pneumophila*, as the free-living stage of the bacteria's lifecycle inhabits oligotrophic freshwater, an environment with limited nutrients. The availability of nutrients plays such a key role in the lifecycle of *L. pneumophila* that the organism has tied its differentiation cycle to the levels of amino and fatty acids. As mentioned in the previous section the LCV becomes flooded with nutrients during infection, which triggers differentiation via a RelA/SpoT-mediated change in levels of ppGpp. While the pathways of differentiation in *L. pneumophila* have received extensive attention, the mechanisms by which nutrients are acquired in the first place are less well understood. Microscopy reveals that the LCV associates closely with

host organelles, most prominently the ER and mitochondria (Horwitz, 1983). This interaction is likely responsible for the increase in available nutrients in the LCV, as both the ER and the mitochondria are sources of energy-rich intermediates and metabolic precursors. The mechanisms by which *L. pneumophila* recruits and exploits these energy sources are not fully worked out, but it is likely that HtpB is involved. Seventy % of internalized beads coated in HtpB are able to attract mitochondria to the vesicles in which they reside, as opposed to 20% of BSA-coated beads (Chong et al., 2009). As only 80% of *L.pneumophila*-containing phagosomes were associated with mitochondria, HtpB is therefore nearly sufficient to explain the recruitment of mitochondria to the LCV. The fact that HtpB attracts mitochondria but is not observed to recruit ER is informative; a homologue to bacterial chaperonins (mtHsp60) exists within mitochondria, and is known to interact with mtHsp10, the mitochondrial co-chaperonin (reviewed in Gupta, 1995). It is therefore possible that HtpB units embedded in the LCV are able to recruit mitochondria through an interaction with mtHsp10. Because the mitochondrial genes responsible for synthesis of mtHsp60 and mtHsp10 have migrated into the eukaryotic nucleus, synthesis of these chaperonin homologues occurs outside the mitochondria and must be translocated inside (Singh, Patel, Ridley, Freeman & Gupta, 1990). Because cytosolic proteins targeted to the mitochondria rely on mitochondrial surface proteins for import (reviewed in Alberts *et al.*, 2002), it is plausible that mitochondria always have at least some surface expressed mtHsp60. Once close enough to the LCV, mitochondrial proteins could be taken advantage of by *L. pneumophila* through the actions of Ankyrin B, a secreted *Legionella* protein similar to ubiquitin ligase which is responsible for promoting the breakdown of host proteins into amino acids (Price *et al.*, 2009).

HtpB and Modification of Cytoskeletal Processes: As an intracellular pathogen, *L. pneumophila* is known to modify host actin in order to promote its own uptake and to alter the host environment in favour of bacterial survival. The modes of entry for *L. pneumophila* are multiple and are difficult to tease apart due to genetic redundancy. Dot/Icm effector proteins are generally thought of as essential for enhanced internalization, as mutations resulting in a non-functional Dot/Icm system result in deficient entry into amoebae and human macrophages, as well as a reduced ability to prevent phagosome-lysosome fusion (Vogel, Andrews Wong and Isberg 1998). *L. pneumophila* likely has multiple methods of altering host actin, however, as pH-induced stress is able to restore entry into human macrophages and amoeba in *dotA* mutants (Bandyopadhyay, Xiao, Coleman, Price-Whelan & Steinman, 2004). While it is true that low pH alone may induce cytoskeletal processes (as actin self-assembles more efficiently at low pH due to lower critical concentrations requirements for cations) (Wang, Sampogna & Ware, 1989), Bandyopadhyay *et al.* report that recovery of the entry phenotype is dependent on pH treating the bacteria (not the macrophages), implicating a stress activated entry mechanism independent of the Dot/Icm system. As well, during entry virulent (but not avirulent) *L. pneumophila* stimulates the polymerization of actin in host cells by stimulating PI3K/Akt signalling through an unknown mechanism (Tachado, Samrakandi & Cirillo, 2008). *L. pneumophila* may also modify host actin using HtpB. In addition to having increased uptake by CHO cells, beads coated in HtpB are also able to delay phagosome-lysosome fusion (Chong, Lima, Allan, Nasrallah & Garduño, 2009); both processes involve the modification of host actin. During infection of CHO cells by HtpB-coated beads, a phenomenon known as “framing” is observed in which host actin is

significantly polymerized at the cell periphery and depolymerized from the cell center (Chong *et al.*, 2009). While this behavior is not observed during infection with virulent *L. pneumophila* (instead, the organism seems to cause association of polymerized actin with host endosomes to reroute intracellular trafficking) it does indicate that HtpB alone has an effect on host actin. Furthermore, HtpB can directly interact with actin (Chong and Garduño 2013). Collectively, these effects of HtpB could promote bacterial survival by recruiting vesicles and organelles for increased nutrients, inhibiting cytoskeleton-dependent bacterial killing events, or both. HtpB modification of host actin may be redundant in real-world infections, such that the process is only important when other methods of actin rearrangement are inhibited. Additionally, the process could be additive, where HtpB is partially responsible for actin rearrangement in conjunction with other bacterial factors.

HtpB as a Metabolic Protein: As mentioned above, nutrient levels in the LCV control the lifecycle of *L. pneumophila* and are key external signals for the organism. *L. pneumophila* possesses entire suites of genes devoted to assessing nutrient levels and initiating responses designed to maximize nutrient uptake. One class of nutrients important for *L. pneumophila* is the polyamine group, organic molecules with multiple amino residues. Polyamines can have many functions, and are known to act as signaling molecules, chelating agents and developmental regulators in eukaryotes (Bachrach, Wang & Tabib, 2001; Harris, Murase, Timmons & Martell, 1978; Kaur-Sawhney, Tiburcio, Altabella & Galston, 2003). Their functions in bacteria are not fully explored, but they are known to facilitate growth, act in acid resistance (Chattopadhyay & Tabor, 2013) and enhance biofilm formation (Patel *et al.*, 2006; Zhang X., Zhang Y., Liu J. & Liu H.,

2013; reviewed in Karatan & Michael, 2013). In *L. pneumophila*, the pharmacological inhibition of polyamine biosynthesis in host cells restricts bacterial growth intracellularly, and the addition of polyamines enhances growth. *L. pneumophila* lacks the ability to synthesize most polyamines, and would therefore need to infect host cells in order to accumulate appreciable amounts. HtpB is known to bind eukaryotic SAMDC (S-Adenosyl Methionine Decarboxylase, an enzyme required for polyamine production), and may therefore function to increase available levels of certain polyamines (Nasrallah *et al.*, 2011). Therefore, it has been hypothesized that HtpB could directly enhance the levels of available polyamines to be used as metabolites, in addition to indirectly assisting energy generation by attracting nutrient- and energy-rich organelles.

HtpB as a Filamentation Factor: When experiencing stress, many bacteria are known to undergo a filamentation process in which cell division is impeded but growth is not, such that bacterial cells end up with a significantly lengthened morphology. This change is known to increase the ability of bacteria to form biofilms, enhance surface area (leading to increased nutrient uptake and enhanced expression of adhesion and invasion factors), and deter certain immune responses (reviewed in Yang, Blair and Salama, 2016). In *E.coli*, filamentation is mediated by the stress-induced accumulation of SulA, a protein which binds FtsZ to prevent polymerization of the latter (Trusca, Scott, Thompson & Bramhill, 1998). Although *L. pneumophila* has no known homologue to *sulA*, it is known to be capable of filamentation in response to temperature stress (Piao, Sze, Barysheva, Iida & Yoshida, 2006). Filamentous *L. pneumophila* is also able to out-compete rod-shaped *L. pneumophila* in terms of attachment to human lung epithelium, suggesting that filamentation enhances pathogenesis (Prashar *et al.*, 2012). Theoretically, the ability to

enhance biofilm formation and deter predation could help *L. pneumophila* survive the harsh conditions of its natural habitat.

HtpB may play a role in the filamentation of *L. pneumophila*. In addition to being induced by the same trigger as filamentation (i.e., temperature stress), overexpression of HtpB results in increased levels of *L. pneumophila* filamentation (Garduño, unpublished). Higher levels of filamentation also seem to correlate with higher expression of HtpB (natively, without overexpression), although causation is difficult to prove as both filamentation and HtpB induction are responses to stress (Garduño, unpublished). While the specific mechanism by which HtpB could cause filamentation is unclear, HtpB is known to alter the distribution of cytoskeletal components (see above). It is therefore possible that HtpB may possess an analogous interaction with the FtsZ ring, or with another mediator of filamentation.

1.3 Translocation and Secretion

1.3.1 Secretion is a Key Aspect of Pathogenesis in *L. pneumophila*

In order to persevere and proliferate within an environment, a pathogen must first be capable of manipulating it. To this end, the mechanisms of secretion available to a bacterial species can define its pathogenesis, as the ability to subvert host defenses often rests with the ability to secrete effector proteins. To date, seven main mechanisms of secretion have been defined in Gram negative bacteria (reviewed in Costa *et al.*, 2015). The diversity of secretion systems and their wide spread within the bacterial domain are testaments to the centrality of this phenomenon in the ability of bacteria to survive their environment. Secretion has many uses: to communicate (as in quorum sensing), to hijack

host processes (e.g., pedestal formation seen in intestinal villi during infection by pathogenic *E. coli*), to eliminate host resistance (e.g., the various toxins secreted by *Bordetella pertussis*), and even to gain adaptive advantages (e.g., DNA uptake in many bacterial species). Given these uses, the selective advantage conferred by the proper secretion of effectors is potentially enormous. This is perhaps even more so in *L. pneumophila*, as an intracellular pathogen must, by definition, replicate within an organism that will be attempting to kill it. To *L. pneumophila*, then, secretion is a mechanism by which host processes conducive to bacterial survival may be enhanced, and those detrimental to bacterial survival may be halted. *L. pneumophila* possesses multiple secretion systems and a massive suite of effectors which are secreted in a regulated manner during infection (Zhu *et al.*, 2011; Aurass *et al.*, 2016). This is easily explained as a product of the organism's lifecycle: not only does *L. pneumophila* require internalization into hostile host cells in order to replicate, it is also known to invade a range of seemingly unrelated hosts. Redundancy in secreted effectors is therefore high, with the loss of a single effector rarely resulting in a noticeable infection defect (Luo & Isberg, 2004).

Prior research has definitively proven that HtpB reaches the cytoplasm of host cells. Not only do fusions between HtpB and CyaA (the adenylate cyclase of *Bordetella pertussis*) result in increased cAMP levels during infection, but the multiple functions of HtpB listed in the previous section would require exposure to the host cell in order to occur (Chong, 2007). As well, immunogold microscopy of HtpB and GroEL has revealed that the former reaches the periplasm, cell surface, and LCV in *L. pneumophila* whereas the latter is confined to the cytoplasm in *E. coli* (Garduño *et al.*, 1998). Trypsinization of cell

surfaces also results in the breakdown of HtpB (as identified by western blot), which could only occur if HtpB were exposed on the cell surface (Garduño, Garduño & Hoffman, 1998). These data taken together confirm that HtpB is present on the cell surface of *L. pneumophila*, and is able to reach the LCV and host cell cytoplasm. Despite the unusual multifunctional nature of HtpB and the central role it may play in infection, very little research has gone into the mechanism by which HtpB reaches extracytoplasmic compartments, or unequivocally defining whether HtpB is actually secreted.

1.3.2 Outline of Known Secretion Mechanisms in *L. pneumophila*

Below is an outline of known secretion systems of *L. pneumophila*, the candidates for the secretion of HtpB.

Type II Secretion in *L. pneumophila*: The Type II secretion system is common in Gram negative bacteria, and is the major terminal of the general secretion pathway (reviewed in Pugsley, 1993). Type II secretion is a two-step process in which the translocation from the cytoplasm to the periplasm is distinct from the translocation to the outer membrane and beyond. The first step relies on either the Sec system or TAT (Twin Arginine Translocase) system in order to move effectors from the cytoplasm to the periplasmic space (reviewed in Natale, Bruser & Driesson, 2008). Once there, proteins are secreted further through the outer membrane by a multi-protein complex known as a secreton. *L. pneumophila* possesses a Type II secretion system known as the Lsp system. This system is responsible for the secretion of many enzymes, including a metalloprotease (ProA), an acid phosphatase (Map), lipases (LipA and LipB), phospholipase C (PlcA) and others (Rossier, Dao & Cianotto, 2008; Aragon, Kurtz, Flieger, Neumeister & Cianciotto, 2000;

Aragon, Rossier & Cianciotto, 2002). The Lsp system is, however, a poor candidate for the secretor of HtpB for several reasons. Firstly, both the Sec and TAT systems require N-terminal signal peptides on their respective targets in order to facilitate their translocation. No such signal peptide is present in HtpB. Secondly, mutations in the Sec and TAT pathways do not result in a decreased secretion of HtpB, indicating that this system is not essential for chaperonin secretion. While this would seem to rule out the Type II secretion of HtpB, it should be noted that some putatively Type II substrates (based on proteomic analysis) are secreted via the Type IV secretion pathway during infection (de Felipe *et al.*, 2008). It is therefore possible that environmental pressures cause the different secretion systems and their substrates to interact with one another in a manner not yet fully understood.

L. pneumophila and Type IV Secretion: Type IV secretion systems are some of the oddest and most multifunctional virulence factors in bacteria. First discovered in *Agrobacterium tumefaciens*, the Type IV secretion system was initially characterized as a mechanism of translocating DNA to host cells in order to alter host processes (Ward *et al.*, 1988). It was soon determined, however, that Type IV secretion systems are also capable of translocating proteins, and have many different uses. Type IV secretion systems are known to function in competence, conjugation, and pathogenesis, making them critical to the lifecycles of many bacteria. *L. pneumophila* possesses two Type IV secretion system types, Type IVA and Type IVB systems. The Type IVA system, known as the Lvh system, is homologous to the VirB system found in *A. tumefaciens* and is thought to be responsible for the secretion of plasmid DNA (Segal, Russo & Shuman, 1999; reviewed in Lammertyne & Anné, 2004). The genes of the Lvh system themselves

are encoded on a plasmid-like element; a long region of DNA that can be either mobile or chromosomally integrated depending on the strain of *L. pneumophila* and the environment in which the organism is grown (Steinert, Heuner, Buchrieser, Albert-Weisenberger & Glöckner, 2007). Additionally, the unusually high GC content of the Lvh-encoding genes suggests that this system was acquired via horizontal gene transfer (Segal *et al.*, 1999). The function of the Lvh system is somewhat disputed, as it seems to be dispensable for infection but may have differing roles depending on environmental context. Deletion of the *lvhB3* gene causes a roughly 100-fold reduction in the internalization of *L. pneumophila* into human epithelial and monocytic cell lines, but only at 30°C and not 37°C (Ridenour, Cirillo S.L., Feng, Samrakandi & Cirillo J.D., 2003). Additionally, the Lvh system seems to partially restore the defects in pathogenesis and survival seen in Dot/Icm mutants. While the Lvh system is therefore considered ancillary, it may possess many functions that depend on environmental contexts not replicated in the laboratory.

The Type IVB system, also known as the Dot/Icm system, is unambiguously the most important virulence factor in pathogenic *L. pneumophila*. Mutations that eliminate Dot/Icm function are not fatal to *L. pneumophila* in and of themselves, but result in a bacterium that has reduced entry into host cells and an inability to replicate inside these cells. This is due to the overarching function of most Dot/Icm effectors: to modify host processes such that clearance is evaded and replication is favoured. The ‘secretome’ of the *L. pneumophila* Dot/Icm system is one of the largest currently known, with nearly three hundred effectors being secreted by the system (Zhu *et al.*, 2011). These vary wildly in function, but include adhesins, guanine exchange factors (RalF and DrrA;

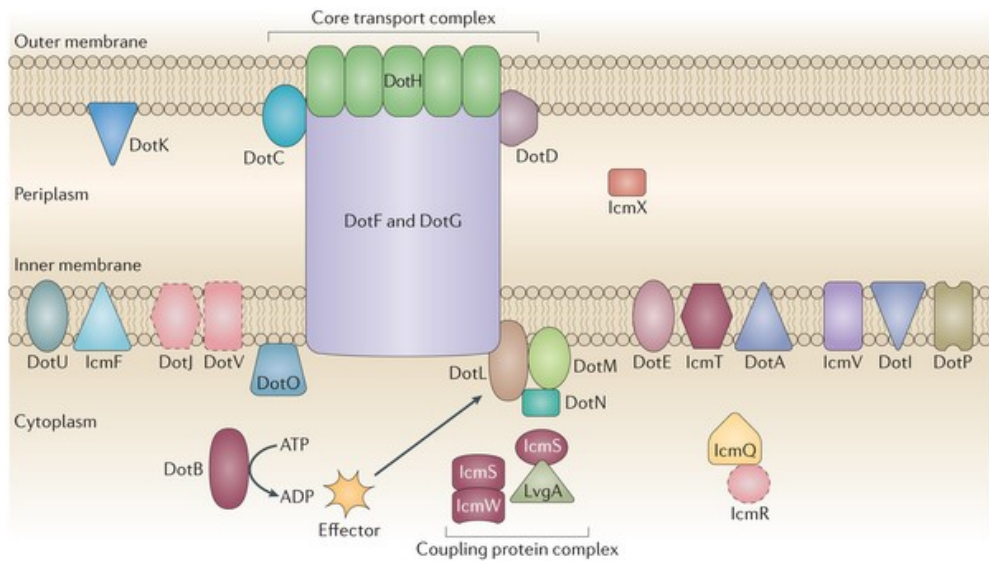
thought to modulate host vesicle trafficking) (Nagai, Kagan, Zhu, Khan & Roy, 2002; Murata *et al.*, 2006), glucosyltransferases (Lgt1, Lgt2 and Lgt3; mediate cytotoxicity by glucosylating eEF1A) (Belyi, Tabakova, Stahl & Aktories, 2008), ubiquitination machinery (LubX and AnkB; may play a role in nutrient acquisition) (Kubori, Hyakutake & Nagai, 2008; Price *et al.*, 2009), and many others (reviewed in Ensminger and Isberg, 2009). Despite intense investigations into the Dot/Icm system, the majority of effectors have no confirmed function. This is partially due to the sheer number of effectors, but also to the extensive redundancy observed in *L. pneumophila*. Knocking out a single effector rarely has a distinguishable phenotype, as most functions are backed up by other effectors. The reason for this redundancy is unknown, but may be due to a wide host range; different freshwater protozoan hosts would require slightly different responses from *L. pneumophila* during infection. Study of essential proteins such as HtpB and their relationship to the Dot/Icm system is therefore doubly difficult, as knockouts result in non-viable mutants, whose differing phenotypes would likely be affected by the choice of hosts in any case.

The structure of the Dot/Icm system has yet to be fully resolved, as have the functions of many Dot/Icm components. The current model suggests that a multimeric complex consisting of DotCDFGH is the core translocon, responsible for secreting substrates. DotF and DotG are inner-membrane proteins that interact with the outer membrane, and are thought to mediate the transfer of energy and substrates from the cytoplasm, through the periplasm to the outer membrane (Vincent *et al.*, 2006). The outer membrane protein DotH likely functions as a secretin, forming a secretion pore composed of multiple DotH subunits. DotC and DotD act as lipid anchors, and are necessary for the correct formation

of the DotH multimer (Vincent *et al.*, 2006). A second complex putatively exists in the inner membrane: the DotLMN complex, which is assisted by the cytoplasmic proteins IcmSW (Buscher *et al.*, 2005). IcmSW are thought to be adaptor proteins which mediate the binding of Dot/Icm substrates to the secretion machinery. IcmSW are known to interact with DotL, which is thought to ‘pass off’ substrates from the adaptor proteins to the DotCDFGH complex (Sutherland, Nguyen, Tseng & Vogel, 2012). DotM and DotN have unknown functions, but complex with DotL (Figure 3) (Vincent Friedman, Jeong, Sutherland & Vogel, 2013) (reviewed in Vincent & Vogel, 2008).

In addition to these proteins, the Dot/Icm complex consists of many additional components with unknown functions. Many of these are integral proteins on the inner membrane, including DotA. Adding to the complexity of studying the Dot/Icm system, no surefire method of predicting Dot/Icm substrates has been identified. Common patterns of Dot/Icm effectors are reported to be a hydrophobic amino acid at the -3 or -4 locus in the C-terminus (Nagai *et al.*, 2005), a C-terminal enrichment of glutamic acid residues (the so-called “E-blocks”)(Huang *et al.*, 2011), a depletion of negative amino acids at -1 to -6 and an enrichment of these amino acids at -8 to -18, a depletion of hydrophobic amino acids at -8 to -12 and an enrichment at -1 to -3, and an enrichment of serine and threonine at -3 to -11 (Burststein *et al.*, 2009). Predictions of Type IVB effectors in *L. pneumophila* require computational analysis in order to identify and scale all of these factors; however some ambiguity exists regarding the relative importance of markers. It is likely then that Dot/Icm effectors lie along a ‘gradient’ with some being secreted more easily than others depending on how strongly they match the biochemical ideal of a Type IV effector. What can be clearly seen from previous research is that the

Figure 3: The current model of the Dot/Icm secretion system. Cartoon depicting the putative structure of the Dot/Icm secretion system. DotCDH form a secretion pore in the outer membrane, DotLMN form an inner-membrane structure, and the two are connected by the DotFG secretion channel. IcmSW act as chaperones to bring substrates in contact with the DotLMN complex. DotB acts to energize the system using ATP. The functions of the other Dot/Icm components are largely unknown, and their deletion has variable effects on secretion efficiency. Reprinted by permission from Macmillan Publishers Ltd: *Nat. Rev. Microbiology*, van Schaik, Chen, Mertens, Weber and Samuel, 2013, copyright 2013.



Nature Reviews | Microbiology

amino acid composition of the C-terminus is critical for determining whether or not a protein can interact with the Dot/Icm system. In several cases the C-terminus alone is necessary and sufficient for secretion, as the last 20 and 35 amino acids of RalF and SidG (respectively) were able to drive secretion through the Dot/Icm system (Nagai et al., 2005; Cambronne and Roy, 2007), supporting the hypothesis that C-terminal signals are responsible for substrate recognition in the Dot/Icm system. Primary sequence similarity in Dot/Icm effectors is notoriously poor, but the secondary structure of RalF (as determined by crystallography) reveals that the C-terminus is held separate from the main body of the protein by an α -helix (Amor *et al.*, 2005). This may implicate secondary structure as a key determinant of substrate recognition in the Dot/Icm system.

The Type IVB Dot/Icm secretion system in *L. pneumophila* is likely involved in the secretion of HtpB. Deletion of DotA or DotB, proteins essential for a functional Dot/Icm system, reduces surface-exposed HtpB (indicated by a reduction in trypsin sensitivity of HtpB in these mutants) (Chong, Riveroll, Allan, Garduño & Garduño, 2006). Further, mutations in *dotG*, which encodes a protein known to function in Dot/Icm secretion but not be essential for it, result in an intermediate phenotype: trypsin degradation of HtpB occurs, but is greatly reduced. This indicates that the ability of HtpB to reach the surface of *L. pneumophila* relies directly upon Dot/Icm secretion. It cannot be emphasized enough, however, that this does not mean HtpB must be a Dot/Icm substrate. The Dot/Icm system is a complicated biological machine with many uncharacterized components; it is possible that one or more of these components acts to fold, stabilize, anchor, or otherwise interact with HtpB. The IcmSW proteins, for example, are known to act as chaperones for Dot/Icm substrates, and enhance their secretion by delivering them

to the main inner-membrane component of the system. HtpB, therefore, may be secreted by a mechanism independent of Dot/Icm secretion, and yet still rely on the formation of a Dot/Icm system for efficient translocation.

Other Forms of Secretion in *L. pneumophila*: For the sake of completeness, it must be mentioned that other forms of secretion exist in *L. pneumophila* but are far less studied than Type II or Type IV. The *L. pneumophila* genome is known to code for a Type I secretion system and a flagella apparatus, and is suspected to be capable of Type V and OMV secretion. Type I secretion systems are dual-membrane spanning ‘ABC’ complexes that secrete from the cytoplasm to the extracellular environment in a single step. While *L. pneumophila* is known to express a Type I secretion system (encoded by the *lssXYZABD* locus), to date the only known substrate is the toxin RtxA (Jacobi and Heuner, 2003). Type I secretion is a poor candidate mechanism to explain the translocation of HtpB, as evidence suggests the presence of a periplasmic intermediate (see above). The flagellar apparatus is not usually considered an independent secretion system (as it is generally assumed to only secrete proteins necessary for the formation of the flagellar complex), but is distantly related to the Type III secretion system (Gophna, Ron & Graur, 2003). There have been documented examples of pathogens secreting virulence factors through the flagellar apparatus (such as the apoptosis-inducing protein FspA in *Campylobacter jejuni*) (Poly *et al.*, 2007), however no such examples have been discovered in *L. pneumophila* to date. Type V secretion systems, also known as autotransporters, are proteins which enter the periplasm via the Sec system and then mediate their own further translocation by using their C-terminal sequence as a β -barrel structure through which to pass the inner membrane (reviewed in Dautin & Bernstein, 2007). While prior research

does indicate that the C-terminus of chaperonins can insert into lipid membrane (Torok *et al.*, 1997), it is unlikely that HtpB is secreted through a Type V mechanism. Firstly, the C-terminal β -barrel structure necessary for autotransportation is not predicted to occur in HtpB. Secondly, deletion of the Sec system does not inhibit HtpB translocation.

Finally, *L. pneumophila* releases Outer membrane vesicles (OMVs), which are thought by some to constitute a form of secretion (Galka *et al.*, 2008). OMVs consist of small membrane vesicles which bud from the bacterial surface and which may contain proteins, either packaged within the vesicle or integrally bound to the vesicle membrane itself. MALDI-TOF analysis of *L. pneumophila* OMVs has revealed that they do contain HtpB, although it is not currently known if this is an intentional act of delivery to potential hosts, or if HtpB is an accidental passenger in OMVs (as it is known to be an abundant surface protein) (Galka *et al.*, 2008). These OMVs are shed extracellularly in the absence of hosts, indicating that HtpB may be an unintentional part of the OMV secretome, although the regulation of OMV secretion levels in *L. pneumophila* is not nearly well studied enough to draw conclusions. Alternatively, OMV secretion may be the main mechanism of translocating HtpB to host cells, and the Dot/Icm system may only be necessary for recruiting, anchoring, or modifying HtpB such that it is capable of undergoing secretion in OMVs. It may also be the case that HtpB is secreted through both OMVs and the Dot/Icm system, as other proteins found in OMVs are known effectors of other secretion systems (such as Map) (Galka *et al.*, 2008; Rossier *et al.*, 2008). Ultimately the interaction between the Dot/Icm system and OMV secretion in *L. pneumophila* is largely unknown, but merits further investigation; at least insofar as the two methods of secretion contribute in tandem to virulence.

1.4 Hypotheses and Intent

The aim of this study is to investigate the mechanism by which *L. pneumophila* secretes HtpB. From the information presented above, two tentative hypotheses have been drawn: Firstly, that the C-terminus of HtpB facilitates the protein's translocation from the cytoplasm to the periplasm, and secondly that a functional Dot/Icm system is required for further translocation to the cell surface and extracellular locations. Throughout this thesis, an attempt is made to test these hypotheses and generate evidence for accepting or rejecting them, as well as to fit them into the current framework of known *Legionella* pathogenesis.

2. Materials and Methods

2.1 General Techniques

2.1.1 Growth of Bacterial Strains

E. coli DH5 α and BL-21 were grown in liquid culture by inoculation in LB medium and incubation in a rotary shaker at 200 rpm and 37 °C. In solid culture, *E. coli* was grown on LB plates in a 37 °C incubator. Antibiotics (all obtained from Sigma Chemicals Canada, Oakville ON) were used for plasmid maintenance in the following concentrations: ampicillin 100 μ g/mL, chloramphenicol 20 μ g/mL, kanamycin 50 μ g/mL. JR32 *L. pneumophila* was grown in liquid culture by inoculation in BYE medium supplemented with 0.04 % L-cysteine and 0.1 % ferric pyrophosphate, followed by incubation in a rotary shaker at 200 rpm and 37 °C. In solid culture *L. pneumophila* was grown on BCYE plates consisting of BYE medium supplemented with 15 g/L agar and 2 g/L charcoal, then grown in a humid incubator at 37 °C with 5 % CO₂. Antibiotics (all Sigma) were used for plasmid maintenance in the following concentrations: chloramphenicol 5 μ g/mL, kanamycin 25 μ g/mL. Strains are listed in Table 1.

2.1.2 Growth of Eukaryotic Cell Lines

U937 human monocyte cells were inoculated in RPMI 1640 medium (ThermoFisher Scientific, Massachusetts USA) supplemented with 10 % FBS (ThermoFisher), and 0.5 mM β -mercaptoethanol (Sigma). One hundred μ g/mL of streptomycin and penicillin (ThermoFisher) were also added to prevent bacterial contamination of cell stocks. U937 cells were then grown in a humid incubator at 37 °C with 5 % CO₂. To create monolayers of adherent, macrophage-like cells, U937 cells were counted in a

Table 1: Strains used in this study.

Name	Species of Origin	Description	Other Characteristics	Source
DH5a	<i>E.coli</i>	Common cloning strain	<i>fhuA2</i> , <i>lac(del)U169</i> , <i>phoA</i> , <i>glnV44</i> , $\Phi80'$, <i>lacZ(del)M15</i> , <i>gyrA96</i> , <i>recA1</i> , <i>relA1</i> , <i>endA1</i> , <i>thi-1</i> , <i>hsdR17</i>	Garduño Lab stock
JR32	<i>L. pneumophila</i>	Lab derivative of clinical <i>Legionella</i> isolate	Strep ^R , restriction-minus	Garduño Lab stock
<i>phoA</i> KO <i>E.coli</i>	<i>E.coli</i>	In-frame, markerless deletion of <i>phoA</i>	K-12 derivative, Δ <i>phoA</i>	Dr. John Rohde
BL-21	<i>E. coli</i>	Common strain	PhoA+	Dr. John Rohde
L929	Mouse	Fibroblast cell line	Immortalized	Garduño Lab stock
U937	Human	Monocyte cell line	Immortalized, differentiates to macrophage-like cells	Garduño Lab stock
ATCC 30010	<i>A. castellanii</i>	Freshwater amoebae		Commercial (American Type Culture Collection)

haemocytometer, activated to differentiate into macrophages using 60 ng/mL of PMA, and then seeded in a twelve-well cell culture plate at a density of 2×10^6 U937 cells per well. Cells were incubated for two days (with medium changes on both days containing no PMA), then checked by microscopy to confirm differentiation before proceeding to bacterial infection. Cells were considered to be differentiated once they were adherent and possessed a spread out, lumpy morphology (as opposed to the detached, rounded monocytes). The activated U937 cells used in experimentation are subsequently referred to as 'U937-derived macrophages'.

L929 mouse fibroblast cells were inoculated in MEM (ThermoFisher) with 10 % FBS (ThermoFisher). Cells were grown in the same manner as the U937 cells. To create an infectable monolayer, cells were detached from their flask using MEM with 0.04 % Trypsin/EDTA (ThermoFisher), counted in a haemocytometer, and plated in six-well plates at a density of 10^5 cells per cm^2 surface area. Infections were carried out the following day.

A. castellanii 30010 were grown in Peptone Yeast Glucose (PYG) at 30 °C. Cells were seeded in six-well plates at a density of 10^5 cells per cm^2 surface area and allowed to grow to confluence.

2.1.3 PCR with *Taq*

Taq DNA polymerase (New England Biolabs Ltd. Canada, Whitby ON) was used for routine detection PCR. Twenty μL of a PCR master mix was made up according to the manufacturer's instructions (final concentration of 200 μM deoxynucleosides, 0.75 units polymerase). Two μL of both the appropriate forward and reverse primers (Table 2) were

then added (to a final concentration of 0.1 μM), as was 1 μL of the appropriate template, for a reaction total of 25 μL . This reaction was then run in a thermocycler (T1 Thermo, ThermoFisher) for 20-35 cycles with a denaturation temperature of 95 $^{\circ}\text{C}$, an extension temperature of 72 $^{\circ}\text{C}$, and an annealing temperature 5 $^{\circ}\text{C}$ lower than the lowest T_{M} of the primer pair. Extension times were calculated as one minute per kilo-base pair of the sequence to be amplified. All PCR products were purified using a PCR purification kit according to the manufacturer's instructions (Qiagen, Toronto ON).

2.1.4 PCR with *Pfx*

High fidelity Platinum *Pfx* DNA polymerase (Invitrogen, now ThermoFisher) was used to amplify genomic segments for direct cloning. Forty μL of a PCR master mix was made up according to the manufacturer's instructions. Four μL of both the appropriate forward and reverse primers (to a final concentration of 0.1 μM) were then added, as was 2 μL of the appropriate template, for a reaction total of 50 μL . This reaction was then run in a thermocycler (T1 Thermo, ThermoFisher) for 20-35 cycles with a denaturation temperature of 94 $^{\circ}\text{C}$, an extension temperature of 68 $^{\circ}\text{C}$, and an annealing temperature 5 $^{\circ}\text{C}$ lower than the lowest T_{M} of the primer pair. All PCR products were purified using a PCR purification kit (Qiagen).

2.1.5 Restriction Digestion

Digestions were carried out in 40 μL reactions. Four μL of the appropriate 10x digestion buffer, 4 μL of BSA (NEB), and 4 μL of DNA restriction digestion enzyme (NEB) (or 2 μL each of two enzymes in double digestions) were mixed in a 0.6 mL Eppendorf tube. Then, 0.5-3 μg of DNA (depending on the sample cut; always diluted to 20 μL total volume) were added, and PCR grade water (ThermoFisher) was used to constitute the

reaction volume up to 40 μ L. The reactions were then placed in a 37 °C water bath for at least 4 hours. The digested DNA was then purified either directly using a PCR CleanUp kit (Qiagen), or else electrophoresed in an agarose gel and purified with a Gel Extraction kit (Qiagen).

2.1.6 Ligation

Ligation was performed as directed by the manufacturer (NEB). Briefly, a 3:1 mixture of linearized vector and an appropriately digested fragment were mixed with 2 μ L ligation buffer, 1 μ L T4 DNA Ligase (NEB), and PCR grade H₂O (ThermoFisher) to a volume of 20 μ L. The reaction was then mixed and incubated in a thermocycler at 15 °C overnight.

2.1.7 Generating Electrocompetent Cells

DH5 α was grown in 1 L of LB (37 °C, 200 rpm in a shaking incubator) to an OD₆₀₀ of 0.6-0.9, and was then pelleted down at 4200 \times g. The supernatant was discarded, and the pelleted cells kept on ice for the rest of the procedure. The pellet was first resuspended in 20 mL of ice-cold ddH₂O, pelleted as before, and drained of the supernatant. The pellet was then resuspended in 20 mL of 20 % glycerol, pelleted as before, and drained of the supernatant. The pellet was then resuspended in 2 mL of 20 % glycerol, and was divided into 40 μ L aliquots. These aliquots were kept frozen at -80 °C until required.

JR32 was grown as a lawn on BCYE plates for 3 days, and the growth was then scraped and suspended into 20 mL ddH₂O to an OD₆₀₀ of 2 units. JR32 was then pelleted, washed and frozen as described above for DH5 α .

2.1.8 Plasmid Extraction, Purification and Transformation

Single colonies bearing the plasmid of interest were inoculated into 10 mL of broth with an appropriate antibiotic overnight. This was then pelleted in a centrifuge (Universal 32R; Hettich Lab Technology, Massachusetts USA) at 4200 *xg* for 6 min. The supernatant was then discarded. Plasmid DNA was extracted from the cells via the alkaline lysis/silica binding method using a Qiagen Miniprep kit (Qiagen) according to the manufacturer's instructions. For electroporation, 2 μ L of the purified plasmid was then pipetted into an aliquot of thawed electrocompetent cells. The cells were then moved to a 2 mm gap electroporation cuvette and shocked at either 2.5 kV (DH5 α) or 2.1 kV (JR32) for 5 ms. The shocked cells were then flooded with 1 mL of LB (DH5 α) or BYE (JR32) and incubated on a rotary shaker at 37 °C and 100 rpm. Cells were left to recover for 1 (DH5 α) or 3 (JR32) hours, and were then plated on solid media with appropriate selection. Resulting single colonies were further tested by either PCR or restriction digestion to confirm transformation (Table 3).

2.1.9 SDS-PAGE

Protein samples were reconstituted in 5x Laemmli's buffer and 0.5 % β -mercaptoethanol. Samples were then placed in a dry heating block at 95 °C for five minutes, and loaded into a 1.5 mm, 12% acrylamide gel (topped with 1.5 cm of 5 % acrylamide loading gel). Gels were run at 40 mA per gel until the dye front extruded through the bottom of the plates. Gels were then used for either visualization via Coomassie staining, or transfer via western blotting.

For Coomassie Blue staining, gels were first briefly rinsed in ddH₂O and then gently agitated in Express Coomassie stain (2 g of Brilliant Blue R250 in 50 % ddH₂O, 40 % methanol and 10 % acetic acid) for 3 hours. The gels were then transferred to cleaning

Table 3: Plasmids used in this study.

Name	Resistance	Other Characteristics	Source	Reference	Notes
pBRDX	Cm, Km	<i>rdx, sacB</i>	Dr. Karen Brassinga	Brassinga <i>et al.</i> , 2006	Suicide plasmid used for recombination. Produces toxic levans in the presence of sucrose.
pMMB	Cm		Garduño Lab stock	Morales, Bäckman and Bagdasarian, 1991	General cloning plasmid in <i>L. monocytogenes</i> .
pBS SK	Amp	<i>lacZ</i>	Stratagene	Alting-Mees & Short, 1989	General cloning plasmid in <i>E. coli</i>
pMMB <i>gsk::htpB</i>	Cm	<i>gsk, htpB</i>	This study	n/a	pMMB backbone containing GSK tag fused to gene encoding HtpB
pMMB <i>gsk::legC6</i>	Cm	<i>gsk, legC6</i>	This study	n/a	pMMB backbone containing GSK tag fused to gene encoding LegC6; positive control for GSK assay
pMMB <i>gsk::mdh</i>	Cm	<i>gsk, mdh</i>	This study	n/a	pMMB backbone containing GSK tag fused to gene encoding Mdh; negative control for GSK assay
pPho-H50	Amp	<i>modified phoA</i>	This study (synthesized by IDT)	n/a	Contains a version of <i>phoA</i> with no signal peptide. Fused to a region encoding the last 100 amino acids of HtpB

Table 3: Plasmids used in this study.

pPho-H100	Amp	<i>modified phoA</i>	This study (synthesized by IDT)	n/a	Contains a version of <i>phoA</i> with no signal peptide. Fused to a region encoding the last 100 amino acids of HtpB
pMMB + HtpB6xHis	Cm		This study	n/a	Contains <i>htpB</i> with a 3' fusion to a sequence encoding six histidine residues
pBRDX- DKO	Cm, Km, Met	<i>rdx, sacB</i>	This study	n/a	Contains fragments homologous to <i>dotA</i> flanking a kanamycin resistance cassette

solution 1 (40 % ddH₂O, 50 % methanol, and 10 % acetic acid) for three hours and left in cleaning solution 2 (88 % ddH₂O, 5 % methanol, and 7 % acetic acid) overnight. Gels were then imaged in an Epson ES-1200C scanner. For western blotting, gels were placed on a nitrocellulose membrane and sandwiched with filter paper in a common “wet-blot” transfer apparatus. Power was applied at a constant 90 V for 90 min. The nitrocellulose was then removed and placed in 10 % Ponceau stain (Sigma) for 5 min. The excess Ponceau stain was washed off with ddH₂O, and the stained nitrocellulose membrane was imaged to confirm homogeneity of transfer, quality of loading, and to semi-quantify proteins by densitometry. The membrane was then de-stained in Phosphate Buffered Saline (PBS), washed in Tween-20 Tris Buffered Saline (TTBS) for 10 minutes, and placed in blocking buffer. Blocking buffer consisted of either 10 % gelatin in TTBS (for any Western Blots using the anti-6xHis antibody) or 2 % skim milk powder + 0.2 % BSA in TTBS (for all other western blots). Membranes were blocked for 1 hour, then washed three times in TTBS. Membranes were then incubated with agitation in the primary antibody (at an antibody-specific dilution; see Table 4) for two hours at room temperature. Membranes were then washed three times in TTBS, and incubated with the secondary antibody diluted in TTBS (1:1000 for AP anti-mouse; 1:5000 for AP anti-rabbit). Membranes were then washed three times in TTBS, twice in TBS, and twice in Alkaline Phosphatase (AP) buffer. Membranes were then developed in 10 mL of AP buffer containing 33 µL of NZT and 44 µL of BCIP.

2.1.10 Total Protein Quantification

Protein concentration was measured before western blotting using a Biorad Bradford assay kit (Bio-Rad Laboratories, California USA) as directed by the manufacturer.

Table 4: Antibodies used in this study

Name	Clonality	Animal Species of Origin	Target Antigen	Dilution Used for Western Blot	Source or Reference
α 6xHis	monoclonal	mouse	6x Histidine tag	1:1000	Abcam Ab18184
α HtpB	monoclonal	mouse	HtpB	1:1000	Garduño Lab
α GSK	monoclonal	rabbit	GSK	1:1000	Cell Signalling Technology #9315
α P-GSK	monoclonal	rabbit	phospho-GSK	1:1000	Cell Signalling Technology #9336
α DsbA	monoclonal	mouse	DsbA2	1:10,000	Jameson-Lee <i>et al.</i> , 2011
α ICDH	polyclonal	rabbit	Icd	1:5000	Matsuno <i>et al.</i> , 1999

Briefly, Bradford dye was diluted 1:5 in ddH₂O and 200 μ L were pipetted into each well of a 96-well microplate. Standards were generated by diluting 10 mg/mL BSA (NEB) to achieve concentrations in the 1-5 μ g/ μ L range. Ten μ L of each standard as well as 10 μ L of each sample were then pipetted into individual wells containing dye, mixed, and incubated at room temperature for five min. The microplate was then assayed for OD₅₉₅ absorbance in a Benchmark Plus Microplate Spectrophotometer (Biorad). Values for standards were plotted in Microsoft Excel to generate a formula connecting OD₅₉₅ absorbance to protein concentration. This formula was then applied to the OD₅₉₅ absorbance values of the sample to determine their concentration. If any sample appeared offscale (i.e., above 5 μ g/ μ L) it was diluted and re-assayed to bring it within the linear range of the assay.

2.2 Generation of Bacterial Strains

2.2.1 Generation of a *dotA* deletion mutant in *L. pneumophila* strain JR32

A Dot/Icm secretion mutant was created by double homologous recombination of *dotA* (*lpg2686*). A 982 base pair fragment corresponding to a region upstream of *dotA* was amplified using the primer pair P1 and P2 in a *pfx* reaction (All primers ordered from Integrated DNA Technologies, Iowa USA). This upstream region was then cut with *NotI* and *BamHI* and ligated into a pBS vector cut with the same enzymes. A 1005 base pair region corresponding to the downstream region of *dotA* was amplified using the primer pair P3 and P4 in a *pfx* reaction. This downstream region was cut with *XhoI* and *BamHI* and then ligated into the pBS vector containing the upstream region. A kanamycin resistance (Km^R) fragment flanked by *BamHI* sites was cut with *BamHI* and then inserted between the upstream and downstream regions in the pBS vector. The entire insert

(encompassing the upstream region, Km^R fragment, and downstream fragment) was then digested out of pBS using *NotI* and *XhoI*, cleaned by gel extraction, and ligated into pBRDX cut with the same enzymes. This plasmid (named pBRDX-DKO, for *dotA* knockout) was electroporated into parent strain JR32 and selected for on BCYE containing kanamycin. Once transformation had been confirmed (by PCR with Taq using primer pair P1 and P4) colonies were streaked onto BCYE containing kanamycin and sucrose. Transformants resistant to kanamycin and sucrose but susceptible to chloramphenicol were considered to have recombined native *dotA* for the flanked Km^R insert of pBRDX-DKO, and were therefore named JR32 $\Delta dotA$. To confirm the absence of native *dotA*, a PCR was performed using primer pair P5 and P6, which amplify a region internal to *dotA*.

2.2.2 Genetic Complementation of the *dotA* Deletion Mutant

The *dotA* gene was cloned from genomic JR32 DNA using a *pxf* PCR with primer pair P18 and P19. This *dotA* fragment and pMMB were then cut with *SacI* and *PstI*. The linear pMMB was gel-purified, and the *dotA* was cleaned in a PCR cleanup kit. The *dotA* fragment was then ligated into the pMMB, and the resulting plasmid was electroporated into $\Delta dotA$ JR32 to generate the complement strain.

2.2.3 Generation of JR32 Strains Carrying the GSK Reporter Construct

A recombinant gene consisting of the promoter region of *htpB* (*lpg0688*) followed by the gene region encoding for thirteen amino-acids of the eukaryotic reporter protein GSK3 β (see Garcia *et al.*, 2006) was ordered from IDT's Minigene service (IDT). This fragment was then cut with *BamHI* and *SalI* and ligated into pMMB cut with the same enzymes. The *L. pneumophila* genes *htpB*, *legC6* (*lpg1588*) and *mdh* (*lpg2352*) were then amplified

in *pfx* reactions using primer pairs P7 and P8, P9 and P10, and P11 and P12 respectively. These amplicons were then cut with *SalI* and *SphI* and ligated separately into pMMB containing the *gsk3β* fragment. This resulted in the creation of the pMMB *gsk::htpB*, pMMB *gsk::legC6* and pMMB *gsk::mdh* plasmids, which were electroporated into parent strain JR32 and sequence confirmed.

2.2.4 Generation of JR32 Strains Carrying the IcdH-HtpB C-terminal Fusion

A version of the *L. pneumophila* housekeeping (i.e., non-secreted) gene *icdH* (*lpg0816*) lacking a stop codon was generated from genomic JR32 DNA by amplification with the primer pair P13 and P14 in a *pfx* reaction. This amplicon was cut with *NotI* and *BamHI* and then ligated into pMMB cut with the same enzymes. Gene regions containing the last 50 and 100 codons of *htpB* were then amplified from genomic JR32 DNA with the primer pairs P15 and P17, and P16 and P17, respectively. These amplicons were cut with *BamHI* and *XhoI* and separately ligated into the pMMB vector containing the *icdH* insert. This resulted in the creation of the pICD-CTER50 and pICD-CTER100 plasmids, which were electroporated into JR32 and sequence confirmed.

2.2.5 Generation of a JR32 Strain Carrying a 6 x His-Tailed *htpB* Gene Construct

The *htpB* gene, including the upstream promoter region, was amplified from JR32 genomic DNA in a *pfx* PCR reaction using primer pair P25 and P26. Primer P26, the reverse primer for *htpB*, encodes a sequence which is translated into six histidine residues. This 6 x His-tagged version of *htpB* was then cut with *SphI* and *XbaI* and ligated into pMMB cut with the same enzymes.

2.3 Other Techniques Used in This Study

2.3.1 Infection of Mammalian Cells

JR32 in early stationary phase was resuspended in RPMI (containing chloramphenicol and/or IPTG when appropriate) and added to the L929 cells at an MOI of 600:1. The culture plates were then centrifuged at 200 $\times g$ for five min to promote infection of the monolayer. The infected L929 cells were then incubated at 37 °C with 5 % CO₂ for two hours to allow for translocation of *Legionella* effectors. Following this, each well was washed three times in warm PBS to remove non-internalized bacteria. One hundred μ L of 2 x Laemmli buffer (containing anti-protease and anti-phosphatase inhibitors, Sigma) was then added and wells were scraped to promote lysis.

In parallel, control wells were run to check the number of internalized bacteria.

Following the washes with PBS, these wells were incubated with RPMI containing 100 μ g/mL gentamicin for two hours. These cells were then washed three times with PBS to remove excess antibiotic. One mL ddH₂O was then added to lyse the L929 cells (but not the osmo-tolerant *Legionella*). This sample was then serially diluted in ddH₂O and plated to determine the number of internalized JR32 cells. U937-derived macrophages were infected as described above for L929 cells, with the exception that infection times of both two and four hours were tried.

2.3.2 Osmotic Shock of *L. pneumophila* and Fractionation of Soluble and Membrane-associated Proteins

Osmotic shock experiments were based on the protocol outlined by Nossal and Heppel, as modified by Gerhardt *et al.* (Nossal & Heppel, 1966; Gerhardt *et al.*, 1994). Cells were grown to early-stationary phase and then washed twice in room-temperature buffer containing 10 mM Tris and 33 mM NaCl. Cells were then resuspended in 40 mL 33 mM

Tris buffer. An equal portion of 33 mM Tris buffer containing 40 % w/v sucrose was then slowly poured into the samples with gentle agitation, resulting in a final suspension of 80 mL 33 mM Tris with 20 % sucrose. 0.1M disodium EDTA (Sigma) was added to a final concentration of 0.1mM during agitation. Cells were then pelleted at 500 xg for ten min. The supernatant was then poured off, and cells were gently resuspended in ice-cold ddH₂O containing 0.5 mM MgCl. Cells were then re-pelleted at 500 xg for ten min, and the supernatant (containing periplasmic protein) was collected. This periplasmic fraction was concentrated down to ~1 mL volume by forcing it through a 30 kDa filter (Merck Millipore) using an N₂-pressurized concentration chamber (Amersham PLC, now GE Healthcare, Mississauga ON). In parallel, the post-shockate pellet (containing cytoplasmic and membrane-bound proteins, but not periplasmic proteins) was resuspended in 500 μ L of TE buffer and sonicated (10 second bursts followed by 30 sec on ice for 10 rounds). This lysed material was loaded into an Optima MAX ultracentrifuge (Beckman-Coulter Inc., California USA) and centrifuged at 1×10^5 xg for 90 minutes. The supernatant (containing soluble cytoplasmic proteins) was then collected. The pellet (containing insoluble, envelope-bound proteins) was resuspended in TE and collected.

To confirm the purity of fractionation, samples were immunoblotted and tested using a chromogenic substrate. For the immunoblot, samples were set equal in concentration and then diluted 1/100. These samples were then run on an acrylamide gel and transferred to a nitrocellulose membrane as described above. Membranes were blotted using α DsbA (a periplasmic protein) to confirm fractionation efficiency (Figure 4). In tandem, fractionated protein samples were incubated with the chromogenic *para-*

Nitrophenylphosphate which turns yellow in the presence of alkaline phosphatase. Fifty micrograms of total protein from each fraction was incubated with 1 mg/mL of paranitrophenol in reaction buffer. The reaction was allowed to proceed for five minutes at room temperature, then each fraction was assessed for A_{405} each minute until a total reaction time of ten minutes was reached. An increase in A_{405} corresponds to alkaline phosphatase activity (Figure 4).

2.3.3 Densitometry and Statistical Analysis

Following immunoblotting of cytoplasmic, periplasmic and membrane-associated fractions using the α -ICDH antibody, membranes were imaged with an $\alpha 6000$ camera (Sony Corporation Canada, Toronto ON). The resulting images were then imported into FIJI, a variant of ImageJ (Schindelin *et al.*, 2012). Images were converted to 8-bit colour (greyscale) and densitometry was assessed using the ‘ANALYZE→GELS→PLOT LANES’ function. Densitometry values were converted into True Secretion Ratios (TSRs) using the process described in Figure 5. P-values were determined using a two-tailed, one-value student’s t-test. Values were considered significant if they differed from the assumed population mean of 0 (no secretion) at p-value <0.05.

2.3.4 Immunogold Electron-Microscopy

Bacterial samples were grown to the phase with the highest expression of the protein of interest (usually early stationary phase). Bacteria were then collected by centrifugation (Biofuge Pico model, Heraeus Germany) at 16000 xg for two min and washed twice with 0.1 M sodium cacodylate. Samples were then fixed in cacodylate buffer containing 4 % w/v freshly depolymerized paraformaldehyde for 30 minutes. The fixing solution was then eliminated with two washes in cacodylate buffer, and the samples were delivered to

Figure 4: Quality of fractionation was confirmed by western blotting and enzymatically. (A) The Cytoplasmic (labeled C), Periplasmic (labeled P) and envelope-associated (labeled M) fractions from the IcdH100 shockate experiment were diluted 1/100 and run in an acrylamide gel. Samples were then transferred to a membrane and run against α DsbA. The resulting band corresponding to DsbA (~27kDa) was stronger in the periplasm than the other two fractions, confirming that the techniques used result in proper fractionation. (B) Graphical plot of the A_{405} of the three fractions from both Icd50 and Icd100 (Icd fused with the last 50 or 100 amino acids of HtpB) shockate experiments during incubation with paranitrophenol. ~50 μ g of total protein from each fraction was incubated with 1 mg/mL of p-nitrophenol in reaction buffer. The reaction was allowed to proceed for five minutes at room temperature, then each fraction was assessed for A_{405} each minute until a total reaction time of ten minutes was reached. An increase in A_{405} corresponds to alkaline phosphatase activity. As the vast majority of this activity was found in the membrane and periplasm fractions, fractionation was confirmed.

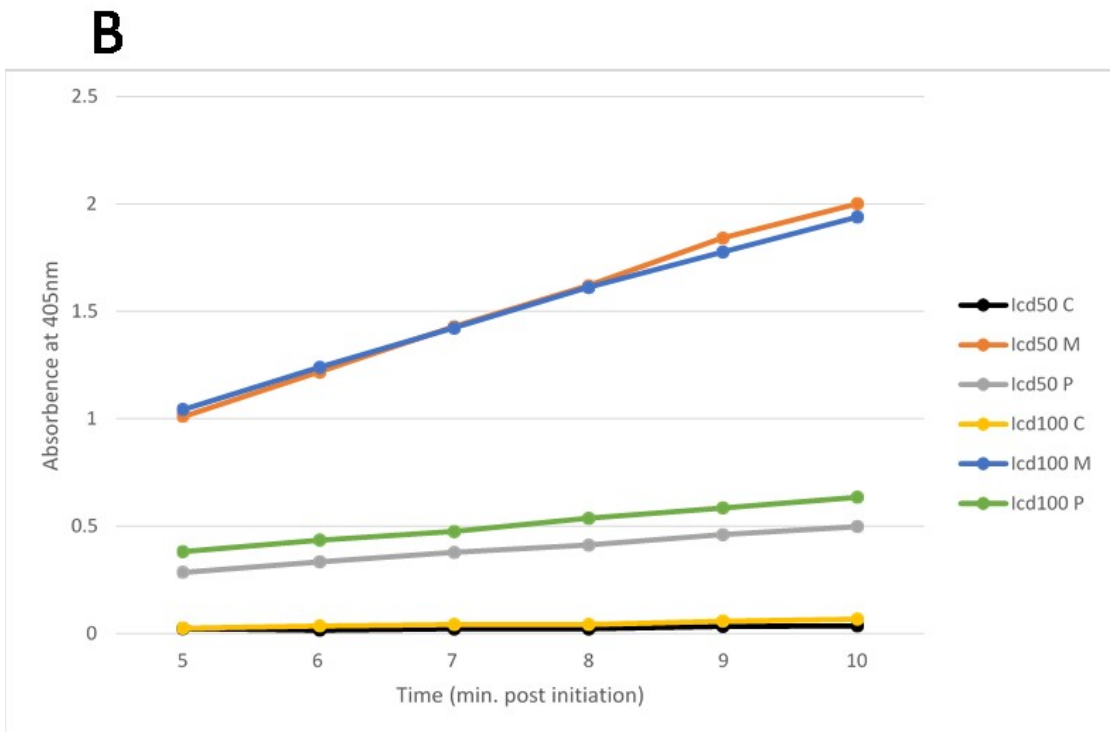
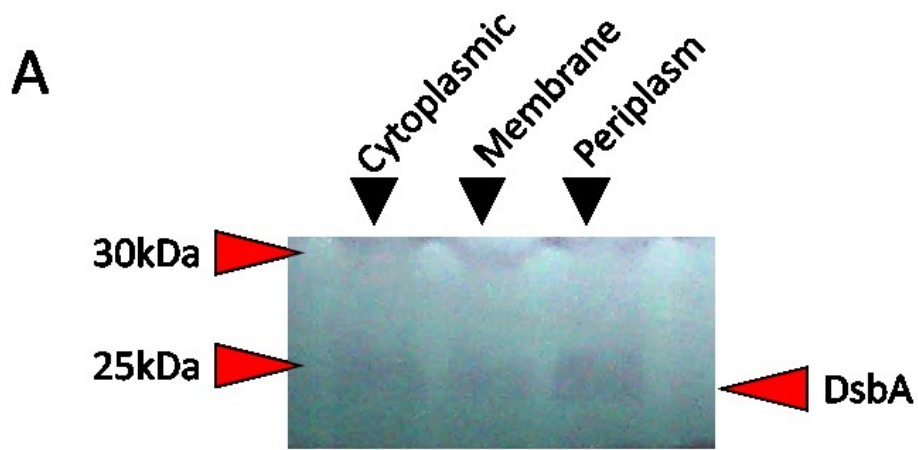
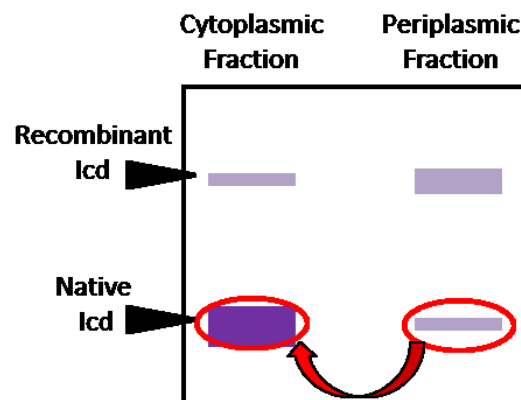


Figure 5: A graphical representation of the formula used to determine the TSR values from densitometric western blotting. (A) The formula used to determine the TSR values of periplasmic and membrane-associated recombinant Icd. (B) A graphical representation of how TSR values are derived from a western blot. The native and recombinant Icd (purple bands) present in the cytoplasmic, periplasmic, and membrane-associated (omitted) fractions were quantized densitometrically using FIJI and the resulting values were processed according to the steps listed. Red circles and arrows indicate which physical bands were mathematically processed during each step of the formula to generate TSR values.

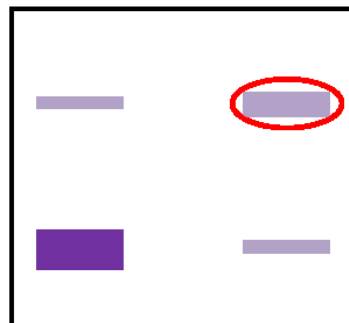
$$\text{TSR} = [(\text{HPS}/\text{ACS}) - 1] * 100$$

Where: $\text{HPS} = (\text{Recombinant Icd Density in Periplasm}) * [(\text{Native Icd density in Cytoplasm}) / (\text{Native Icd density in Periplasm})]$

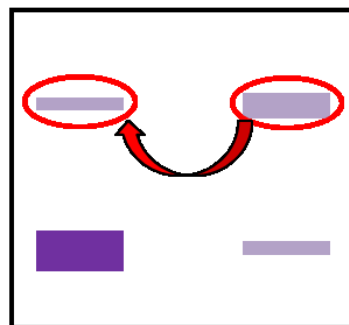
And $\text{ACS} = (\text{Recombinant Icd Density in Cytoplasm})$



1. Divide native cytoplasmic density by native periplasmic density to determine ratio



2. Multiply periplasmic recombinant density by the ratio in step 1. This describes how much periplasmic recombinant Icd would exist if the Native Icd in the cytoplasmic and periplasmic fractions were equal.



3. Divide normalized periplasmic recombinant fraction (derived in step 2) by cytoplasmic recombinant fraction. This number represents the extent to which the periplasmic Icd density is more or less prevalent than expected through lysis alone.

Mary-Ann Trevors (Electron Microscope core facilities, Dalhousie University) for embedding (in LR white resin), sectioning, and mounting on nickel grids. Grids with mounted ultrathin sections were then floated sequentially on drops of 1 mg/mL sodium borohydride for 10 minutes, 30 mM glycine in borate buffer (10 mM sodium borate, 150 mM sodium chloride, pH 9.6) for 10 min, and blocking solution (1 % skim milk and 1 % BSA in TBS) for 45 min. Grids were then briefly washed in TBS and incubated with primary antibody (1:50 dilution in TBS) overnight at 4°C. Grids were then washed three times in washing buffer (10 mM Tris, 0.3 M sodium chloride, pH 8.1) and incubated with the secondary antibody (1:50 dilution, room temperature) for one hour. Grids were again washed three times in washing buffer and then fixed in cacodylate buffer containing 2.5% w/v glutaraldehyde for 15 minutes. Grids were then washed in ddH₂O for three minutes three times, dried, and imaged in a JEOL 1230 model transmission electron microscope (JEOL Ltd, Tokyo Japan). All photos were taken at 60,000x magnification using a Hamamatsu ORCA-HR camera (Hamamatsu Photonics, Japan) and an acceleration voltage of 80 kV.

2.3.5 Resistance-to-salt Testing

The salt testing protocol was adapted from Li *et al.*, 2010 which was itself based on Byrne & Swanson, 1998. Bacterial strains undergoing salt testing were grown to early stationary phase (OD₆₀₀ of 2.0). Strains were then serially diluted in water to create a range of samples from 10⁻⁴ to 10⁻⁹. Twenty µL of each sample was then spotted onto BCYE and BCYE+100 mM NaCl (parent strain JR32 and $\Delta dotA$ JR32) or onto BCYE+Cm⁵ and BCYE+Cm⁵+100 mM NaCl (complemented $\Delta dotA$ JR32 and vector control $\Delta dotA$ JR32). Plates were then incubated for three days and imaged.

2.3.6 Testing for AP Activity

Sixty $\mu\text{g/mL}$ of BCIP was added to LB or Modified M9 agar following autoclaving. The media were then poured and allowed to solidify as normal. Strains being tested were allowed to grow to an OD_{600} of 1.0 in liquid LB and were then spotted in 20 μL drops on the media containing BCIP. Cultures were grown at 37°C overnight and photographed. Formation of blue coloured colonies was considered indicative of AP activity.

3. Results

Part I: Translocation of HtpB to the cytoplasm of *L. pneumophila*-infected cells relies on a functional Dot/Icm system

3.1 HtpB has some, but not all, markers of a Dot/Icm effector

3.1.1 HtpB does not have the hydrophobicity index of a Dot/Icm effector

As Dot/Icm effectors are known to generally possess either a hydrophobic residue or a proline at the -3 or -4 position relative to the C-terminus, HtpB was evaluated for this criteria. Both the -3 and -4 residues in HtpB are glycine, a mildly hydrophilic amino acid (-0.4 on the Kyte-Doolittle scale), meaning that HtpB does not meet this criterion for a Dot/Icm effector. However, the glycines are flanked by methionine, a moderately hydrophobic amino acid (+1.9 on the Kyte-Doolittle scale). Whether or not this can compensate for the lack of hydrophobic residues at positions -3 and -4 is unknown at this point, mainly because the reason why these residues tend to be hydrophobic in Dot/Icm effectors has yet to be determined.

3.1.2 HtpB does not possess amino acid enrichments characteristic of a Dot/Icm effector

HtpB was evaluated for amino acid enrichments known to be associated with Dot/Icm effectors. HtpB was not found to be enriched in negatively charged amino acids at positions -8 to -18, or to be depleted of these residues at -1 to -6. The protein was also not depleted of hydrophobic amino acids at -8 to -12, and no enrichment of serine or threonine was present at -3 to -11. HtpB therefore does not possess the amino acid profile associated with Dot/Icm effectors (Figure 6).

3.1.3 HtpB has a degenerate E-block motif

The C-terminus of HtpB was examined for an E-block motif, meaning a chain of glutamic acid residues usually followed by isoleucine and/or valine, associated with Dot/Icm effectors. HtpB was found to possess two glutamic acid residues followed by a valine just outside of the canonical -10 to -17 position (Figure 6). While this is small for an E-block motif (which generally have three to five glutamic acid residues) it may indicate a semi-functional or degenerated motif.

3.2 HtpB has sequence similarity to several known Cell Penetrating Peptides (CPPs)

The sequence of HtpB was examined for homology to CPPs using a BLAST assay against a library of ~1800 known CPPs (Gautam *et al.*, 2012; Agrawal *et al.*, 2016; <http://www.imtech.res.in/raghava/cppsite/index.html>). HtpB had weak similarity to several CPPs, including SR6 (a synthetic modification of the CPP pVEC; Rajpal, Khanduri, Naik & Ganguli, 2012) and LL-37 (a human anti-microbial peptide; reviewed in Durr, Sudheendra & Ramamoorthy, 2006) and Inv3.7 (a small portion of the MceA1 protein in *M. tuberculosis* responsible for translocation of the MceA1 into the cytoplasm of *Mycobacterium*-infected host cells; Lu, Tager, Chitale & Riley, 2006) (Figure 7).

3.3 Translocation of a GSK tagged HtpB

3.3.1 A *dotA* deletion mutant was created and complemented *in-trans*

The *dotA* gene of JR32 was interrupted by the process outlined in Figure 8. Successful knockout was confirmed genetically by PCR (using primer pair P5 and P6) against an internal region of *dotA*. Parent strain JR32 exhibited amplification, whereas neither of the $\Delta dotA$ strains tested did, suggesting that *dotA* was successfully replaced (Figure 9). All strains were capable of amplifying a region internal to *enhA* (a housekeeping gene; tested

Figure 6: HtpB does not possess most amino acid characteristics of a typical Dot/Icm effector. A diagram of several key areas of the C-terminus of HtpB reveal that it does not possess many of the traits associated with known Dot/Icm effectors such as SidM. Residues that correspond to Dot/Icm effector traits are highlighted in blue, while residues that contradict these traits are highlighted in red.

	HtpB	SidM
Enriched in negative residues (-8 to -18)	GAGDMGGMGGM	EETRESIKSQE
Depleted in negative residues (-1 to -6)	GMGGMM	QTIKIK
Depleted in hydrophobic residues (-8 to -12)	GMGGM	IKSQE
Enriched in Ser/Thr residues (-3 to -11)	MGGMGGMGG	KSQERQTIK

Figure 7: HtpB displays sequence similarity to several known Cell-Penetrating Peptides. A BLAST search of the entire HtpB amino acid sequence against a library of ~1800 known CPPs (Gautam *et al.*, 2012; Agrawal *et al.*, 2016) revealed areas of HtpB with similarity to many CPPs, including S6R, Inv3.7 and LL-37 (similar sequences highlighted in blue). CPP sequences are given in full, while HtpB segments are labeled by amino acid number from the N-terminus. E-values correspond to the expect value for the BLAST search.

Identity	Sequence	E-Value
HtpB LL-37	168 EKVGE + LLGDFFRKSKEKIGKEFKRIVQRIKDFLRNLPRTESC 173	4.8
HtpB Inv3.7	321 KRIVVTKENTTIIDGEGKATEINA + + + TKRRITPKDVIDVESVTEINT 345	6.3
HtpB S6R	442 NILRRAIESPMRQ LLHILRRSIR—RQAHAIRR 454	0.34

Figure 8: Diagram showing the sequential steps followed to construct the knockout vector used to create the $\Delta dotA$ mutant. (A) Based on the DNA sequence of the *dotA* locus obtained from NCBI the *dotA* upstream (US) and downstream (DS) regions were amplified by PCR. The purple box represents the *dotA* open reading frame and the black lines at the sides of this box represent the flanking chromosomal regions, upstream to the left and downstream to the right. The green triangles indicate the relative position (not to scale) of the forward and reverse primers used to generate the *dotA* upstream region amplicon (box labeled *dotA* US). The yellow triangles indicate the relative position (not to scale) of the forward and reverse primers used to generate the *dotA* downstream region amplicon (box labeled *dotA* DS). (B) Construction in plasmid pBlueScript (pBS) of the knockout vector intermediate. The *dotA* US and *dotA* DS amplicons were ligated to the km^R kanamycin resistance cassette (in red) using the restriction sites indicated by the black arrowheads. (C) The knockout vector intermediate was subcloned in plasmid pMMB207c (pMMB) using the restriction sites XhoI and NotI, to generate the knockout vector used for the allelic replacement of the *L. pneumophila* wild-type *dotA* chromosomal gene. The two recombination events required for the allelic replacement are represented by the two sets of crossing dotted lines.

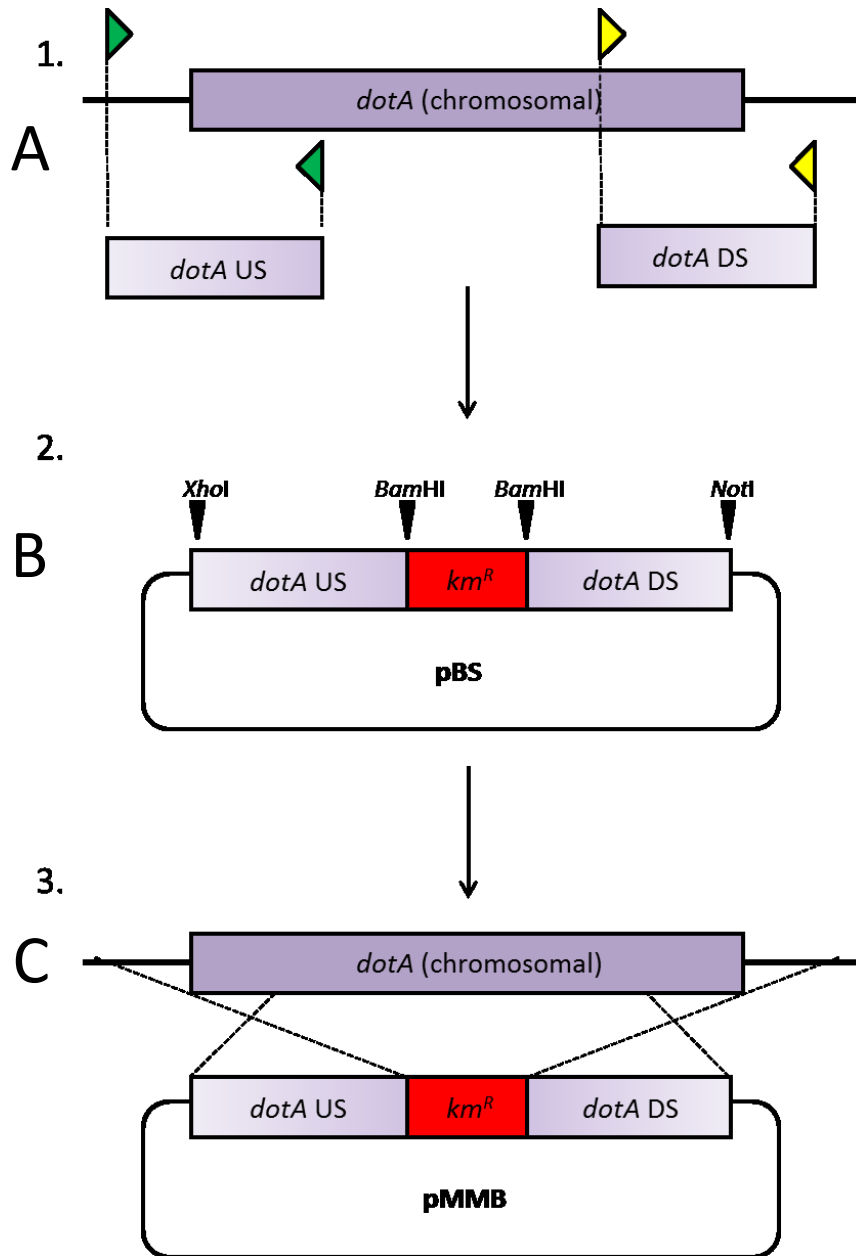
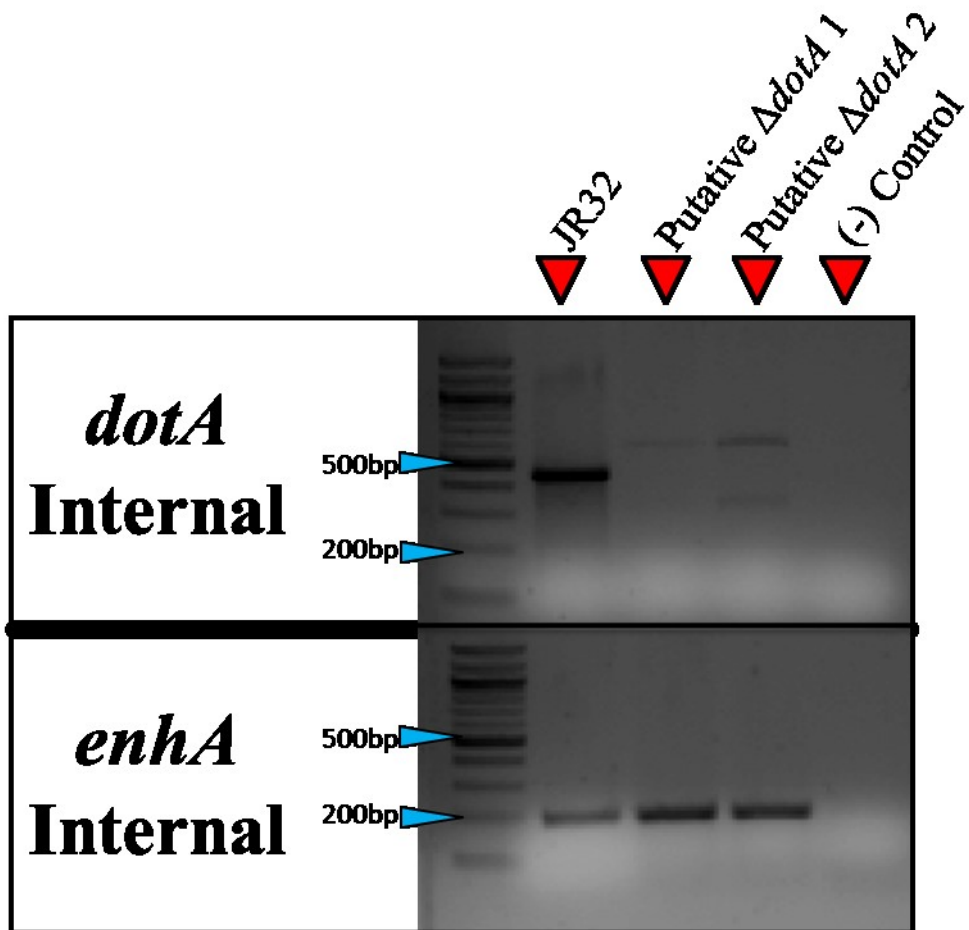


Figure 9: Agarose gels of a PCR for *dotA* and a control gene in parent strain JR32 and two $\Delta dotA$ mutants. A 30-cycle amplification of a 400bp region internal to *dotA* was performed on genomic DNA from parent strain JR32 as well as two putative $\Delta dotA$ mutants and a negative (no DNA template) control. These samples were run on a 1.0% agarose gel for thirty minutes to assess the PCR results, with a 100bp DNA ladder (NEB N3231) run for size analysis (darker bands correspond to 500bp and 1kbp). PCR confirmed the presence of the region in the parent strain as indicated by an amplified DNA fragment of ~400 base pairs, which was absent in both mutants. PCR to amplify a region internal to *enhA* (a housekeeping gene) resulted in positive DNA bands for all strains, demonstrating the ability of all DNA samples to support PCR reactions.



with primer pair P27 and P28), demonstrating that the absence of a *dotA* PCR product was not due to a lack of DNA in the mutant samples (Figure 9). As both mutant strains seemed equally correct, strain 1 was chosen for further experimentation, and is hereafter referred to as strain $\Delta dotA$. The $\Delta dotA$ mutant was then complemented in trans with pMMB containing the *dotA* gene of JR32.

To test the mutant and complement strains phenotypically, they were subjected to the salt test. Growth of stationary phase *L. pneumophila* is greatly inhibited by the presence of sodium, but only when the Dot/Icm system is functional. Parent strain JR32 was significantly inhibited in growth by the presence of 100 mM NaCl compared to $\Delta dotA$, indicating that the mutant exhibits salt tolerance typical of a Dot/Icm mutant (Figure 10). Complementation restored sensitivity to NaCl compared to a vector control ($\Delta dotA$ transformed with empty pMMB) (Figure 11), indicating a functional Dot/Icm system. In addition to the salt test, the mutant was tested phenotypically by infecting a monolayer of *A. castellanii*. Parent strain JR32, the Δdot mutant, and a Δdot strain complemented with pMMB::*dotA* were grown to early stationary phase ($OD_{600} \sim 2$) and used to infect amoeba monolayers at an MOI of 100:1. Following 16 hours of incubation at 37 °C, the parent strain JR32 and complement strains had caused significant rounding and lysis to the amoebae, while the amoebae infected with Δdot remained relatively unchanged (Figure 12).

To ensure that all strains grew equally, parent strain JR32, the Δdot mutant, and the Δdot complement strain were inoculated at OD_{600} of 0.05 and grown for 20 hours. OD_{600} was recorded every hour (Figure 13; some early values not shown). No significant differences in growth were detected.

Figure 10: Pictures of BCYE plates showing the growth patterns of the *L. pneumophila* parent strain JR32 and its Δ dotA derived mutant in the presence or absence of sodium chloride. Pictures were taken 72 hours after spotting 20 μ L of a series of dilutions from a bacterial suspension of \sim 2 OD. The dilutions spotted are indicated at the top of the figure, where the value of “x” is given in the second top row. It is known that Na⁺ inhibits the growth of virulent *L. pneumophila*, whereas non-virulent Dot/Icm mutants are salt-tolerant. The BCYE plate at the bottom contains 100 mM NaCl. The top two rows of spots on each plate correspond to the parent strain (JR32) and the bottom two rows to the Δ dotA mutant (each dilution was spotted in duplicate).

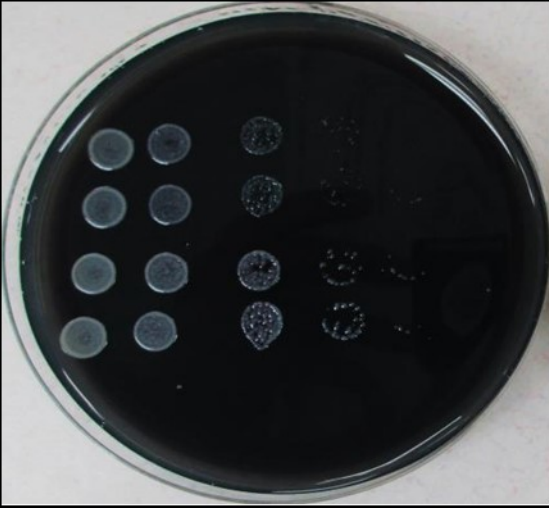
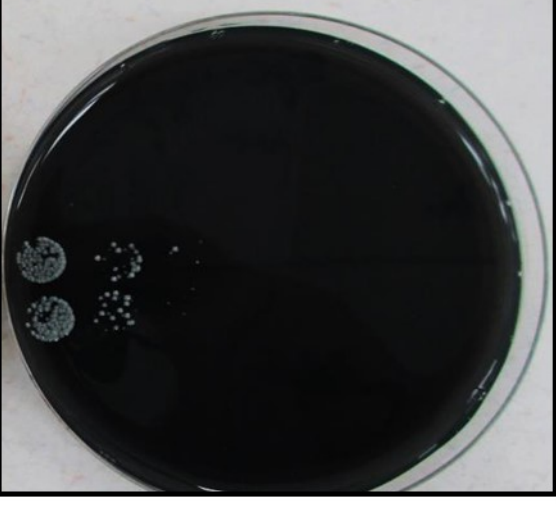
		Dilution (10 ^X)				
		-5	-6	-7	-8	-9
BCYE	<i>ΔdotA</i>					
	JR32					
BCYE + 100mM NaCl	<i>ΔdotA</i>					
	JR32					

Figure 11: Pictures of BCYE plates showing the growth patterns of the *L. pneumophila* $\Delta dotA$ mutant complemented in trans with pMMB::*dotA* and a vector control consisting of $\Delta dotA$ containing empty pMMB in the presence or absence of sodium chloride. Pictures were taken 72 hours after spotting 20 μ L of a series of dilutions from a bacterial suspension of ~ 2 OD. The dilutions spotted are indicated at the top of the figure, where the value of “x” is given in the second top row. It is known that Na⁺ inhibits the growth of virulent *L. pneumophila*, whereas non-virulent Dot/Icm mutants are salt-tolerant. The BCYE plate at the bottom contains 100 mM NaCl. The top two rows of spots on each plate correspond to the parent strain (JR32) and the bottom two rows to the $\Delta dotA$ mutant (each dilution was spotted in duplicate).

		Dilution (10 ^X)					
		-4	-5	-6	-7	-8	-9
BCYE + Cm5	Vector Control						
	<i>dotA</i> Complement						
BCYE + Cm5 + 100mM NaCl	Vector Control						
	<i>dotA</i> Complement						

Figure 12: Light micrographs of *A. castellanii* following sixteen hours of infection with parent strain, *dotA* deletion mutant, and *dotA* complemented *L. pneumophila*. Monolayers of *A. castellanii* were infected with parent strain JR32, $\Delta dotA$ deletion mutants, *dotA* complement, or nothing (uninfected controls) at an MOI of 100:1 and incubated for 16 hours. *A. castellanii* in the uninfected control and $\Delta dotA$ groups display healthy phenotypes (adherent trophozoites, at high density and with an irregular amoeboid outline), whereas those in the parent strain and *dotA* complement groups display phenotypes indicative of severe infection (detachment of trophozoites [floating cells], low density [suggesting lysis of trophozoites], and obvious change in morphology [rounding]). Scale bars all 100 μm .

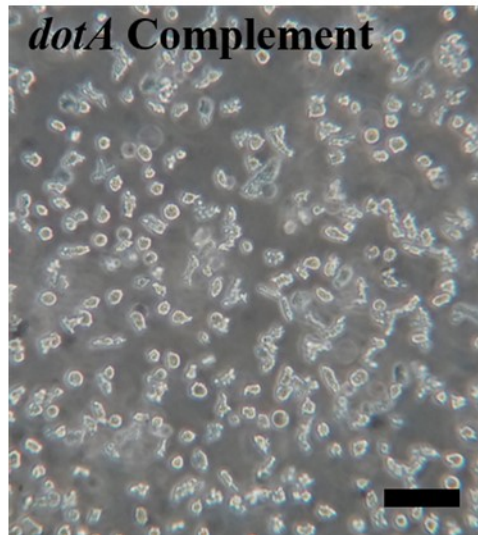
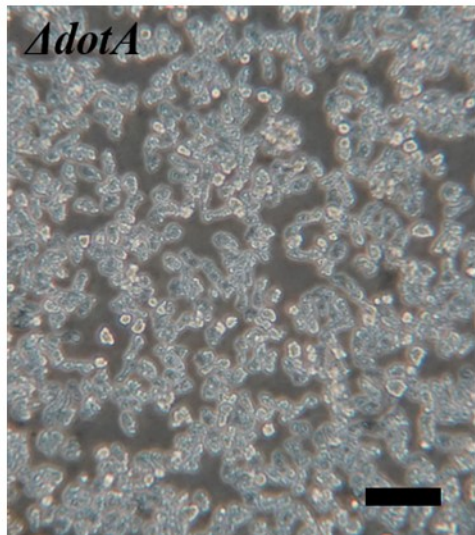
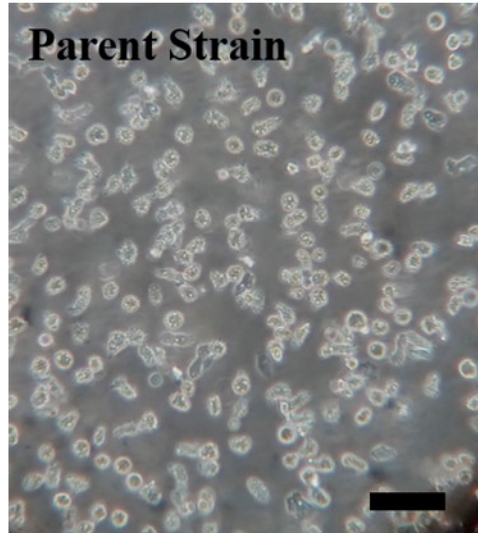
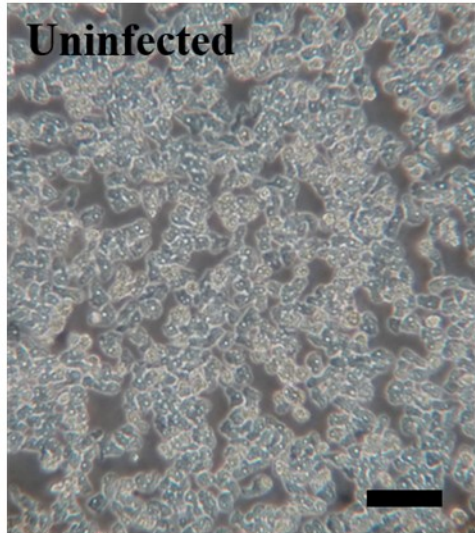
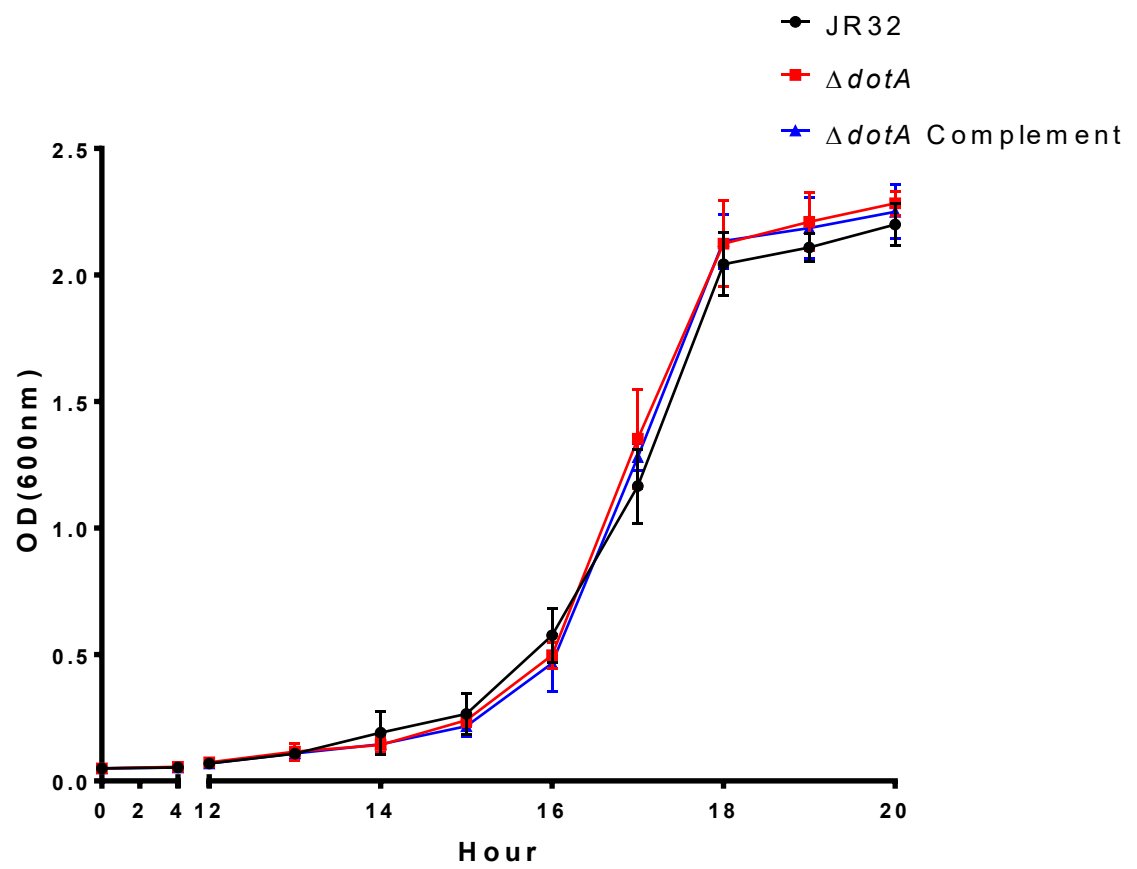


Figure 13: Growth curves of parent strain, *dotA* deletion mutant, and *dotA* complemented *L. pneumophila*. Parent strain JR32 (black), $\Delta dotA$ deletion mutants (red), and *dotA* complement (blue) *L. pneumophila* were incubated in BYE for 20 hours and OD₆₀₀ was measured each hour. Error bars correspond to standard deviation of three replicates.



3.3.2 HtpB and appropriate controls were tagged with GSK

The gene products of *legC6* (*lpg1588*, encoding a secreted effector), *mdh* (*lpg2352*, encoding a non-secreted metabolism protein) and *htpB* (*lpg0688*, encoding the protein of interest) were tagged with small GSK fragments as depicted in Figure 14. The resulting strains were termed WT-G-LegC6, WT-G-Mdh, WT-G-HtpB (for constructs transformed into parent strain JR32), Δ -G-LegC6, Δ -G-Mdh and Δ -G-HtpB (for constructs transformed into a *ΔdotA* background). To confirm expression of the GSK-tag, western blots were run on lysates of all strains using α -GSK and α -pGSK antibodies. As expected, all recombinant proteins resulted in a band when incubated with α -GSK but not with α -pGSK, indicating that the GSK tags are expressed, and are not phosphorylated in *L. pneumophila* (Figure 15).

3.3.3 GSK tagged HtpB is not phosphorylated in a Dot/Icm mutant

To test whether or not HtpB is translocated during infection, all GSK tagged strains were used to infect L929 mouse fibroblast cells. Following infection, lysates were extracted and immunoblotted to determine the phosphorylation status of the GSK tag. The GSK tags of all three proteins (LegC6, Mdh and HtpB) in both backgrounds (parent strain and *Δdot*) were picked up using α -GSK antibody, indicating that all recombinant proteins were expressed and recoverable by this procedure (Figure 16). When using the α -pGSK antibody, the LegC6 band (the positive control) reacts in the parent strain but not the *Δdot* strain. The MDH band (the negative control) does not react in either background. Like LegC6, HtpB reacts in the parent background but not in the *Δdot* background, confirming that HtpB is reliant on a functional Dot/Icm system for its translocation to the cytoplasm

Figure 14: Diagram describing the cloning procedures to generate GSK fusion proteins. The *gsk* construct (light blue; consisting of the promoter region of *htpB* followed by the sequence encoding the GSK tag) was synthesized by IDT's geneblock service and possessed *Bam*HI and *Sal*I flanking cut sites. The *gsk* construct was cut with these flanking cut sites and ligated into pMMB upstream of an *Sph*I site. Genes encoding for the positive, negative and test proteins (*legC6* in orange, *mdh* in purple and *htpB* in light red, respectively) were amplified by PCR to have *Sal*I and *Sph*I cloning sites. The target genes were then cut with *Sal*I and *Sph*I and ligated into the pMMB::*gsk* construct to generate the *gsk* fusion genes.

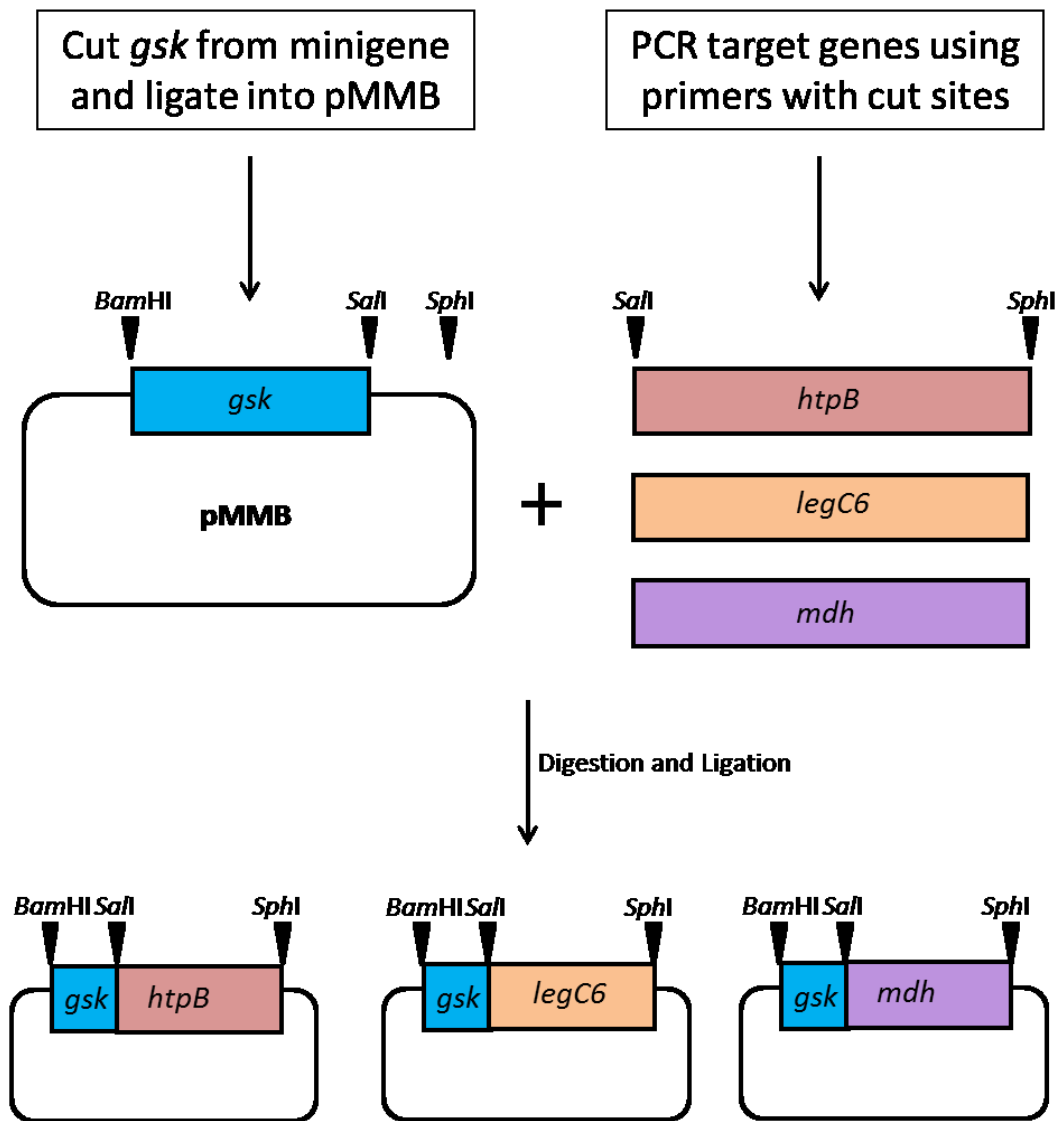


Figure 15: Immunoblots of lysed JR32 strains carrying *gsk* constructs reveal that the GSK tag is not phosphorylated by *L. pneumophila*. (A) Lysates of control parent strain JR32, as well as parent strain and Δdot JR32 carrying a plasmid encoding for the GSK-tagged version of HtpB, were immunoblotted using α GSK. Both strains encoding the plasmid developed bands corresponding to HtpB-GSK, whereas the control JR32 (which was loaded at a higher level of protein) developed only an irrelevant band at ~ 27 kDa. (B) Lysates of control parent strain JR32, as well as parent strain and Δdot JR32 carrying a plasmid encoding for the GSK-tagged version of HtpB, were immunoblotted using α -P-GSK. No bands were developed. Loading controls correspond to Ponceau stains of the actual membranes shown.

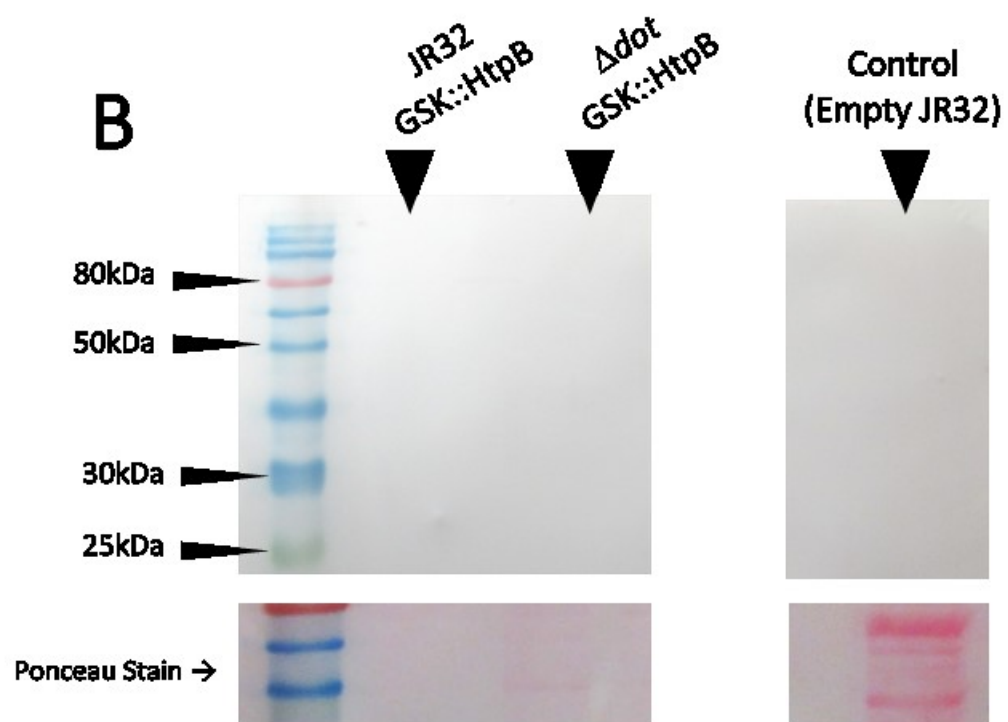
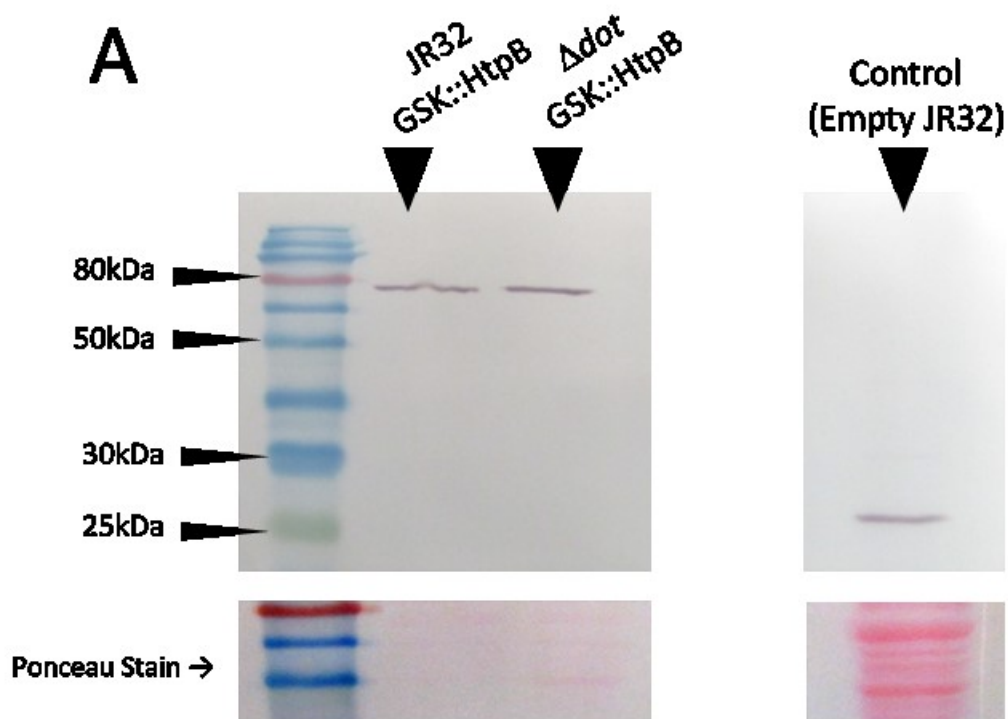


Figure 16: A western blot of lysates recovered following an infection of L929 cells by parent strain JR32 and the $\Delta dotA$ mutant expressing HtpB-GSK, LegC6-GSK and Mdh-GSK. L929 cells were infected by these strains at an MOI of 600:1, and infection was allowed to proceed for two hours. Samples were then lysed by boiling in Laemmli's buffer and run on a 12% polyacrylamide gel. Samples were transferred to a membrane and a western blot using α -GSK was performed to confirm the presence and expression of all GSK-tagged constructs. Bands developed corresponding to GSK-tagged HtpB, LegC6 and MDH (red boxes), confirming that all constructs are well expressed and recovered by the infection protocol in both the parent and $\Delta dotA$ strains. Molecular weight in kilodaltons indicated left (red arrows), based on the running pattern of Colorplus Prestained Protein Ladder, Broad Range (NEB P7712).

**Parent
JR32**

**$\Delta dotA$
JR32**

HtpB-
Gsk
▼

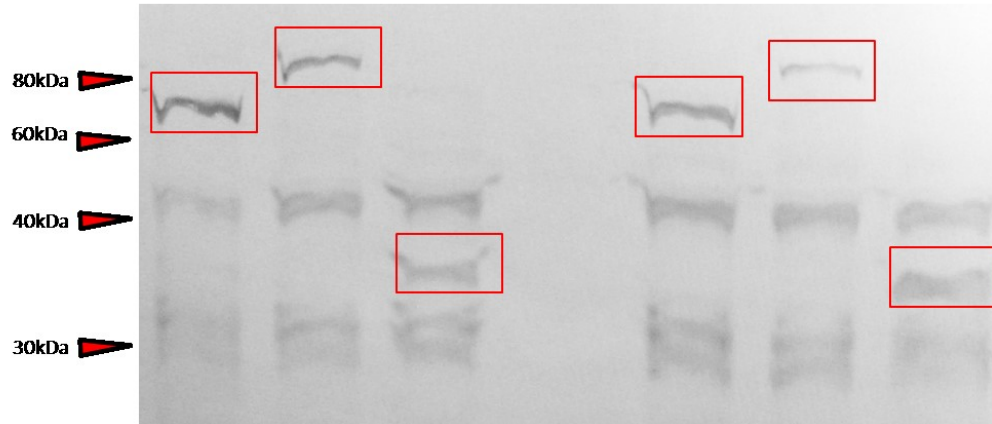
LegC6-
Gsk
▼

MDH-
Gsk
▼

HtpB-
Gsk
▼

LegC6-
Gsk
▼

MDH-
Gsk
▼



of host cells (Figure 17). An attempt was made to conduct the same experiment in U937-derived human macrophages, however native U937 proteins obscured results and made the results uninterpretable (Figure 18).

Part II: The C-terminus of HtpB is involved in its translocation across the inner membrane of *L. pneumophila*

3.4 Adding the C-terminus of HtpB to a non-secreted form of PhoA does not restore its translocation to the periplasm

A version of *phoA* lacking the region encoding a secretion signal peptide was obtained commercially as a G-block (IDT). The gene encoding this non-secreted PhoA was then tagged (at the 3' end, corresponding to the C-terminus) with a region encoding the last 50 or 100 amino acids of the C-terminus of HtpB. The recombinant, plasmid-borne versions of *phoA* were then transformed into *phoA* KO *E. coli*. Since PhoA only has alkaline phosphatase activity after it has entered the periplasm, the PhoA-H100 strain was plated onto LB supplemented with BCIP to assess whether the HtpB tail could restore translocation of PhoA. While the PhoA + BL-21 strain of *E. coli* developed the blue colour associated with alkaline phosphatase activity, neither the PhoA-H100 nor *phoA*-KO strains developed colour (Figure 19). This indicates that the HtpB tail was not able to restore translocation of PhoA across the inner membrane.

To rule out the possibility that a component of the LB medium was responsible for the alkaline phosphatase activity (or lack thereof) the test was repeated identically on modified M9 medium (see Appendix). Results were identical to those from the LB test, with BL-21 turning blue and the PhoA-H100 and *phoA*-KO strains staying white (Figure 19).

Figure 17: A western blot of lysates recovered following an infection of L929 cells by parent strain JR32 and the $\Delta dotA$ mutant expressing HtpB-GSK, LegC6-GSK and Mdh-GSK. L929 cells were infected by these strains at an MOI of 600:1, and infection was allowed to proceed for two hours. Samples were then lysed by boiling in Laemmli's buffer and run on a 12% polyacrylamide gel. Samples were transferred to a membrane and a western blot using α -p-GSK was performed to test whether or not the GSK-tagged constructs had been translocated into host cells. LegC6-GSK (the positive control) and HtpB-GSK were found to be phosphorylated in parent strain JR32 but not in $\Delta dotA$. MDH-GSK (the negative control) was not phosphorylated in either background. Red boxes correspond to the expected locations of the GSK constructs. Molecular weight in kilodaltons indicated left (red arrows), based on the running pattern of Colorplus Prestained Protein Ladder, Broad Range (NEB P7712).

**Parent
JR32**

***ΔdotA*
JR32**

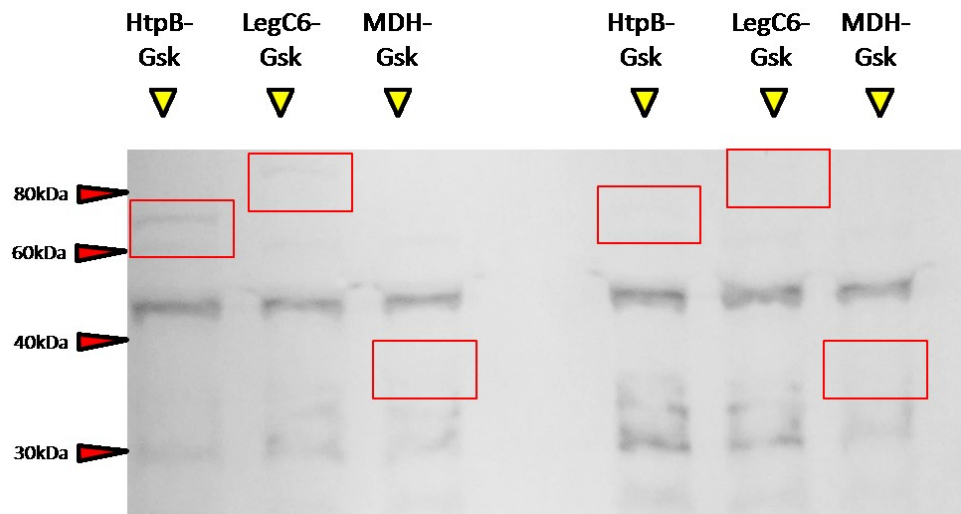


Figure 18: A western blot of lysates recovered following an infection of U937 cells by parent strain JR32 and the $\Delta dotA$ mutant expressing HtpB-GSK, LegC6-GSK and Mdh-GSK. U937-derived macrophages were infected by these strains at an MOI of 600:1, and infection was allowed to proceed for four hours. Samples were then lysed by boiling in Laemmli's buffer and run on a 12% polyacrylamide gel. Samples were transferred to a membrane. western blots were performed on samples recovered from the infection assay. (A) incubation with α -GSK reveals that although HtpB-GSK and MDH-GSK are expressed and recoverable (red boxes), LegC6-GSK is obscured by cross-reaction with a high molecular weight U937 protein (black boxes). (B) incubation with α -p-GSK reveals that no GSK construct gives a signal strong enough to detect, except possibly MDH-GSK, which is again obscured by cross-reactive U937 proteins (red boxes correspond with expected location of GSK constructs). Molecular weight in kilodaltons indicated left (red arrows), based on the running pattern of Colorplus Prestained Protein Ladder, Broad Range (NEB P7712).

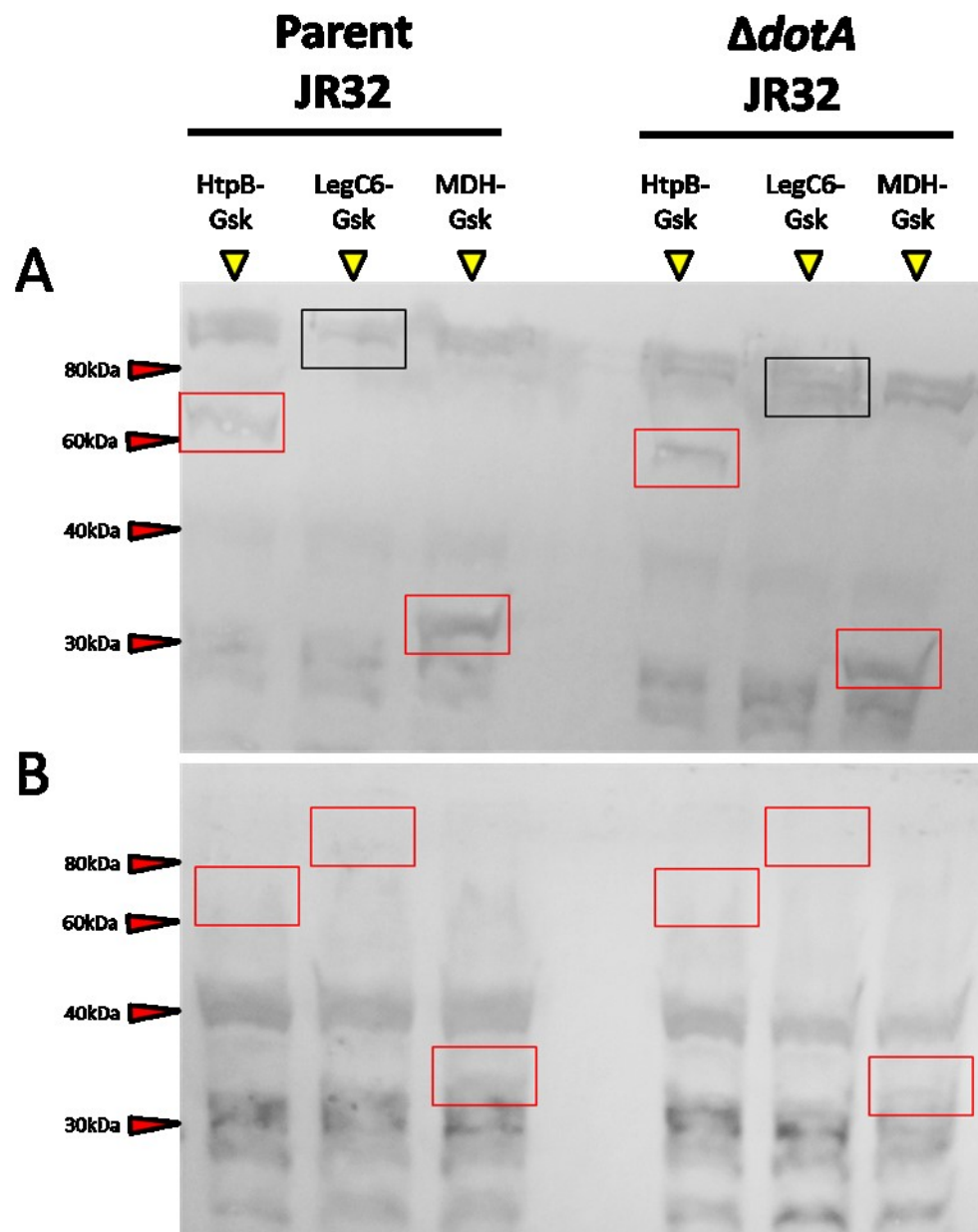
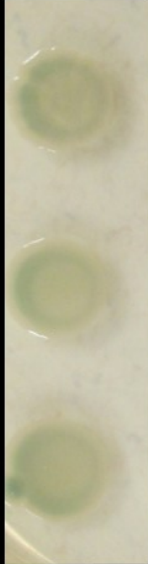




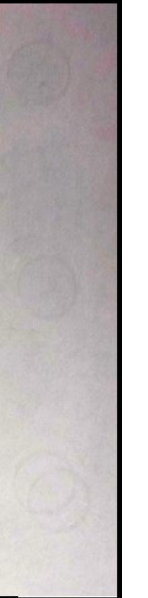


Figure 19: Images of BL21, and *phoA* KO *E.coli* carrying recombinant *phoA* with an HtpB ‘tail’, incubated on agar containing a chromogenic substrate which assays alkaline phosphatase activity. The *phoA::htpB50* and *phoA::htpB100* strains are *phoA* KO *E.coli* that have been transformed with pMMB carrying recombinant *phoA*. This recombinant *phoA* has been modified to lack a secretion signal, and to encode the last 50 or 100 amino acids of the C-terminal region of HtpB. Twenty μL of a liquid bacterial culture at $\sim 1 \text{ OD}_{600}$ was spotted in triplicate on LB and M9 media containing 40mg/mL of BCIP. Blue coloration indicates alkaline phosphatase activity, which only occurs when *phoA* reaches the periplasm. Media type is indicated in top box, strains are indicated at left.

	LB + Cm20	Modified M9
Pho+ Control		
<i>phoA::</i> <i>htp50</i>		
<i>phoA::</i> <i>htp100</i>		

3.5 Post-osmotic shock fractionation of soluble and insoluble proteins indicates that the HtpB C-terminus associates with the *L. pneumophila* envelope

Recombinant proteins were generated by PCR/restriction digestion such that the gene coding for isocitrate dehydrogenase (*icd*, *lpg0816*) was tagged with a gene region encoding the last 50 or 100 amino acids of the HtpB C-terminus. These recombinant genes were mobilized on pMMB and transformed separately into parent strain JR32 to generate the strains IcdH50 and IcdH100 (Figure 20). These strains were subjected to the osmotic shock procedure in order to separate sub-cellular fractions. The fractions were then western blotted with α -Icd and evaluated by densitometry to determine the sub-cellular localization of Icd (Figure 21). By evaluating the True Secretion Ratio (the percentage of recombinant Icd found in the membrane or periplasmic fractions that cannot be explained by cell lysis; see Materials and Methods) it was determined that recombinant IcdH-50 and IcdH-100 protein localize to the membrane fraction (TSRs of 0.814 and 0.754, p-values <0.05). In the periplasmic fraction, the recombinant Icd-100 protein is found to a greater extent than can be explained by lysis alone (TSR of 0.139, p-value <0.05) but the Icd-50 protein is not (TSR of 0.126, p-value 0.14) (Figure 22).

To determine the quality of fraction separation, western blotting and enzymatic assays were carried out on the three fractions. In western blotting, the cytoplasmic, membrane and periplasmic fractions were set equal by Bradford assay and diluted 1:10, 1:100 and 1:500 on an acrylamide gel. Following transfer, the membrane was developed with α -DsbA antibody (Table 4).

3.6 Immunogold microscopy indicates that the C-terminus of HtpB is involved in determining the sub-cellular localization of HtpB

3.6.1 Blocking the C-terminus results in a Cytoplasmic build-up of HtpB

Figure 20: Recombinant *icdH* with an *htpB* ‘tail’ is expressed at the protein level in JR32. A western blot using α -IcdH was performed on parent strain JR32, as well as two strains carrying recombinant *icd* (designed to express a C-terminal fusion of the last 50 or 100 amino acids of HtpB). As expected, the parent strain only developed one band at the expected molecular weight of IcdH (predicted to be ~47kDa) whereas the recombinant strains expressed parent strain IcdH as well as recombinant IcdH. Recombinant IcdH is of noticeably higher molecular weight due to the addition of the tail at the C-terminus. Molecular weight in kilodaltons indicated left (red arrows), based on the running pattern of Colorplus Prestained Protein Ladder, Broad Range (NEB P7712).

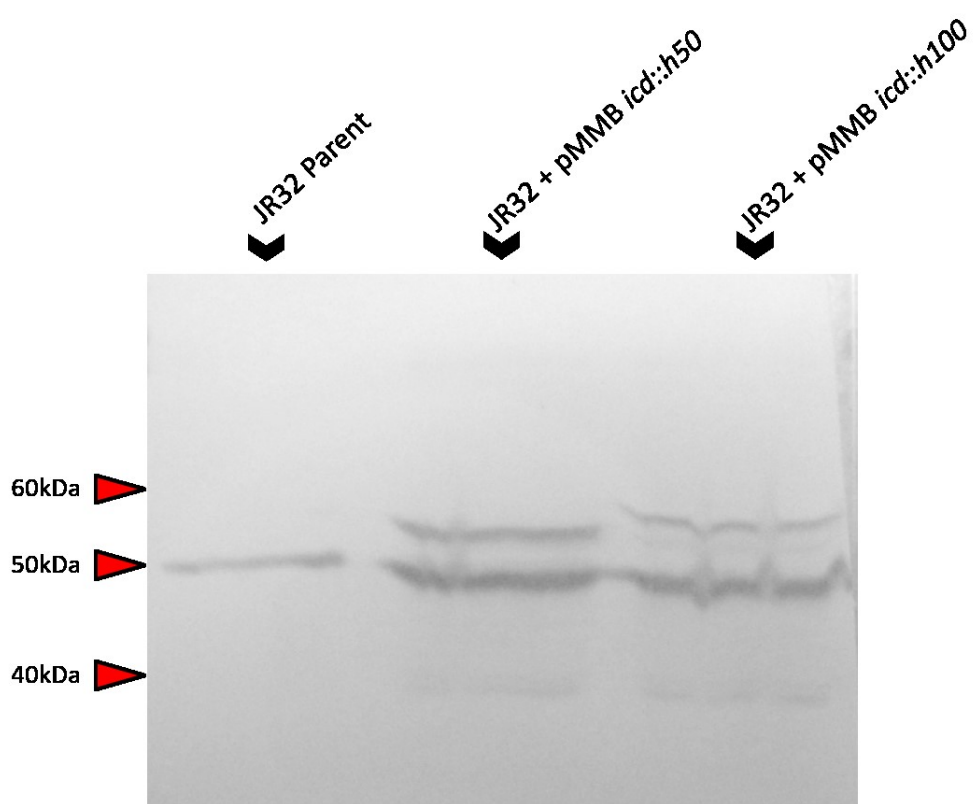


Figure 21: western blots of osmotic shockate samples for Icd-H50 and Icd-H100 and the densitometric analysis of these blots for sub-cellular localization. (A) 100mL of JR32 expressing either Icd-H50 or Icd-H100 were grown to an OD₆₀₀ of ~2, pelleted, and osmotically shocked. The shockate supernatant was considered ‘periplasmic’ while the remaining cytoplasmic and membrane-associated fractions were separated by ultracentrifugation at 100,000xg for one hour. These fractions were assessed for total protein concentration, and 20 mg of each sample was run on a 12% polyacrylamide gel and transferred to a PVDF membrane. western blotting was then performed using α -Icd antibody. (B) Using the ‘gel analysis’ function of FIJI (ImageJ) densitometry profiles were generated for the blots shown in A. The size of the peaks corresponds to the density of the detected band. The distance left→right corresponds to vertical distance (with left being higher and right lower). Broken lines indicate whether the measured peak was recombinant or native Icd.

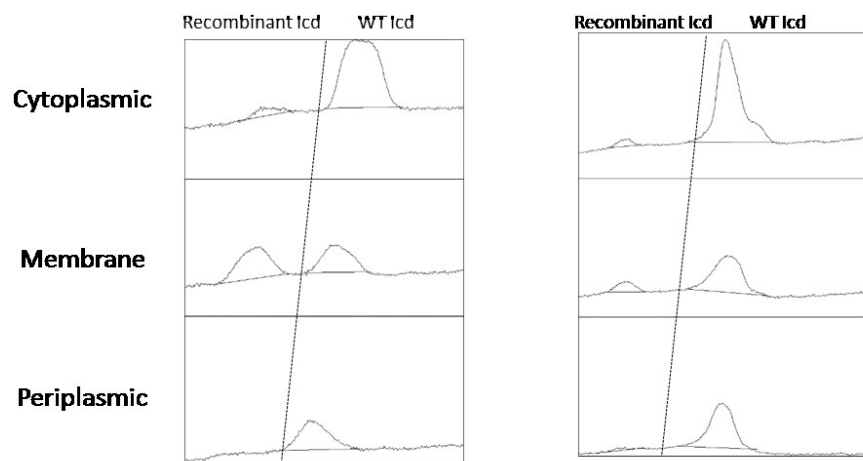
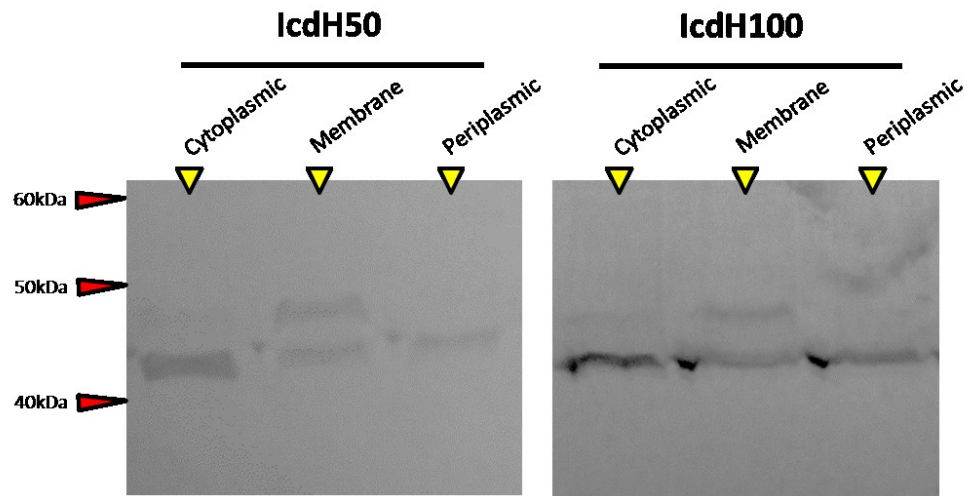
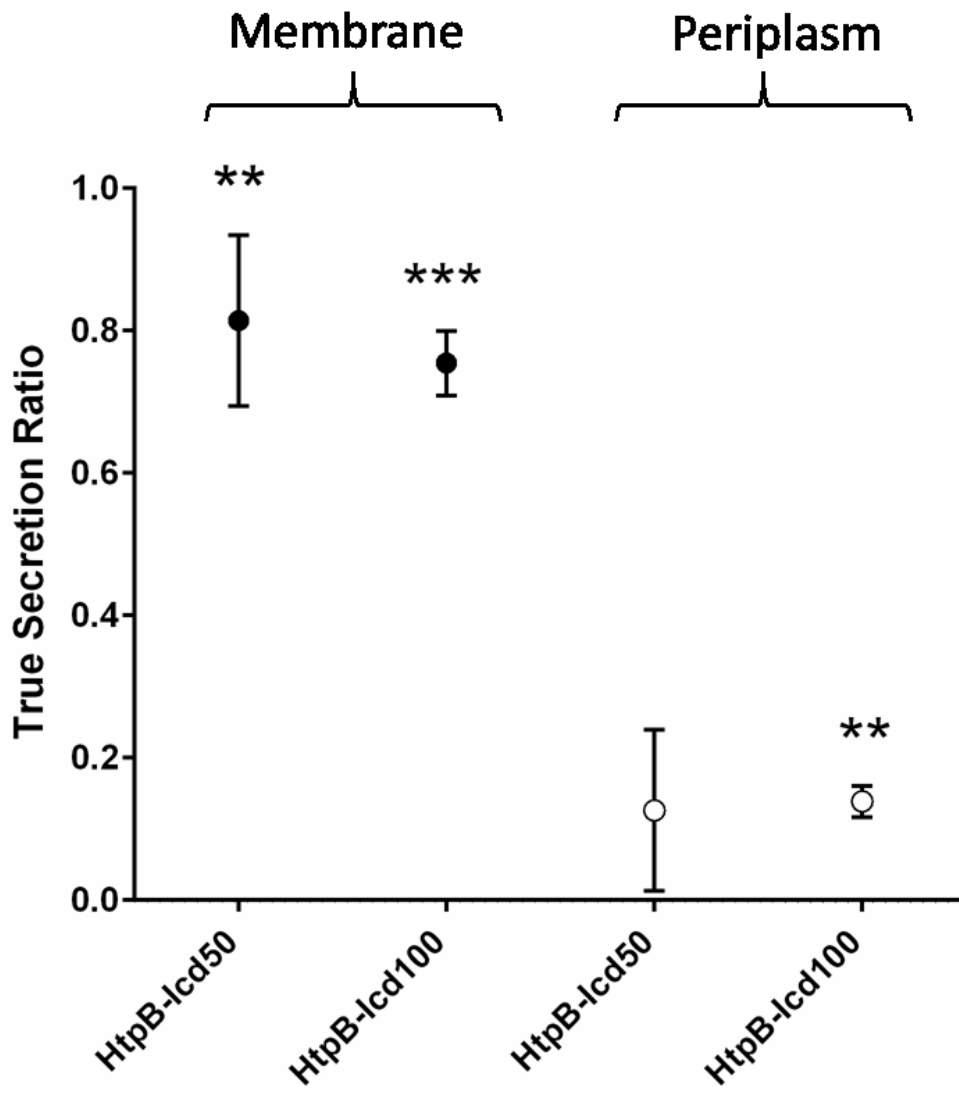


Figure 22: A graphical plot of the ratio relating the amount of recombinant Icd found in the membrane and periplasmic fractions after osmotic shock that cannot be explained by cell lysis. The densitometry values derived from western blotting the osmotic shock fractions were assessed by the formula presented in Figure 5. This resulted in the ‘True Secretion Ratio’, a measure of how much recombinant (i.e. tagged with the HtpB C-terminus) Icd in the periplasmic (white circles) and membrane (black circles) fractions cannot be explained by the lysis of cells during the shock procedure. The ‘0’ value corresponds with all observed translocation being due to lysis, whereas a value of 1 indicates that all observed Icd was legitimately translocated. Error bars indicate standard deviation of three replicates. Asterisks correspond to statistical difference from 0.



Working on the assumption that the C-terminus inserts into or interacts with lipid membranes, a C-terminal 6xHis tag (histidine being a large, potentially charged amino acid) was added to HtpB to disrupt this interaction. In comparison with the most common C-terminal amino acids of HtpB, glycine (which has no side chain) and methionine (which has a sterically unhindered, electrically neutral side chain), the large, ionizable imidazole ring of histidine is unlikely to insert in lipid membrane. As well, the 6xHis tag is a commonly used biomarker that can be detected by antibodies. *htpB* was amplified by PCR in a reaction where the reverse primer contained a sequence encoding for the 6xHis tag (P26). This was then mobilized in pMMB to generate plasmid pMMB + HtpB6xHis (Figure 23). JR32 cells carrying this plasmid and expressing the tagged HtpB were then fixed and sectioned for electron microscopy, then incubated with gold-conjugated α 6xHis antibody (Table 4). After visually scoring the sub-cellular localization of the 6xHis residues, it was determined that these were found in cytoplasmic locations in higher proportion than unmodified HtpB (57% vs. the 39% reported by Garduño *et al.*, 1998) (Figure 24, Figure 25).

3.6.2 Adding the C-terminus of HtpB to Icd causes an increase in translocation

To test whether the C-terminus of Htp was sufficient to cause translocation, the *L. pneumophila* cells expressing Icd-H50 recombinant protein were grown to early stationary phase and prepared for electron microscopy as before. Sections were stained with α ICDH, imaged, visually scored for sub-cellular localization, and compared to images of parent-strain JR32 incubated with α ICDH (Figure 26). It was determined that more Icd was found in extracytoplasmic locations in the strain expressing Icd-50 than in the strain with native Icd only (22% vs. 11% of residues seen) (Figure 27).

Figure 23: Diagram describing the cloning procedures to generate a 6xHis tagged version of HtpB. Chromosomal *htpB* (light red) was amplified in a PCR reaction (primers are light red triangles) in which the reverse primer contained a region coding for six histidine residues (light blue; size not to scale). This amplicon was cut with XbaI and SphI, and then ligated into pMMB cut with the same enzymes to generate plasmid pMMB + *htpB*6xHis. Following translation (second downwards arrow) this resulted in a version of HtpB with six positively charged histidine residues attached to the C-terminus (blue 'H's).

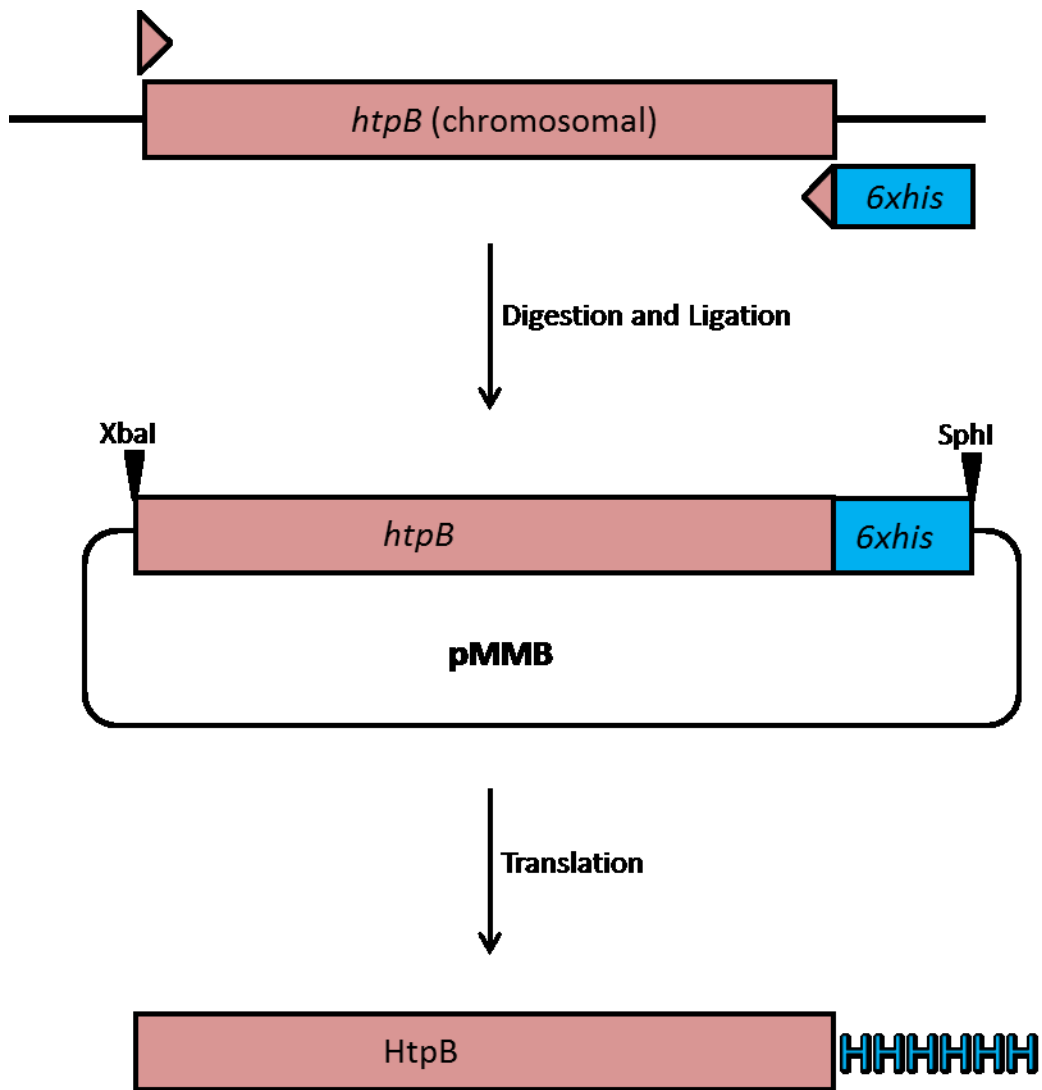
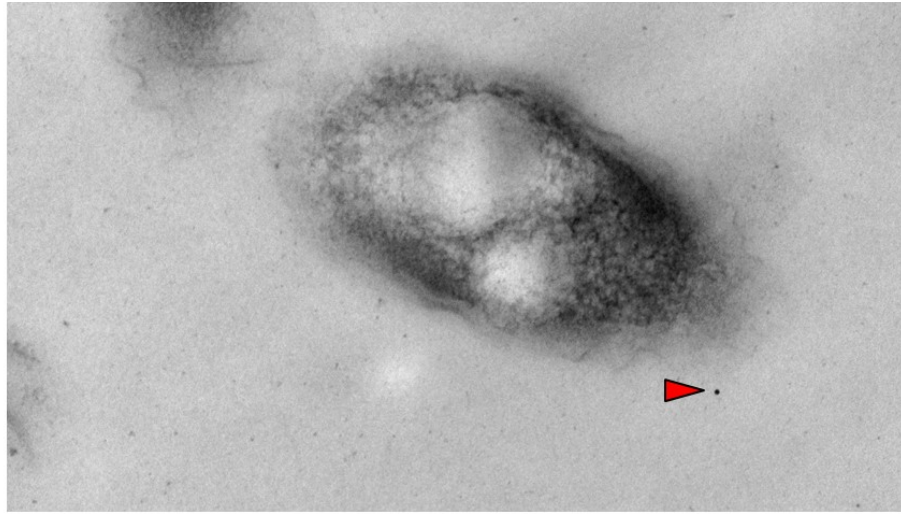
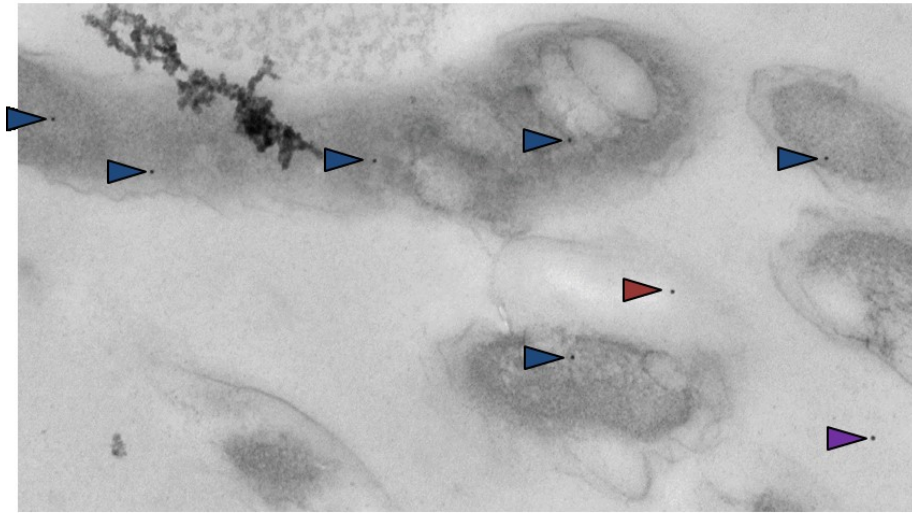


Figure 24: Transmission electron micrographs of JR32 expressing a recombinant HtpB with a C-terminal 6xHis tag. Two representative TEM images of JR32 labelled with gold conjugated antibodies that detect α -6xHis antibodies. Dots were visually scored as either 'Cytoplasmic and Inner-membrane' (blue arrows), 'Outer Membrane' (red arrows), 'Periplasmic' (dark red arrows) or 'Not Associated' (purple arrows). All images taken at 60,000x magnification (scale indicated).



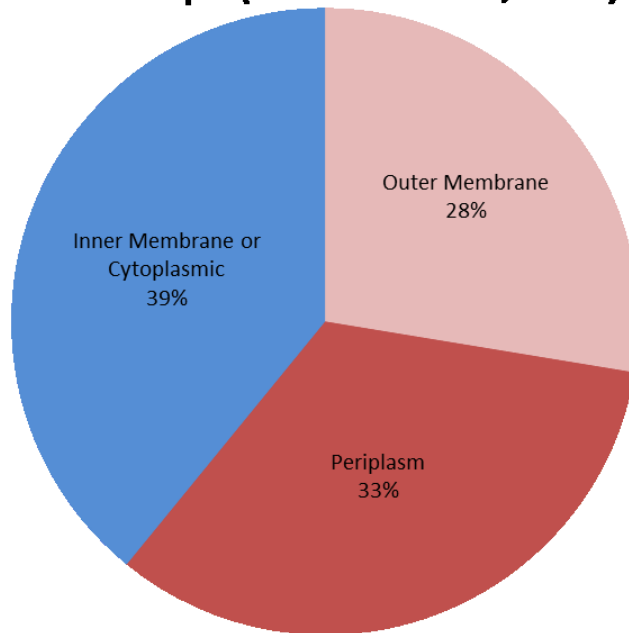
200 nm



200 nm

Figure 25: Graphs representing the sub-cellular distribution of HtpB-6xHis seen in immunogold micrographs. Following visual scoring on the location of HtpB-6xHis, data were collated into percentage format (bottom chart). Data from Garduño *et al.*, 1998 on the subcellular localization of native HtpB was used for comparison (top chart) as time restrictions precluded repeating their protocol.

Native HtpB (Garduno et al., 1998)



6 X His Tag (This study)

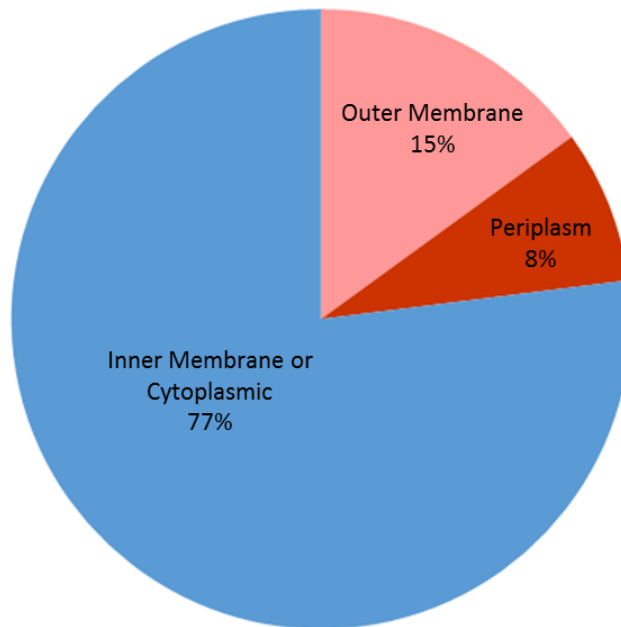
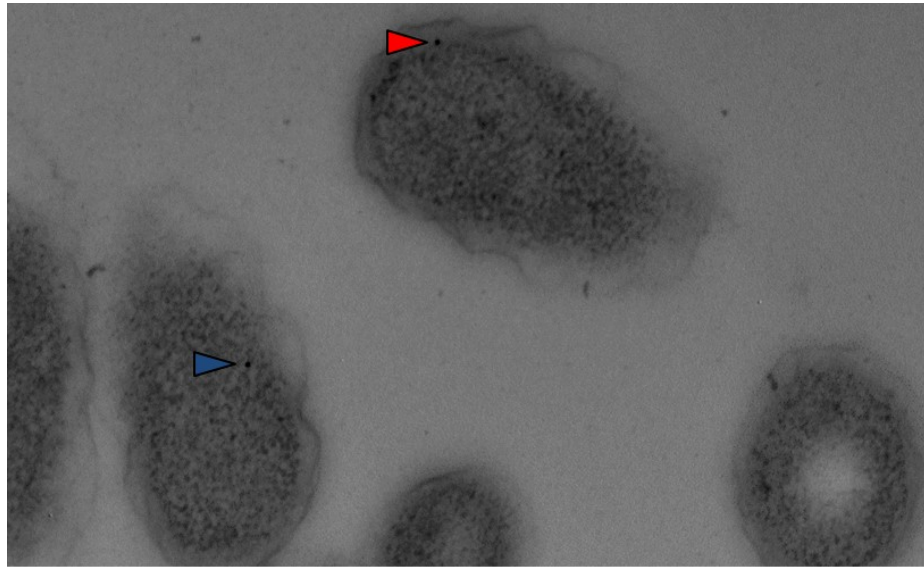
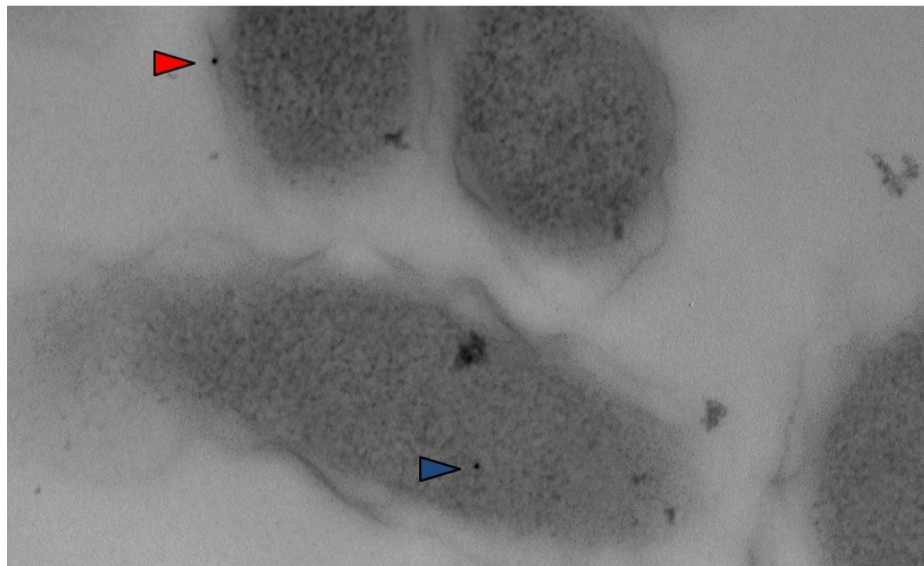


Figure 26: Transmission electron micrographs of JR32 expressing a recombinant Icd tagged with the last 50 amino acids of HtpB.

Following overnight culture, *L. pneumophila* expressing pMMB::IcdH50 was pelleted, fixed in 4% freshly depolymerized paraformaldehyde, sectioned in LR White resin and incubated with 1/100 α -Icd antibodies. Two representative SEM images of JR32 labelled with gold conjugated antibodies that detect α -Icd antibodies are shown. Dots were visually scored as either 'Translocated' (red Arrows) if they were associated with the inner membrane, periplasm, or outer membrane, 'Non-translocated' (blue arrows) if they were associated with the cytoplasm, or 'Background' (not shown) if they weren't associated with a cell. All images taken at 60,000x magnification (scale bars shown).



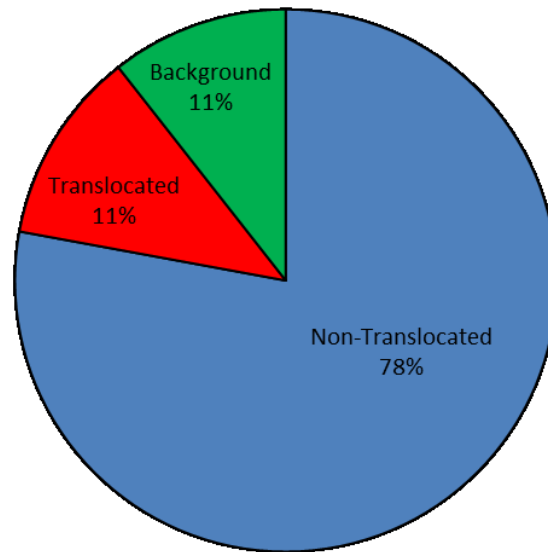
200 nm



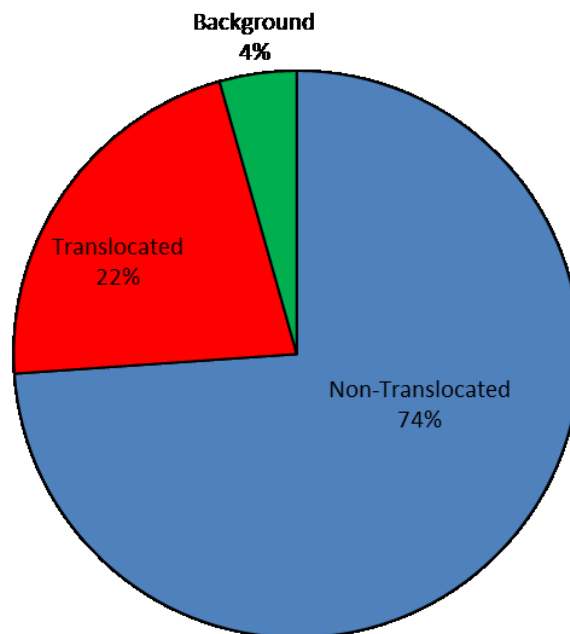
200 nm

Figure 27: Graphs representing the sub-cellular distribution of Icd seen in immunogold micrographs. Following visual scoring on the location of Icd::H50, data were collated into percentage format (bottom chart). Micrographs of Icd::pMMB were also visually scored for comparison.

Icd pMMB



Icd::H50



4. Discussion

4.1 A new Method for Assessing Chaperonin Secretion in *L. pneumophila* was Validated

Without doubt, the most important result of this study is the determination that HtpB relies on a functional Dot/Icm system for efficient translocation into the cytoplasm of *Legionella*-infected cells. Less interesting, but still important for understanding the validity of this study, were the difficulties encountered in attaining this result. Initially, the assay used to test the translocation status of HtpB was a cyclic AMP assay based on gene fusions with *cyaA*. This assay was developed by Chong (2007) who generated three plasmids: pAC17, containing *cyaA* fused to the C-terminal encoding region of *htpB*, pJC158, containing *cyaA* fused to the C-terminal encoding region of *lepA* (which encodes a Dot/Icm secreted protein), and pJC203, containing *cyaA* alone (a negative control). Chong (2007) and Nasrallah, Riveroll, Garduño & Murray (2011b) used these plasmids to assess the translocation status of HtpB; in our hands, however, this approach did not clearly resolve whether or not HtpB was secreted due to several issues. Firstly, the results generated by this assay were not reproducible in this study. The experiment was conducted at least five separate times, which resulted in five different patterns of cAMP expression. The results of these experiments were highly variable and statistically problematic, and indicated that any assay based on cAMP was not ideal for our infection model. The reasons for why this is are not clear, but it is likely that either background noise (i.e. the eukaryotic cells' native cAMP) was too high to measure a clear signal, the expression profiles of the recombinant proteins were different during infection, or both. It may also be that if HtpB is not a canonical Dot/Icm effector, then the secretion status of

HtpB is not the simple ‘yes or no’ answer that the cAMP assay was designed to generate. It is of interest to note that the GSK assay was also difficult to resolve in U937 cells and only worked clearly in L929 cells, indicating that the problems may stem from the cell line itself. As U937-derived macrophages are immune cells and L929 cells are fibroblasts, it may be that the immunity-evasion program of *L. pneumophila* or the response of the macrophages to bacterial invasion results in cellular processes that make translocation assays difficult to perform. In the cAMP assay, this may be due to modulation of the cAMP signal during bacterial infection (reviewed in McDonough and Rodriguez, 2012). It would be a worthwhile experiment to repeat the cAMP assay in the L929 infection model to see if a clearer result could be obtained. In the GSK assay, some proteinacious signal (either native to U937 cells or induced in *L. pneumophila* exposed to immune cells) of around 90kDa reacts to the GSK antibody and obscured the LegC6 positive control (Figure 18). As well, no tagged *L. pneumophila* protein could be detected in the phospho-GSK western blot with the possible exception of Mdh, the negative control. The absence of phosphorylated HtpB-GSK or LegC6-GSK is not surprising, as these signals were very weak in the L929 cells as well (Figure 17). Their absence in the U937 model may be due to an altered translocation profile in a different host, or to an increased ability of U937 cells to degrade translocated proteins. The potential for Mdh to be translocated is surprising (and uncertain, given the weak band in Figure 18) given that it is a metabolic protein that has never been identified as a secretion effector. Carbohydrate metabolism proteins have been suggested as potential components of host-specific differentiation of *L. pneumophila* before, however, so it is possible that Mdh may act in an unknown role (Abdelhady, 2013).

There was also some difficulty employing the controls selected in other studies. During this investigation, it was determined that JR32 *lepA* has a mutation resulting in a premature stop codon (Figure 28). This puts its ability to act as even a negative control in jeopardy, as failure to result in a signal is due to a malformed protein and not a lack of secretion. This does not impugn the results of prior studies, however, as the mutation (a deletion) could very well have been recent. The development of mutations in virulence genes is unfortunately common in lab strains of bacteria, and underlines the importance of sequencing all developed constructs.

The GSK assay involves the addition of the GSK tag, a thirteen residue peptide from the eukaryotic glycogen synthase kinase protein (EC 2.7.11.26). Upon entry to the eukaryotic cytoplasm the tag is phosphorylated at serine-9, an event which can be detected by antibodies. This tag system is superior to the CyaA assay in many ways: the GSK tag is smaller than CyaA and therefore would have reduced steric hindrance, and the assay for the GSK tag is a simple western blot instead of a complicated sandwich ELISA method. The GSK tag assay is also superior to other small protein tag systems, as the GSK tag does not need to enter the nucleus to be phosphorylated and detected (as opposed to the ELK tag, which requires a nuclear kinase) (Garcia *et al.*, 2006). While the GSK tag system has been used to assay type IV secretion effectors before (Hohlfeld *et al.*, 2006), to our knowledge this study is the first use of the GSK tag in *L. pneumophila*, as well as its first use in a type IVB secretion system. To date, most large scale assessments of the *L. pneumophila* proteome for secretion have relied on fusion to bulky molecules such as cyaA or β -lactamases. While these assays are undoubtedly valuable, they often miss proteins with unusual secretion signals or low levels of secretion. The GSK assay, now

Figure 28: An alignment of the sequence encoding the LepA used in this study with the reference sequence of *L. pneumophila* *lepA* (NCBI, Gene ID:19833438). (A) The *lepA* from JR32 used in this study was sequenced (bottom sequence, labelled “Actual”) and compared to the reference sequence of *lepA* (top sequence, labelled “Theoretical”). These sequences were then aligned using Clustal Omega (relevant part of sequence shown; asterisks indicate identical residues). The *lepA* used in this study was found to have a C→T mutation early in the LepA coding region. (B) Following translation, this mutation would result in a premature stop codon.

A

Theoretical	CAAGAAGGTTAGAACAGTTGAAAGATTTAAACCGAATTCGAAATTTTCAATAATTGCC
Actual	CAAGAAGGTTAGAACAGTTGAAAGATTTAAACCGAATTCGAAATTTTCAATAATTGCC *****
Theoretical	ATATTGATCATGGCAAGTCTACGTTGGCTGATCGATTTATCCAAATTTGTGGCGGGTTGA
Actual	ATATTGATCATGGCAAGTCTACGTTGGCTGATCGATTTATCCAAATTTGTGGCGGGTTGA *****
Theoretical	CTGAGCGCGAAATGAGCTCGCAAGTTCTTGATTCTATGGATATTGAACGTGAGCGAGGTA
Actual	CTGAGCGCGAAATGAGCTCGCAAGTTCTTGATTCTATGGATATTGAACGTGAGCGAGGTA *****
Theoretical	TTACCATCAAAGCGCAATGCGTTTCCTTGAATTACACAGCTAAAGATGGAAGACCTATT
Actual	TTACCATCAAAGCGCAATGCGTTTCCTTGAATTACACAGCTAAAGATGGAAGACCTATT *****

B

Theoretical	Met SGRPRTTSFAESVDLFARRLEQLKDL
Actual	Met SGRPRTTSFAESVDLFARRLEQLKDL
Theoretical	NRIRNFSIIAHIDHGKSTLADRFIQICG...
Actual	NRIRNFSIIAHIDHGKSTLADRFI Stop

that it has been validated in the Dot/Icm system, represents an ideal alternative to these other assays as it is cheap, sensitive, and easy to perform. Some questions may be raised as to the accuracy of densitometry for the purposes of assessing *levels* of secretion, but this is at least as quantitative as previously published assays involving the quantification of fluorescence (Zhu *et al.*, 2011).

4.2 The C-terminus of HtpB is essential but not sufficient for translocation

It was hypothesized that the translocation of HtpB is dependent on the Dot/Icm system, and that the C-terminus of HtpB promotes or facilitates this translocation. The former hypothesis was conclusively supported by the results of this study, while the latter was strongly suggested. To begin with the less conclusive position, the addition of the C-terminus of HtpB to the cytoplasmic protein Icd caused association with the membrane fraction, and the addition of a 6xHis tag to the C-terminus of HtpB decreased association with membrane in immunogold microscopy. As well, the addition of the C-terminus to a version of the PhoA protein with no secretion signal did not restore translocation to the periplasm. Taken together, it can be concluded that the C-terminus is not sufficient for the translocation of HtpB across the cytoplasmic membrane, but seems to play a role in promoting the interaction of HtpB with this membrane; either associating with the actual bilayer or with an integral membrane factor (such as a glycoprotein, glycolipid, or lipoprotein). However, the role of the C-terminus cannot be conclusively demonstrated by this work. The target for the C-terminus was not identified, and the binding of the C-terminus to this target must be unequivocally demonstrated in future experiments. This study relied on tangential evidence provided by the localization of recombinant proteins; a necessity borne of the fact that the way in which the C-terminus interacts with

membrane is unknown. A more in-depth bioinformatics analysis of the HtpB C-terminus may reveal the likely interaction partner, helping to guide further experiments that demonstrate association directly. Such analysis was able to determine the structural component of enolase (a protein previously thought to be cytoplasmic-only) which contributed to its secretion in *B. subtilis* (Yang *et al.*, 2011). As well, better controlled immunogold microscopy experiments would help reinforce the interpretation that the HtpB C-terminus and membrane associate. Much difficulty was encountered in labelling unmodified HtpB (the control for Figure 24). This is especially surprising considering the density of HtpB residues seen by Garduño *et al.*, 1998 using the same antibody, but may be a result of the antibody's age. Experiments were planned using new materials, however time and funding considerations precluded this. This weakens the conclusions that can be drawn from the intracellular buildup of HtpB as this study was forced to rely on reproduction of data from Garduño *et al.*, 1998 to estimate a control result (Figure 24). Still, the results of this study are enough to strongly indicate that the association occurs. In the context of the model presented above, this author suggests that the C-terminus' affinity for lipid membrane puts HtpB in close proximity with whichever factor is responsible for mobilizing it across the inner membrane. The ability of a chaperonin C-terminus to associate with lipid membrane and act as a lipochaperonin has already been demonstrated in GroEL (Torok *et al.*, 1997) giving HtpB a valid evolutionary rationale for localizing there. There would seem to be no good reason for a shift to the periplasm to be selected for, but if the periplasmic intermediate hypothesis presented earlier is correct, HtpB may fold, stabilize or otherwise interact with other periplasmic effectors. Once in the periplasm the transition to being a fully secreted effector is simpler to envision; HtpB

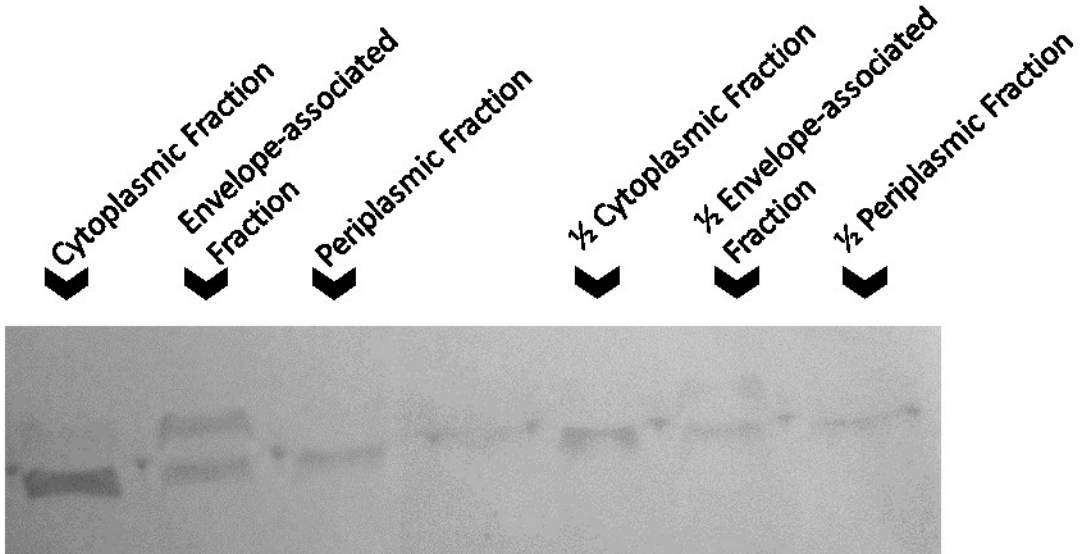
could diffuse out of the DotCDH pore. This could occur passively, as HtpB diffuses through a DotCDH pore not associated with a DotFG translocation channel, or actively, as some periplasmic protein guides HtpB to such a pore. Canonically the Dot/Icm system doesn't do this (as it spans both membranes, proteins are pulled from the cytoplasm straight to the extracellular environment), however the fact that the knockout of *dotFG* (singularly or together) does not eliminate secretion suggests that the channel is either redundant or not necessary for secretion (Kubori *et al.*, 2014). An affinity for membrane would favour HtpB's development into a virulence factor, as once outside the cell it could lodge in either the outside of the outer membrane or the inner wall of the LCV. This interpretation of HtpB's evolutionary history does rely on HtpB being able to act as a lipochaperonin (or having another function which favours association with lipid membrane) which has not yet been proven. While (Torok *et al.*, 1997) demonstrated that the C-terminus of GroEL acts as a lipochaperonin, and chaperonins have very high sequence identity, the C-terminus is one area where GroEL and HtpB differ significantly. GroEL is not known to secrete, however, so the differences in sequence may be due to HtpB having to dissociate with lipid membrane as it translocates, or may have to do with another of its many functions. To help clarify this, repeating the experiments of Torok *et al.*, 1997 on HtpB instead of GroEL to confirm lipochaperonin capabilities would be beneficial.

Because of the way in which densitometry was used in this study, experiment-specific data analysis posed some interesting statistical challenges. While densitometry is a widely accepted method of semi-quantitation, it is known that even differences in commonly used techniques can cause p-values to shift dramatically (Gassmann,

Grenacher, Rohde & Vogel, 2009). Because the experiment in which Icd was tagged with an HtpB tail and fractionated has a unique design (in which the lytic control is the untagged version of the same protein), normal techniques become difficult or impossible to employ. For example, it is almost universal to include a loading control during western blotting. In this experiment a loading control would be uninformative and misleading. Because the samples in this experiment are fractionated, there is no reason to assume that any band should be equivalent even if total protein was equal. To counteract this problem total protein from each sample was always measured, and equivalent amounts were run, but there is always some variation in transfer efficiency that cannot be accounted for by this method. The amount of protein run in each lane is irrelevant in this case, however, because the data analysis method used here relates the recombinant Icd to the native Icd within the same band. The comparison, therefore, is whether or not the ratio between recombinant Icd and native Icd in the periplasm and membrane is bigger or smaller than the same ratio in the cytoplasm. The major danger in this type of assay, then, is not having uneven levels of protein but going off of the linear scale. Because this study used colorimetric blotting and a regular, man-operated camera to image blots, no software was present to determine when the bands had reached saturation. To ameliorate this issue, blots were always run with internal duplicates diluted by half (Figure 29). During image analysis, the density values of these controls were checked against the fully concentrated sample bands to make sure the ratio between them was ~ 0.5 (i.e. $\frac{1}{2}$ dilution). If the ratio was higher than 0.6, the fully concentrated bands were considered to be saturated and were not used for final analysis. Ideally, samples would be run in triplicate, but low concentrations of protein in the periplasmic fractions and several

Figure 29: Immunoblot of fractionated lysate dilutions intended to ensure linearity-of-scale during densitometry analysis. (A) An immunoblot used for densitometry, with the corresponding 2x dilutions. (B) An example of the analysis performed to ensure that densitometry values were within linear range. The densitometry values for the 2x dilution samples were divided by the densitometry values for the 1x samples, generating a ratio. A perfect dilution corresponds to a ratio of 0.500; samples were discarded if the ratio exceeded 0.600 (indicative of saturation in the stronger band) or fell below 0.400 (indicative of insufficiently controlled loading or poor dilution) allowing for +/-10% error.

A



B

Fraction	Dilution	Raw Densitometry Value (1x band)	Raw Densitometry Value (1/2x band)	Densitometry Ratio
Cytoplasm	2x	7942	3510	0.442
Envelope-associated	2x	2376	1236	0.520
Periplasm	2x	2466	1202	0.487

technical difficulties precluded this. If these experiments were to be repeated, it is suggested that luminescent blotting chemistry be used in place of colorimetric. Because luminescent blots are usually imaged in a machine by a computer, saturation is a much less important problem: data can be collected in a time-dependent manner (meaning that the linear emission is always captured) and many programs will automatically detect saturation and adjust exposure accordingly. Luminescence has the added advantage of being more sensitive, and being strippable (so that fractionation controls like the DsbA antibody can be run much more easily).

To clearly demonstrate that the densitometry presented here proves the point that the C-terminus of HtpB causes accumulation of Icd in the membrane, extreme care was taken to interpret and present the data in Figure 21. Because of the way data was analyzed, the zero value is a placeholder for the recombinant Icd found in the cytoplasm due to lysis. When the p-value of a result is <0.05 in this assay, it indicates that across three replicates there was significantly more recombinant Icd in the periplasm or membrane than could be explained by lysis alone (i.e. the ratio does not statistically encompass 0). The corollary of this, that there could be less recombinant Icd than can be explained by lysis alone, is a mathematical artifact with no physical basis (as it would imply that the periplasm is secreting a cytoplasmic protein to the cytoplasm). While this method is not fully quantitative, it does thoroughly support the hypothesis that the C-terminus localizes to the membrane.

As a technique, densitometry exists in a bit of a grey area in science; it attempts to add objectivity to an inherently subjective interpretation. Despite this, osmotic shock is a feasible, reproducible method of assessing sub-cellular localization. While both

quantitative and qualitative experiments exist that would prove the point more thoroughly, osmotic shock was selected here for its practicality compared to the alternatives. On the quantitative side, an alternative to densitometry would be mass spectrometry of the fractions. This has the disadvantage of being expensive and technically difficult, as well as requiring numerous controls, making it unfeasible for most labs. On the qualitative side, the HtpB C-terminus could have been fused to an enzyme that is only active in the periplasm (such as PhoA) and added to media with BCIP for a colour assay. While the actual data collection part of this experiment would be much easier to perform than the densitometry experiments, too many difficulties would be encountered in setting up this experiment. Firstly, a negative result would make no distinction between the HtpB tail lodging PhoA in the inner membrane and the HtpB tail doing nothing, as the enzyme must reach the periplasm to function. Secondly, *L. pneumophila* already possesses an active PhoA, and this author did not possess a mutant *phoA* KO strain. In an attempt to circumvent these issues and still help validate the densitometry data, fusions between PhoA and HtpB were carried out in *E. coli*. While these did help confirm the results of the densitometry (i.e. the HtpB tail does not cause secretion alone) this experiment was not without issue. The relevance of any experiment carried out in a proxy organism must immediately be questioned; *E. coli* does not have any Dot/Icm complex. This might be seen as an advantage, however, as it allows us to determine what effects the HtpB protein has on its own secretion in the absence of other relevant machinery. This experiment does definitively demonstrate that HtpB requires more than just its C-terminus to translocate across lipid membrane.

Given the manipulations performed on the HtpB C-terminus in this study, it is fair to inquire why a C-terminal truncation was not done. Such an experiment is both scientifically and conceptually challenging for a variety of reasons, foremost of which is that HtpB is an essential protein. This means that a truncation can only eliminate so many residues before HtpB is rendered non-functional and *L. pneumophila* dies. In GroEL, a 20 residue truncation of the C-terminus resulted in a 25% slower folding cycle (from eight seconds to ten) (Suzuki *et al.*, 2008), and a fully intact C-terminus has been implicated in determining the size of the folding cage (which has implications for how efficiently folding occurs) (Tang *et al.*, 2006). It is therefore reasonable to assume that even if an HtpB truncation were viable, it would not be directly comparable to wild-type *Legionella* due to differences in protein processing abilities. This is assuming that an HtpB truncation could be cleanly inserted, as one would need to remove the native HtpB without killing the organism. As double homologous recombination is a multi-step process (involving integration and then excision) the odds of continual output of functional HtpB is low. CRISPR editing would be more likely to work, so long as repair mechanisms in *L. pneumophila* are swift enough to avoid depletion of HtpB.

4.3 The translocation of HtpB is explained by non-canonical, Dot/Icm dependent secretion

When trying to integrate the results of this study with previous research, difficulty ensues. Any attempts to form a logical model of chaperonin secretion is complicated by the fact that the Dot/Icm system is complex and understudied. To help combat this issue, the process of chaperonin secretion is best laid out in a series of sequential steps that can be logically derived from what is known. It is known that HtpB is synthesized in the

bacterial cytoplasm and can be translocated to host cytoplasm; it follows that various processes must transport the protein through the intervening spaces and barriers. To get from one cytoplasmic space to the other, HtpB must cross the inner bacterial membrane, the periplasm, the outer bacterial membrane, the LCV, and the LCV membrane. While the exact mechanisms of all of these steps are unresolved, this study and prior research allows division of these processes based on their dependence on the Dot/Icm system. Previous research has demonstrated that the translocation of HtpB from the cytoplasm to the periplasm is Dot/Icm independent, this study confirms that at least one stage later in the secretion process is dependent on Dot/Icm. This demonstrates that the secretion of HtpB is non-canonical: it occurs in a process with at least two distinct steps, one of which is independent of the classical Dot/Icm pathway.

To begin, HtpB must cross from the cytoplasm to the periplasm. In traditional Dot/Icm secretion this would occur through the DotFG translocation channel, and HtpB would travel from the bacterial cytoplasm to the extracellular space without any actual exposure to the periplasm itself. In practice HtpB has a distinct, periplasmic existence. Function-loss mutations in the Dot/Icm system cause HtpB to build up in the periplasm, not the cytoplasm (Chong, *et al.*, 2006). How HtpB translocates across the inner membrane in the absence of the Dot/Icm system is unknown, but this author proposes that the C-terminus of HtpB itself plays a role. The C-terminus was seen to cause an affinity for lipid membrane (Figure 21), suggesting that it binds either membrane itself or a membrane-associated protein. The latter is more likely, as the C-terminus of HtpB was not sufficient to cause translocation of PhoA in *E. coli*, indicating that another *L. pneumophila* specific component is needed for translocation (Figure 19). Investigating

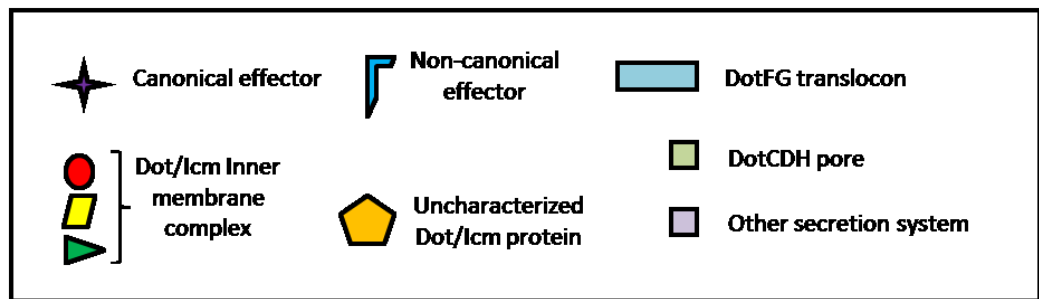
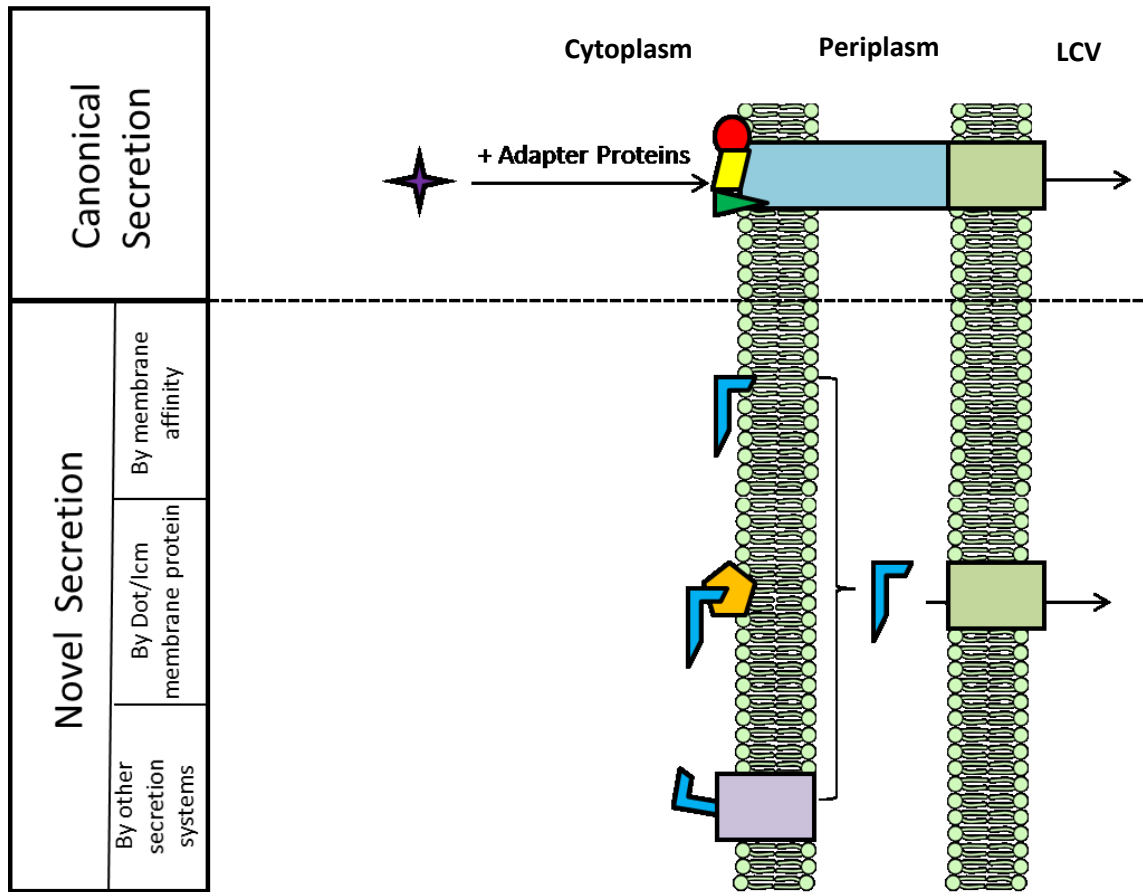
the interactions between HtpB and the inner-membrane proteome of *L. pneumophila* (by such techniques as yeast-two-hybrid or FRET) could help determine what component is responsible for translocation across the membrane. It is critical to stress that this inner membrane component could still be a Dot/Icm protein, as this translocation process is known to be independent of Dot/Icm secretion, not of the individual Dot/Icm components themselves. It is also possible that HtpB is capable of causing its own translocation, and the reason why PhoA was not translocated is that a part of HtpB outside of the C-terminus is needed. This could occur in a manner similar to the translocation of CPPs or autotransporters, although HtpB does not match the typical structure of those proteins. Short portions of HtpB did, in fact, show similarity to several CPPs, including a known translocation molecule of *M. tuberculosis* (Figure 7). This could indicate that parts of HtpB act in a similar fashion to CPPs, especially if post-translational cleavage results in a portion of HtpB with strong similarity to a CCP breaking off from the rest of the protein. This theoretical fragment could potentially be one of the ‘breakdown’ products of HtpB seen during immunoblotting of *L. pneumophila* lysate (mentioned above). This finding may be an artifact of an inappropriate use of BLAST given that a large polypeptide was BLASTed against a library of smaller fragments (the large E-values of the BLAST results indicate a high chance of false positive results). This problem is, in some sense, inevitable when BLASTing a large polypeptide (in this case, HtpB) against a library of smaller fragments (the CPPs) as the increased number of potentially matchable residues increases noise to the point where signal is not easily detected. This result could be reinforced if one of the small fragments of HtpB (currently thought to be breakdown products) were isolated and found to be identical to one of the sequences listed in Figure

7. A graphical summary of the mechanisms proposed for non-canonical secretion by this author is presented in Figure 30.

While the translocation to the periplasm is independent of the Dot/Icm system, this study demonstrates that one of the steps which follows does not occur in the absence of Dot/Icm secretion. Following translocation to the periplasm, HtpB must be further secreted to the bacterial cell surface and the lumen of the LCV. If HtpB can translocate across the inner membrane of its own accord, then it may similarly translocate across the outer membrane. More likely is that HtpB exits through a pore, like most Dot/Icm effectors. This step provides an opportunity to link up Dot/Icm dependence with the post periplasmic movement of HtpB, because the Dot/Icm system makes such a pore. In wild-type *L. pneumophila*, the DotCDH complex forms a pore in the outer membrane which is thought to link up with the DotFG channel and allow effectors to exit the cell. It is possible that HtpB exits through a DotCDH pore, either actively or passively. This would DotCDH pore is not formed when Dot/Icm secretion is eliminated. The pore is still formed in a *dotG* mutant but is differently shaped, which may explain why *dotG* mutants have a periplasmic build-up of HtpB but still express some levels of HtpB on their surface.

It should be mentioned at this point that there is a way in which HtpB could bypass the LCV entirely, going straight from the periplasm to host cytoplasm. HtpB is known to be present in OMVs, which generally contain periplasmic and outer membrane proteins. Shedding of OMVs in the LCV could lead to HtpB entering the host cytoplasm without exposure to the LCV lumen. While this may occur, it is unlikely to account for the

Figure 30: A diagram depicting elements of the putative new model for Dot/Icm secretion. In canonical secretion (top) effectors are brought to the inner membrane by Dot/Icm chaperones, secreted through a DotFG translocon, and exit via a DotCDH pore. In the putative new model (bottom), effectors with affinity for either membrane or membrane proteins are secreted to the periplasm by autotransport, an uncharacterized Dot/Icm inner-membrane protein, or the machinery of secretion systems other than Dot/Icm. These effectors then leak through the DotCDH pore or are packaged in an OMV.



majority of HtpB translocation seen during infection. Immunostaining indicates that HtpB is present in the LCV diffusely, not in clusters as one would expect if HtpB were packaged in OMVs. OMV secretion also does not explain why the elimination of Dot/Icm secretion halted HtpB translocation in this study, as OMV formation is not dependent on Dot/Icm.

Following translocation across the outer membrane via a pore, a self-mediated mechanism, or through another unknown pathway, HtpB is able to present on the cell surface and further extrude into the LCV. The order and relationship between these two options are unknown, but some educated guesses may be put forward. If HtpB does have the ability to associate with membrane (or with membrane components) then it may be secreted 'freely' through the inner membrane, with some HtpB molecules shedding into the LCV and others being attracted to their outer membrane partner. Alternatively, the HtpB might be automatically stuck in the outer membrane during its translocation and rely on some enzyme to cleave it free so that it can diffuse into the LCV. Which enzyme would do this is impossible to speculate upon without knowing how HtpB is connected to the outer membrane, but *L. pneumophila* is known to secrete several proteases and lipases (Aragon, *et al.*, 2000). Whatever the mechanism by which HtpB is either retained on the membrane or released to the LCV, it is likely to be differentially regulated, as the different environments encountered by *L. pneumophila* present different selective pressures. In an LCV, *L. pneumophila* is better served to shed HtpB as the protein must reach host cytosol to perform most of its functions. When free-living, however, shed HtpB would be wasted into the environment, whereas that retained in the outer membrane

could act as an adhesin for attachment to hosts. Like so many other processes in *L. pneumophila*, the secretion of HtpB could be linked into the organism's lifecycle.

Upon secretion to the LCV, HtpB must then make one final transition across the LCV membrane in order to contact host cytosol. This offers another opportunity to connect HtpB translocation to the Dot/Icm system, as the creation and manipulation of the LCV is dependent upon Dot/Icm. *L. pneumophila* is known to anchor Dot/Icm effectors (such as SidM and LidA) to the LCV membrane by targeting them to mono-phosphorylated phosphoinositide glycerolipids (reviewed in Hilbi, Weber & Finsel, 2011). These proteins then modify the LCV to the bacteria's liking, stealing host metabolites and preventing phagosome lysosome fusion. As *L. pneumophila* imports and exports multitudes of effectors and metabolites to prevent its own killing and modify the intracellular compartment, it is likely that highly expressed proteins have ample opportunity to leak out of the LCV. It is known, in fact, that the LCV is somewhat porous, as PAMPS such as flagellin are able to enter the host cytoplasm (a process not intended by the bacteria, as PAMP recognition often leads to apoptosis). As well, the ability of *L. pneumophila* to form pores in eukaryotic membrane is well known; *L. pneumophila* is often observed in the cytoplasm during the late stages of infection and certain host cells exhibit contact-dependent lysis caused by pores. This presents an interesting possibility that HtpB may make it to the LCV lumen without the assistance of the Dot/Icm system, but can't exit without the LCV modifications that Dot/Icm effectors mediate. It may seem odd that HtpB is Dot/Icm dependent without being a Dot/Icm effector, but there is precedent for this in the "secretion" of the flagellin protein. The export of flagellar components is independent of Dot/Icm, being mediated by the flagellar secretion apparatus (distantly

related to type III secretion systems, not type IV). The recognition of FlaA flagellin by BMM cells, however, seems to occur in a manner dependent on Dot/Icm. This indicates that FlaA is being translocated to host cytosol (i.e. leaked) in a Dot/Icm dependent manner, despite the fact that FlaA is not a Dot/Icm effector (Molofsky *et al.*, 2006).

4.4 Final Thoughts

While ultimately this study leaves the secretion of HtpB unresolved, I feel that sufficient uncertainties have been raised herein to justify further study of chaperonins in *L. pneumophila*, and of the Dot/Icm secretion system as a whole. Because of its ubiquitous environmental nature, its infection of freshwater eukaryotes, and its infrequent infection of humans, *L. pneumophila* presents a unique opportunity to study a bacterium on the precipice of pathogenicity. The secretion of multifunctional HtpB is simply one example of how this pathogen is being driven to cope with new environments, and an in depth study of the organism may reveal why human pathogens have evolved the way they have. It must be remembered that pathogens are not simply conjured from aether, but are a result of environmental or zoonotic bacteria transmitting to human hosts. While this is intensively studied in the field of virology (with the fear that zoonotic strains of Influenza may mix with human-infectious strains) the complexity of prokaryotes and (relatively) slower infection cycle has rendered this a dark area in bacteriology. More effort must be put into studying *L. pneumophila* and other bacteria like it if we are to fully understand evolutionary pathogenesis. From a more pragmatic (and fundable) viewpoint, *L. pneumophila* can act as a safer model for *C. burnetii*, which also possesses a Dot/Icm system. Since *C. burnetii* is one of the most infectious bacteria ever found, and is a prime candidate for biological warfare, understanding (and treating) its pathogenesis could be of

importance. *L. pneumophila* is therefore an understudied pathogen and a prime candidate for further investigation.

References

- Abdelhady, H., & Garduño, R. A. (2013). The progeny of *Legionella pneumophila* in human macrophages shows unique developmental traits. *FEMS microbiology letters*, *349*(2), 99-107.
- Agrawal, P., Bhalla, S., Usmani, S. S., Singh, S., Chaudhary, K., Raghava, G. P., & Gautam, A. (2016). CPPsite 2.0: a repository of experimentally validated cell-penetrating peptides. *Nucleic acids research*, *44*(D1), D1098-D1103.
- Alberts, B., Johnson, A., Lewis, J., Raff, M., Roberts, K., & Walter, P. (2002). The Transport of Proteins into Mitochondria and Chloroplasts. In B. Alberts, A. Johnson, J. Lewis, M. Raff, K. Roberts & P. Walter (Eds.), *Molecular Biology of the Cell 4th edition*. New York: Garland Sciences. Available from: <http://www.ncbi.nlm.nih.gov/books/NBK26828/>
- Alting-Mees, M. A., & Short, J. M. (1989). pBluescript II: gene mapping vectors. *Nucleic acids research*, *17*(22), 9494.
- Amor, J. C., Swails, J., Zhu, X., Roy, C. R., Nagai, H., Ingmundson, A., ... & Kahn, R. A. (2005). The structure of RalF, an ADP-ribosylation factor guanine nucleotide exchange factor from *Legionella pneumophila*, reveals the presence of a cap over the active site. *Journal of Biological Chemistry*, *280*(2), 1392-1400.
- Aragon, V., Kurtz, S., Flieger, A., Neumeister, B., & Cianciotto, N. P. (2000). Secreted Enzymatic Activities of Wild-Type and pilD-Deficient *Legionella pneumophila*. *Infection and immunity*, *68*(4), 1855-1863.
- Aragon, V., Rossier, O., & Cianciotto, N. P. (2002). *Legionella pneumophila* genes that encode lipase and phospholipase C activities. *Microbiology*, *148*(7), 2223-2231.
- Artsimovitch, I., Patlan, V., Sekine, S. I., Vassylyeva, M. N., Hosaka, T., Ochi, K., ... & Vassylyev, D. G. (2004). Structural basis for transcription regulation by alarmone ppGpp. *Cell*, *117*(3), 299-310.
- Aurass, P., Gerlach, T., Becher, D., Voigt, B., Karste, S., Bernhardt, J., ... & Flieger, A. (2016). Life stage-specific proteomes of *Legionella pneumophila* reveal a highly differential abundance of virulence-associated Dot/Icm effectors. *Molecular & Cellular Proteomics*, *15*(1), 177-200.
- Bachrach, U., Wang, Y. C., & Tabib, A. (2001). Polyamines: new cues in cellular signal transduction. *Physiology*, *16*(3), 106-109.
- Baine, W. B. (1985). Cytolytic and phospholipase C activity in *Legionella* species. *Journal of general microbiology*, *131*(6), 1383-1391.

- Bandyopadhyay, P., Xiao, H., Coleman, H. A., Price-Whelan, A., & Steinman, H. M. (2004). Icm/dot-independent entry of *Legionella pneumophila* into amoeba and macrophage hosts. *Infection and immunity*, 72(8), 4541-4551.
- Barbaree, J. M., Fields, B. S., Feeley, J. C., Gorman, G. W., & Martin, W. T. (1986). Isolation of protozoa from water associated with a legionellosis outbreak and demonstration of intracellular multiplication of *Legionella pneumophila*. *Applied and Environmental Microbiology*, 51(2), 422-424.
- Belyi, Y., Tabakova, I., Stahl, M., & Aktories, K. (2008). Lgt: a family of cytotoxic glucosyltransferases produced by *Legionella pneumophila*. *Journal of bacteriology*, 190(8), 3026-3035.
- Berk, S. G., Ting, R. S., Turner, G. W., & Ashburn, R. J. (1998). Production of Respirable Vesicles Containing Live *Legionella pneumophila* Cells by Two *Acanthamoeba* spp. *Applied and Environmental Microbiology*, 64(1), 279-286.
- Berk, S. G., Faulkner, G., Garduño, E., Joy, M. C., Ortiz-Jimenez, M. A., & Garduño, R. A. (2008). Packaging of live *Legionella pneumophila* into pellets expelled by *Tetrahymena* spp. does not require bacterial replication and depends on a Dot/Icm-mediated survival mechanism. *Applied and environmental microbiology*, 74(7), 2187-2199.
- Bozue, J. A., & Johnson, W. (1996). Interaction of *Legionella pneumophila* with *Acanthamoeba castellanii*: uptake by coiling phagocytosis and inhibition of phagosome-lysosome fusion. *Infection and Immunity*, 64(2), 668-673.
- Brassinga, K. C., Croxen, M. A., Shoemaker, C. J., Morash, M. G., LeBlanc, J. J., Hoffman, P. S. (2006). NOVEL USE OF HELICOBACTER PYLORI NITROREDUCTASE (rdxA) AS A COUNTERSELECTABLE MARKER IN ALLELIC VECTOR EXCHANGE TO CREATE LEGIONELLA PNEUMOPHILA PHILADELPHIA-1 MUTANTS. In N. P. Cianciotto, Y. Abu Kwaik, P.H. Edelstein, B. S. Fields, G. F. Geary, T. G. Harrison, C. A. Joseph, R. M. Ratcliff, J. E. Stout, & M. S. Swanson (Eds.), *Legionella: state of the art 30 years after its recognition* (pp. 339-342). Washington D.C. : ASM Press.
- Brüggemann, H., Hagman, A., Jules, M., Sismeiro, O., Dillies, M. A., Gouyette, C., ... & Buchrieser, C. (2006). Virulence strategies for infecting phagocytes deduced from the in vivo transcriptional program of *Legionella pneumophila*. *Cellular microbiology*, 8(8), 1228-1240.
- Burstein, D., Zusman, T., Degtyar, E., Viner, R., Segal, G., & Pupko, T. (2009). Genome-scale identification of *Legionella pneumophila* effectors using a machine learning approach. *PLoS Pathog*, 5(7), e1000508.

- Buscher, B. A., Conover, G. M., Miller, J. L., Vogel, S. A., Meyers, S. N., Isberg, R. R., & Vogel, J. P. (2005). The DotL protein, a member of the TraG-coupling protein family, is essential for viability of *Legionella pneumophila* strain Lp02. *Journal of bacteriology*, 187(9), 2927-2938.
- Byrne, B., & Swanson, M. S. (1998). Expression of *Legionella pneumophila* virulence traits in response to growth conditions. *Infection and immunity*, 66(7), 3029-3034.
- Cambronne, E. D., & Roy, C. R. (2007). The *Legionella pneumophila* IcmSW complex interacts with multiple Dot/Icm effectors to facilitate type IV translocation. *PLoS Pathog*, 3(12), e188.
- Carroll, M. V., Sim, R. B., Bigi, F., Jäkel, A., Antrobus, R., & Mitchell, D. A. (2010). Identification of four novel DC-SIGN ligands on *Mycobacterium bovis* BCG. *Protein & cell*, 1(9), 859-870.
- Chang, B., Kura, F., Amemura-Maekawa, J., Koizumi, N., & Watanabe, H. (2005). Identification of a novel adhesion molecule involved in the virulence of *Legionella pneumophila*. *Infection and immunity*, 73(7), 4272-4280.
- Chattopadhyay, M. K., & Tabor, H. (2013). Polyamines are critical for the induction of the glutamate decarboxylase-dependent acid resistance system in *Escherichia coli*. *Journal of Biological Chemistry*, 288(47), 33559-33570.
- Chong, A., Riveroll, A., Allan, S., Garduño, E., Garduño, R. A. (2006). THE Hsp60 CHAPERONIN OF *LEGIONELLA PNEUMOPHILA*: AN INTRIGUING PLAYER IN INFECTION OF HOST CELLS. In N. P. Cianciotto, Y. Abu Kwaik, P.H. Edelstein, B. S. Fields, G. F. Geary, T. G. Harrison, C. A. Joseph, R. M. Ratcliff, J. E. Stout, & M. S. Swanson (Eds.), *Legionella: state of the art 30 years after its recognition* (pp. 255-260). Washington D.C. : ASM Press.
- Chong, A. (2007). Characterization of the Virulence-Related Roles of the *Legionella pneumophila* Chaperonin, HtpB, in Mammalian Cells (Doctoral dissertation, Dalhousie University). Retrieved January 8th, 2016 from Dalhousie Libraries Graduate Theses Archive (Identifier AAINR27158).
- Chong, A., Lima, C. A., Allan, D. S., Nasrallah, G. K., & Garduño, R. A. (2009). The purified and recombinant *Legionella pneumophila* chaperonin alters mitochondrial trafficking and microfilament organization. *Infection and immunity*, 77(11), 4724-4739.
- Cirillo, J. D., Cirillo, S. L., Yan, L., Bermudez, L. E., Falkow, S., & Tompkins, L. S. (1999). Intracellular growth in *Acanthamoeba castellanii* affects monocyte entry mechanisms and enhances virulence of *Legionella pneumophila*. *Infection and immunity*, 67(9), 4427-4434.

- Collins, H. L. (2008). Withholding iron as a cellular defence mechanism—friend or foe?. *European journal of immunology*, 38(7), 1803-1806.
- Costa, T. R., Felisberto-Rodrigues, C., Meir, A., Prevost, M. S., Redzej, A., Trokter, M., & Waksman, G. (2015). Secretion systems in Gram-negative bacteria: structural and mechanistic insights. *Nature Reviews Microbiology*, 13(6), 343-359.
- Costa, T. R., Felisberto-Rodrigues, C., Meir, A., Prevost, M. S., Redzej, A., Trokter, M., & Waksman, G. (2015). Secretion systems in Gram-negative bacteria: structural and mechanistic insights. *Nature Reviews Microbiology*, 13(6), 343-359.
- Daisy, J. A., Benson, C. E., McKittrick, J., & Friedman, H. M. (1981). Intracellular replication of *Legionella pneumophila*. *Journal of Infectious Diseases*, 143(3), 460-464.
- Dalebroux, Z. D., Edwards, R. L., & Swanson, M. S. (2009). SpoT governs *Legionella pneumophila* differentiation in host macrophages. *Molecular microbiology*, 71(3), 640-658.
- D'Auria, G., Jiménez-Hernández, N., Peris-Bondia, F., Moya, A., & Latorre, A. (2010). *Legionella pneumophila* pangenome reveals strain-specific virulence factors. *BMC genomics*, 11(1), 181.
- Dautin, N., & Bernstein, H. D. (2007). Protein secretion in gram-negative bacteria via the autotransporter pathway*. *Annu. Rev. Microbiol.*, 61, 89-112.
- De Felipe, K. S., Glover, R. T., Charpentier, X., Anderson, O. R., Reyes, M., Pericone, C. D., & Shuman, H. A. (2008). *Legionella* eukaryotic-like type IV substrates interfere with organelle trafficking. *PLoS Pathog*, 4(8), e1000117.
- Deepe Jr, G. S., & Gibbons, R. S. (2002). Cellular and molecular regulation of vaccination with heat shock protein 60 from *Histoplasma capsulatum*. *Infection and immunity*, 70(7), 3759-3767.
- Dolezal, P., Aili, M., Tong, J., Jiang, J. H., Marobbio, C. M., fung Lee, S., ... & Frankel, G. (2012). *Legionella pneumophila* secretes a mitochondrial carrier protein during infection. *PLoS Pathog*, 8(1), e1002459.
- Donlan, R. M., Forster, T., Murga, R., Brown, E., Lucas, C., Carpenter, J., & Fields, B. (2005). *Legionella pneumophila* associated with the protozoan *Hartmannella vermiformis* in a model multi-species biofilm has reduced susceptibility to disinfectants. *Biofouling*, 21(1), 1-7.
- Dürr, U. H., Sudheendra, U. S., & Ramamoorthy, A. (2006). LL-37, the only human member of the cathelicidin family of antimicrobial peptides. *Biochimica et Biophysica Acta (BBA)-Biomembranes*, 1758(9), 1408-1425.

- Ensminger, A. W., & Isberg, R. R. (2009). Legionella pneumophila Dot/Icm translocated substrates: a sum of parts. *Current opinion in microbiology*, 12(1), 67-73.
- Faucher, S. P., Mueller, C. A., & Shuman, H. A. (2011). Legionella pneumophila transcriptome during intracellular multiplication in human macrophages. *Frontiers in microbiology*, 2.
- Faulkner, G., & Garduño, R. A. (2002). Ultrastructural analysis of differentiation in Legionella pneumophila. *Journal of bacteriology*, 184(24), 7025-7041.
- Faulkner, G., Berk, S. G., Garduño, E., Ortiz-Jiménez, M. A., & Garduño, R. A. (2008). Passage through Tetrahymena tropicalis triggers a rapid morphological differentiation in Legionella pneumophila. *Journal of bacteriology*, 190(23), 7728-7738.
- Fayet, O., Ziegelhoffer, T., & Georgopoulos, C. (1989). The groES and groEL heat shock gene products of Escherichia coli are essential for bacterial growth at all temperatures. *Journal of bacteriology*, 171(3), 1379-1385.
- Fraser, D. W., Tsai, T. R., Orenstein, W., Parkin, W. E., Beecham, H. J., Sharrar, R. G., ... & Shepard, C. C. (1977). Legionnaires' disease: description of an epidemic of pneumonia. *New England Journal of Medicine*, 297(22), 1189-1197.
- Galka, F., Wai, S. N., Kusch, H., Engelmann, S., Hecker, M., Schmeck, B., ... & Steinert, M. (2008). Proteomic characterization of the whole secretome of Legionella pneumophila and functional analysis of outer membrane vesicles. *Infection and immunity*, 76(5), 1825-1836.
- Garcia, J. T., Ferracci, F., Jackson, M. W., Joseph, S. S., Pattis, I., Plano, L. R., ... & Plano, G. V. (2006). Measurement of effector protein injection by type III and type IV secretion systems by using a 13-residue phosphorylatable glycogen synthase kinase tag. *Infection and immunity*, 74(10), 5645-5657.
- Garduño, R. A., Faulkner, G., Trevors, M. A., Vats, N., & Hoffman, P. S. (1998). Immunolocalization of Hsp60 in Legionella pneumophila. *Journal of bacteriology*, 180(3), 505-513.
- Garduño, R. A., Garduño, E., & Hoffman, P. S. (1998b). Surface-associated hsp60 chaperonin of Legionella pneumophila mediates invasion in a HeLa cell model. *Infection and immunity*, 66(10), 4602-4610.
- Garduño, R. A., Garduño, E., Hiltz, M., & Hoffman, P. S. (2002). Intracellular growth of Legionella pneumophila gives rise to a differentiated form dissimilar to stationary-phase forms. *Infection and immunity*, 70(11), 6273-6283.

- Garduño, R. A., Chong, A., Nasrallah, G. K., & Allan, D. S. (2011). The Legionella pneumophila chaperonin—an unusual multifunctional protein in unusual locations. *Legionella: from protozoa to humans*, 40.
- Garduño, R. A., & Chong, A. (2013). The Legionella pneumophila chaperonin 60 and the art of keeping several moonlighting jobs. In *Moonlighting Cell Stress Proteins in Microbial Infections* (pp. 143-160). Springer Netherlands.
- Gassmann, M., Grenacher, B., Rohde, B., & Vogel, J. (2009). Quantifying western blots: pitfalls of densitometry. *Electrophoresis*, 30(11), 1845-1855.
- Gautam, A., Singh, H., Tyagi, A., Chaudhary, K., Kumar, R., Kapoor, P., & Raghava, G. P. S. (2012). CPPsite: a curated database of cell penetrating peptides. *Database*, 2012, bas015.
- Gerhardt, P., Murray, R. G. E., Wood, W. A., Krieg, N. R. (Eds). (1994). *Methods for general and molecular biology*. Washington DC: American Society for Microbiology.
- Gophna, U., Ron, E. Z., & Graur, D. (2003). Bacterial type III secretion systems are ancient and evolved by multiple horizontal-transfer events. *Gene*, 312, 151-163.
- Gupta, R. S. (1995). Evolution of the chaperonin families (HSP60, HSP 10 and TCP-1) of proteins and the origin of eukaryotic cells. *Molecular microbiology*, 15(1), 1-11.
- Hammer, B. K., & Swanson, M. S. (1999). Co-ordination of Legionella pneumophila virulence with entry into stationary phase by ppGpp. *Molecular microbiology*, 33(4), 721-731.
- Harada, T., Tanikawa, T., Iwasaki, Y., Yamada, M., Imai, Y., & Miyake, M. (2012). Phagocytic entry of Legionella pneumophila into macrophages through phosphatidylinositol 3, 4, 5-trisphosphate-independent pathway. *Biological and Pharmaceutical Bulletin*, 35(9), 1460-1468.
- Hartl, F. U., Bracher, A., & Hayer-Hartl, M. (2011). Molecular chaperones in protein folding and proteostasis. *Nature*, 475(7356), 324-332.
- Hayer-Hartl, M., Bracher, A., & Hartl, F. U. (2016). The GroEL–GroES chaperonin machine: a nano-cage for protein folding. *Trends in biochemical sciences*, 41(1), 62-76.
- Henderson, B., Fares, M. A., & Lund, P. A. (2013). Chaperonin 60: a paradoxical, evolutionarily conserved protein family with multiple moonlighting functions. *Biological Reviews*, 88(4), 955-987.

- Heuner, K., & Steinert, M. (2003). The flagellum of *Legionella pneumophila* and its link to the expression of the virulent phenotype. *International Journal of Medical Microbiology*, 293(2), 133-143.
- Hilbi, H., Segal, G., & Shuman, H. A. (2001). Icm/Dot-dependent upregulation of phagocytosis by *Legionella pneumophila*. *Molecular microbiology*, 42(3), 603-617.
- Hilbi, H., Weber, S., & Finsel, I. (2011). Anchors for effectors: subversion of phosphoinositide lipids by *Legionella*. *Legionella: from protozoa to humans*, 64.
- Hohlfeld, S., Pattis, I., Püls, J., Plano, G. V., Haas, R., & Fischer, W. (2006). AC-terminal translocation signal is necessary, but not sufficient for type IV secretion of the *Helicobacter pylori* CagA protein. *Molecular microbiology*, 59(5), 1624-1637.
- Horwitz, M. A. (1983). Formation of a novel phagosome by the Legionnaires' disease bacterium (*Legionella pneumophila*) in human monocytes. *The Journal of experimental medicine*, 158(4), 1319-1331.
- Horwitz, M. A. (1984). Phagocytosis of the Legionnaires' disease bacterium (*Legionella pneumophila*) occurs by a novel mechanism: engulfment within a pseudopod coil. *Cell*, 36(1), 27-33.
- Huang, L., Boyd, D., Amyot, W. M., Hempstead, A. D., Luo, Z. Q., O'Connor, T. J., ... & Isberg, R. R. (2011). The E Block motif is associated with *Legionella pneumophila* translocated substrates. *Cellular microbiology*, 13(2), 227-245.
- Isaac, D. T., Laguna, R. K., Valtz, N., & Isberg, R. R. (2015). MavN is a *Legionella pneumophila* vacuole-associated protein required for efficient iron acquisition during intracellular growth. *Proceedings of the National Academy of Sciences*, 112(37), E5208-E5217.
- Ishino, S., Kawata, Y., Taguchi, H., Kajimura, N., Matsuzaki, K., & Hoshino, M. (2015). Effects of C-terminal truncation of chaperonin GroEL on the yield of in-cage folding of the green fluorescent protein. *Journal of Biological Chemistry*, 290(24), 15042-15051.
- Jacobi, S., & Heuner, K. (2003). Description of a putative type I secretion system in *Legionella pneumophila*. *International journal of medical microbiology*, 293(5), 349-358.
- Jameson-Lee, M., Garduño, R. A., & Hoffman, P. S. (2011). DsbA2 (27 kDa Com1-like protein) of *Legionella pneumophila* catalyses extracytoplasmic disulphide-bond formation in proteins including the Dot/Icm type IV secretion system. *Molecular microbiology*, 80(3), 835-852.

- Karatan, E., & Michael, A. J. (2013). A wider role for polyamines in biofilm formation. *Biotechnology letters*, *35*(11), 1715-1717.
- Karunakaran, K. P., Noguchi, Y., Read, T. D., Cherkasov, A., Kwee, J., Shen, C., ... & Brunham, R. C. (2003). Molecular analysis of the multiple GroEL proteins of Chlamydiae. *Journal of bacteriology*, *185*(6), 1958-1966.
- Kaufmann, A. F., McDade, J. E., Patton, C. M., Bennett, J. V., Skaliy, P., Feeley, J. C., ... & Brachman, P. S. (1981). Pontiac fever: isolation of the etiologic agent (*Legionella pneumophila*) and demonstration of its mode of transmission. *American journal of epidemiology*, *114*(3), 337-347.
- Kerner, M. J., Naylor, D. J., Ishihama, Y., Maier, T., Chang, H. C., Stines, A. P., ... & Hartl, F. U. (2005). Proteome-wide analysis of chaperonin-dependent protein folding in *Escherichia coli*. *Cell*, *122*(2), 209-220.
- Kirby, J. E., Vogel, J. P., Andrews, H. L., & Isberg, R. R. (1998). Evidence for pore-forming ability by *Legionella pneumophila*. *Molecular microbiology*, *27*(2), 323-336.
- Klumpp, M., & Baumeister, W. (1998). The thermosome: archetype of group II chaperonins. *FEBS letters*, *430*(1-2), 73-77.
- Koubar, M., Rodier, M. H., Garduño, R. A., & Frère, J. (2011). Passage through *Tetrahymena tropicalis* enhances the resistance to stress and the infectivity of *Legionella pneumophila*. *FEMS microbiology letters*, *325*(1), 10-15.
- Kubori, T., Hyakutake, A., & Nagai, H. (2008). *Legionella* translocates an E3 ubiquitin ligase that has multiple U-boxes with distinct functions. *Molecular microbiology*, *67*(6), 1307-1319.
- Kubori, T., Koike, M., Bui, X. T., Higaki, S., Aizawa, S. I., & Nagai, H. (2014). Native structure of a type IV secretion system core complex essential for *Legionella* pathogenesis. *Proceedings of the National Academy of Sciences*, *111*(32), 11804-11809.
- Lammertyn, E., & Anné, J. (2004). Protein secretion in *Legionella pneumophila* and its relation to virulence. *FEMS microbiology letters*, *238*(2), 273-279.
- LaRue, R. W., Dill, B. D., Giles, D. K., Whittimore, J. D., & Raulston, J. E. (2007). Chlamydial Hsp60-2 is iron responsive in *Chlamydia trachomatis* serovar E-infected human endometrial epithelial cells in vitro. *Infection and immunity*, *75*(5), 2374-2380.

- Lee, W. (2014) Investigating the protein-folding function of high temperature protein B (HtpB), the putative chaperonin of *Legionella pneumophila*. B.Sc. Honors thesis. Department of Microbiology and Immunology, Dalhousie University, Halifax, NS, Canada.
- Li, X. H., Zeng, Y. L., Gao, Y., Zheng, X. C., Zhang, Q. F., Zhou, S. N., & Lu, Y. J. (2010). The ClpP protease homologue is required for the transmission traits and cell division of the pathogen *Legionella pneumophila*. *BMC microbiology*, *10*(1), 1.
- Liles, M. R., Scheel, T. A., & Cianciotto, N. P. (2000). Discovery of a nonclassical siderophore, legiobactin, produced by strains of *Legionella pneumophila*. *Journal of bacteriology*, *182*(3), 749-757.
- Long, K. H., Gomez, F. J., Morris, R. E., & Newman, S. L. (2003). Identification of heat shock protein 60 as the ligand on *Histoplasma capsulatum* that mediates binding to CD18 receptors on human macrophages. *The Journal of Immunology*, *170*(1), 487-494.
- Lu, S., Tager, L. A., Chitale, S., & Riley, L. W. (2006). A cell-penetrating peptide derived from mammalian cell uptake protein of *Mycobacterium tuberculosis*. *Analytical biochemistry*, *353*(1), 7-14.
- Luo, Z. Q., & Isberg, R. R. (2004). Multiple substrates of the *Legionella pneumophila* Dot/Icm system identified by interbacterial protein transfer. *Proceedings of the National Academy of Sciences of the United States of America*, *101*(3), 841-846.
- Matsuno, K., Blais, T., Serio, A. W., Conway, T., Henkin, T. M., & Sonenshein, A. L. (1999). Metabolic imbalance and sporulation in an isocitrate dehydrogenase mutant of *Bacillus subtilis*. *Journal of bacteriology*, *181*(11), 3382-3391.
- McDade, J. E., Shepard, C. C., Fraser, D. W., Tsai, T. R., Redus, M. A., & Dowdle, W. R. (1977). Legionnaires' disease: isolation of a bacterium and demonstration of its role in other respiratory disease. *New England Journal of Medicine*, *297*(22), 1197-1203.
- McDonough, K. A., & Rodriguez, A. (2012). The myriad roles of cyclic AMP in microbial pathogens: from signal to sword. *Nature Reviews Microbiology*, *10*(1), 27-38.
- Molofsky, A. B., Byrne, B. G., Whitfield, N. N., Madigan, C. A., Fuse, E. T., Tateda, K., & Swanson, M. S. (2006). Cytosolic recognition of flagellin by mouse macrophages restricts *Legionella pneumophila* infection. *The Journal of experimental medicine*, *203*(4), 1093-1104.

- Morales, V. M., Bäckman, A., & Bagdasarian, M. (1991). A series of wide-host-range low-copy-number vectors that allow direct screening for recombinants. *Gene*, *97*(1), 39-47.
- Morioka, M., Muraoka, H., Yamamoto, K., & Ishikawa, H. (1994). An endosymbiont chaperonin is a novel type of histidine protein kinase. *Journal of biochemistry*, *116*(5), 1075-1081.
- Murata, T., Delprato, A., Ingmundson, A., Toomre, D. K., Lambright, D. G., & Roy, C. R. (2006). The *Legionella pneumophila* effector protein DrrA is a Rab1 guanine nucleotide-exchange factor. *Nature cell biology*, *8*(9), 971-977.
- Nagai, H., Kagan, J. C., Zhu, X., Kahn, R. A., & Roy, C. R. (2002). A bacterial guanine nucleotide exchange factor activates ARF on *Legionella* phagosomes. *Science*, *295*(5555), 679-682.
- Nagai, H., Cambronne, E. D., Kagan, J. C., Amor, J. C., Kahn, R. A., & Roy, C. R. (2005). A C-terminal translocation signal required for Dot/Icm-dependent delivery of the *Legionella* RalF protein to host cells. *Proceedings of the National Academy of Sciences of the United States of America*, *102*(3), 826-831.
- Nasrallah, G.K., Gagnon, E., Orton, D.J., and Garduño, R.A. (2011). The htpAB operon of *Legionella pneumophila* cannot be deleted in the presence of the groE chaperonin operon of *Escherichia coli*. *Canadian Journal of Microbiology*, *57*, 943-952.
- Nasrallah, G. K., Riveroll, A. L., Chong, A., Murray, L. E., Lewis, P. J., & Garduño, R. A. (2011b). *Legionella pneumophila* Requires Polyamines for Optimal Intracellular Growth. *Journal of bacteriology*, *193*(17), 4346-4360.
- Natale, P., Brüser, T., & Driessen, A. J. (2008). Sec-and Tat-mediated protein secretion across the bacterial cytoplasmic membrane—distinct translocases and mechanisms. *Biochimica et Biophysica Acta (BBA)-Biomembranes*, *1778*(9), 1735-1756.
- Nossal, N. G., & Heppel, L. A. (1966). The release of enzymes by osmotic shock from *Escherichia coli* in exponential phase. *Journal of Biological Chemistry*, *241*(13), 3055-3062.
- Patel, C. N., Wortham, B. W., Lines, J. L., Fetherston, J. D., Perry, R. D., & Oliveira, M. A. (2006). Polyamines are essential for the formation of plague biofilm. *Journal of bacteriology*, *188*(7), 2355-2363.
- Phin, N., Parry-Ford, F., Harrison, T., Stagg, H. R., Zhang, N., Kumar, K., ... & Abubakar, I. (2014). Epidemiology and clinical management of Legionnaires' disease. *The Lancet infectious diseases*, *14*(10), 1011-1021.

- Piao, Z., Sze, C. C., Barysheva, O., Iida, K. I., & Yoshida, S. I. (2006). Temperature-regulated formation of mycelial mat-like biofilms by *Legionella pneumophila*. *Applied and environmental microbiology*, 72(2), 1613-1622.
- Poly, F., Ewing, C., Goon, S., Hickey, T. E., Rockabrand, D., Majam, G., ... & Guerry, P. (2007). Heterogeneity of a *Campylobacter jejuni* protein that is secreted through the flagellar filament. *Infection and immunity*, 75(8), 3859-3867.
- Portaro, F. C., Hayashi, M. A., De Arauz, L. J., Palma, M. S., Assakura, M. T., Silva, C. L., & de Camargo, A. C. (2002). The *Mycobacterium leprae* hsp65 displays proteolytic activity. Mutagenesis studies indicate that the *M. leprae* hsp65 proteolytic activity is catalytically related to the HslVU protease. *Biochemistry*, 41(23), 7400-7406.
- Prashar, A., Bhatia, S., Tabatabaeiyazdi, Z., Duncan, C., Garduño, R. A., Tang, P., ... & Terebiznik, M. R. (2012). Mechanism of invasion of lung epithelial cells by filamentous *Legionella pneumophila*. *Cellular microbiology*, 14(10), 1632-1655.
- Price, C. T., Al-Khodor, S., Al-Quadani, T., Santic, M., Habyarimana, F., Kalia, A., & Kwai, Y. A. (2009). Molecular mimicry by an F-box effector of *Legionella pneumophila* hijacks a conserved polyubiquitination machinery within macrophages and protozoa. *PLoS Pathog*, 5(12), e1000704.
- Pugsley, A. P. (1993). The complete general secretory pathway in gram-negative bacteria. *Microbiological reviews*, 57(1), 50.
- Rajpal, A. M., Khanduri, R., Naik, R. J., & Ganguli, M. (2012). Structural rearrangements and chemical modifications in known cell penetrating peptide strongly enhance DNA delivery efficiency. *Journal of controlled release*, 157(2), 260-271.
- Ridenour, D. A., Cirillo, S. L., Feng, S., Samrakandi, M. M., & Cirillo, J. D. (2003). Identification of a gene that affects the efficiency of host cell infection by *Legionella pneumophila* in a temperature-dependent fashion. *Infection and immunity*, 71(11), 6256-6263.
- Robertson, P., Abdelhady, H., & Garduño, R. A. (2014). The many forms of a pleomorphic bacterial pathogen—the developmental network of *Legionella pneumophila*. *Frontiers in microbiology*, 5.
- Rossier, O., Dao, J., & Cianciotto, N. P. (2008). The type II secretion system of *Legionella pneumophila* elaborates two aminopeptidases, as well as a metalloprotease that contributes to differential infection among protozoan hosts. *Applied and environmental microbiology*, 74(3), 753-761.

- Roy, C. R., Berger, K. H., & Isberg, R. R. (1998). Legionella pneumophila DotA protein is required for early phagosome trafficking decisions that occur within minutes of bacterial uptake. *Molecular microbiology*, 28(3), 663-674.
- Sandegren, L., & Andersson, D. I. (2009). Bacterial gene amplification: implications for the evolution of antibiotic resistance. *Nature Reviews Microbiology*, 7(8), 578-588.
- Santic, M., Molmeret, M., & Kwaik, Y. A. (2005). Maturation of the Legionella pneumophila-containing phagosome into a phagolysosome within gamma interferon-activated macrophages. *Infection and immunity*, 73(5), 3166-3171.
- Sauer, J. D., Bachman, M. A., & Swanson, M. S. (2005). The phagosomal transporter A couples threonine acquisition to differentiation and replication of Legionella pneumophila in macrophages. *Proceedings of the National Academy of Sciences of the United States of America*, 102(28), 9924-9929.
- Schindelin, J., Arganda-Carreras, I., Frise, E., Kaynig, V., Longair, M., Pietzsch, T., ... & Tinevez, J. Y. (2012). Fiji: an open-source platform for biological-image analysis. *Nature methods*, 9(7), 676-682.
- Seeger, E. M., Thuma, M., Fernandez-Moreira, E., Jacobs, E., Schmitz, M., & Helbig, J. H. (2010). Lipopolysaccharide of Legionella pneumophila shed in a liquid culture as a nonvesicular fraction arrests phagosome maturation in amoeba and monocytic host cells. *FEMS microbiology letters*, 307(2), 113-119.
- Segal, G., Russo, J. J., & Shuman, H. A. (1999). Relationships between a new type IV secretion system and the icm/dot virulence system of Legionella pneumophila. *Molecular microbiology*, 34(4), 799-809.
- Silveira, T. N., & Zamboni, D. S. (2010). Pore formation triggered by Legionella spp. is an Nlr4 inflammasome-dependent host cell response that precedes pyroptosis. *Infection and immunity*, 78(3), 1403-1413.
- Singh, B., Patel, H. V., Ridley, R. G., Freeman, K. B., & Gupta, R. S. (1990). Mitochondrial import of the human chaperonin (HSP60) protein. *Biochemical and biophysical research communications*, 169(2), 391-396.
- Steinert, M., Heuner, K., Buchrieser, C., Albert-Weissenberger, C., & Glöckner, G. (2007). Legionella pathogenicity: genome structure, regulatory networks and the host cell response. *International journal of medical microbiology*, 297(7), 577-587.

- Sutherland, M. C., Nguyen, T. L., Tseng, V., & Vogel, J. P. (2012). The Legionella IcmSW complex directly interacts with DotL to mediate translocation of adaptor-dependent substrates. *PLoS Pathog*, 8(9), e1002910.
- Suzuki, M., Ueno, T., Iizuka, R., Miura, T., Zako, T., Akahori, R., ... & Ohdomari, I. (2008). Effect of the C-terminal Truncation on the Functional Cycle of Chaperonin GroEL IMPLICATION THAT THE C-TERMINAL REGION FACILITATES THE TRANSITION FROM THE FOLDING-ARRESTED TO THE FOLDING-COMPETENT STATE. *Journal of Biological Chemistry*, 283(35), 23931-23939.
- Tachado, S. D., Samrakandi, M. M., & Cirillo, J. D. (2008). Non-opsonic phagocytosis of Legionella pneumophila by macrophages is mediated by phosphatidylinositol 3-kinase. *PLoS One*, 3(10), e3324.
- Tang, Y. C., Chang, H. C., Roeben, A., Wischnewski, D., Wischnewski, N., Kerner, M. J., ... & Hayer-Hartl, M. (2006). Structural features of the GroEL-GroES nanocage required for rapid folding of encapsulated protein. *Cell*, 125(5), 903-914.
- Thomas, V., Bouchez, T., Nicolas, V., Robert, S., Loret, J. F., & Levi, Y. (2004). Amoebae in domestic water systems: resistance to disinfection treatments and implication in Legionella persistence. *Journal of applied microbiology*, 97(5), 950-963.
- Török, Z., Horváth, I., Goloubinoff, P., Kovacs, E., Glatz, A., Balogh, G., & Vígh, L. (1997). Evidence for a lipochaperonin: association of active protein folding GroESL oligomers with lipids can stabilize membranes under heat shock conditions. *Proceedings of the National Academy of Sciences*, 94(6), 2192-2197.
- Trusca, D., Scott, S., Thompson, C., & Bramhill, D. (1998). Bacterial SOS checkpoint protein Sula inhibits polymerization of purified FtsZ cell division protein. *Journal of bacteriology*, 180(15), 3946-3953.
- Valenzuela-Valderas, K.N., A.L. Riveroll, P. Robertson, L.E. Murray, and R.A. Garduño. 2016. Legionella pneumophila chaperonin 60, an extra- and intra-cellular moonlighting virulence-related factor. In: Moonlighting Proteins: Novel Virulence Factors in Bacterial Infections, Chapter 6 (edited by B. Henderson). John Wiley & Sons, Inc., Hoboken, NJ, pp. *in press*.
- van Schaik, E. J., Chen, C., Mertens, K., Weber, M. M., & Samuel, J. E. (2013). Molecular pathogenesis of the obligate intracellular bacterium Coxiella burnetii. *Nature Reviews Microbiology*, 11(8), 561-573.
- Vandersmissen, L., De Buck, E., Saels, V., Coil, D. A., & Anné, J. (2010). A Legionella pneumophila collagen-like protein encoded by a gene with a variable number of tandem repeats is involved in the adherence and invasion of host cells. *FEMS microbiology letters*, 306(2), 168-176.

- Victor, L. Y., Zuravleff, J. J., Gavlik, L., & Magnussen, M. H. (1983). Lack of evidence for person-to-person transmission of Legionnaires' disease. *Journal of Infectious Diseases*, 147(2), 362-362.
- Vincent, C. D., Friedman, J. R., Jeong, K. C., Buford, E. C., Miller, J. L., & Vogel, J. P. (2006). Identification of the core transmembrane complex of the Legionella Dot/Icm type IV secretion system. *Molecular microbiology*, 62(5), 1278-1291.
- Vincent, C.D. & Vogel, J.P. (2008). The Dot/Icm Type IVB Secretion System. In K. Heuner & M. Swanson (Eds.), *Legionella: Molecular Microbiology* (pp. 165-179). Norfolk, UK: Caister Academic Press.
- Vincent, C. D., Friedman, J. R., Jeong, K. C., Sutherland, M. C., & Vogel, J. P. (2012). Identification of the DotL coupling protein subcomplex of the Legionella Dot/Icm type IV secretion system. *Molecular microbiology*, 85(2), 378-391.
- Vogel, J. P., Andrews, H. L., Wong, S. K., & Isberg, R. R. (1998). Conjugative transfer by the virulence system of Legionella pneumophila. *Science*, 279(5352), 873-876.
- Wadowsky, R. M., Yee, R. B., Mezmar, L., Wing, E. J., & Dowling, J. N. (1982). Hot water systems as sources of Legionella pneumophila in hospital and nonhospital plumbing fixtures. *Applied and Environmental Microbiology*, 43(5), 1104-1110.
- Wang, F., Sampogna, R. V., & Ware, B. R. (1989). pH dependence of actin self-assembly. *Biophysical journal*, 55(2), 293.
- Ward, J. E., Akiyoshi, D. E., Regier, D., Datta, A. S. I. S., Gordon, M. P., & Nester, E. W. (1988). Characterization of the virB operon from an Agrobacterium tumefaciens Ti plasmid. *Journal of Biological Chemistry*, 263(12), 5804-5814.
- Watarai, M., Derre, I., Kirby, J., Growney, J. D., Dietrich, W. F., & Isberg, R. R. (2001). Legionella pneumophila Is Internalized by a Macropinocytotic Uptake Pathway Controlled by the Dot/Icm System and the Mouse Lgn1 Locus. *The Journal of experimental medicine*, 194(8), 1081-1096.
- Watarai, M., Kim, S., Erdenebaatar, J., Makino, S. I., Horiuchi, M., Shirahata, T., ... & Katamine, S. (2003). Cellular prion protein promotes Brucella infection into macrophages. *The journal of experimental medicine*, 198(1), 5-17.
- Williams, T. A., & Fares, M. A. (2010). The effect of chaperonin buffering on protein evolution. *Genome biology and evolution*, 2, 609-619.
- Yang, C. K., Ewis, H. E., Zhang, X., Lu, C. D., Hu, H. J., Pan, Y., ... & Tai, P. C. (2011). Nonclassical protein secretion by Bacillus subtilis in the stationary phase is not due to cell lysis. *Journal of bacteriology*, 193(20), 5607-5615.

- Yang, D. C., Blair, K. M., & Salama, N. R. (2016). Staying in Shape: the Impact of Cell Shape on Bacterial Survival in Diverse Environments. *Microbiology and Molecular Biology Reviews*, 80(1), 187-203.
- Yoshida, N., Oeda, K., Watanabe, E., Mikami, T., Fukita, Y., Nishimura, K., ... & Matsuda, K. (2001). Protein function: chaperonin turned insect toxin. *Nature*, 411(6833), 44-44.
- Zarankiewicz, T., Madej, J., Galli, J., Bajzert, J., & Stefaniak, T. (2012). Inhibition of in vitro *Histophilus somni* biofilm production by recombinant Hsp60 antibodies. *Polish journal of veterinary sciences*, 15(2), 373-378.
- Zhang, X., Zhang, Y., Liu, J., & Liu, H. (2013). PotD protein stimulates biofilm formation by *Escherichia coli*. *Biotechnology letters*, 35(7), 1099-1106.
- Zhu, W., Banga, S., Tan, Y., Zheng, C., Stephenson, R., Gately, J., & Luo, Z. Q. (2011). Comprehensive identification of protein substrates of the Dot/Icm type IV transporter of *Legionella pneumophila*. *PloS one*, 6(3), e17638.

Appendices

Appendix A: Rights and Permissions

License Agreement for Reproduction of Figure 2

RightsLink Printable License	Page 1 of 3
NATURE PUBLISHING GROUP LICENSE TERMS AND CONDITIONS	
Jul 21, 2016	
<hr/>	
This Agreement between Peter Robertson ("You") and Nature Publishing Group ("Nature Publishing Group") consists of your license details and the terms and conditions provided by Nature Publishing Group and Copyright Clearance Center.	
License Number	3913670348337
License date	Jul 21, 2016
Licensed Content Publisher	Nature Publishing Group
Licensed Content Publication	Nature
Licensed Content Title	Molecular chaperones in protein folding and proteostasis
Licensed Content Author	F. Ulrich Hartl, Andreas Bracher, Manajit Hayer-Hartl
Licensed Content Date	Jul 20, 2011
Licensed Content Volume Number	475
Licensed Content Issue Number	7356
Type of Use	reuse in a dissertation / thesis
Requestor type	academic/educational
Format	print and electronic
Portion	figures/tables/illustrations
Number of figures/tables/illustrations	2
High-res required	no
Figures	Figure 1 (Competing reactions...) and Figure 3 (Folding in...)
Author of this NPG article	no
Your reference number	
Title of your thesis / dissertation	Investigating the Secretion of HtpB, the Multifunctional Chaperonin of Legionella pneumophila
Expected completion date	Aug 2016
Estimated size (number of pages)	160
Requestor Location	Peter Robertson 16 Lewis Drive Bedford, NS B4B1C2 Canada Attn: Peter Robertson
Billing Type	Invoice
Billing Address	Peter Robertson 16 Lewis Drive
https://s100.copyright.com/App/PrintableLicenseFrame.jsp?publisherID=52&publisherN... 2016-07-21	

Bedford, NS B4B1C2
Canada
Attn: Peter Robertson

Total 0.00 CAD

[Terms and Conditions](#)

Terms and Conditions for Permissions

Nature Publishing Group hereby grants you a non-exclusive license to reproduce this material for this purpose, and for no other use, subject to the conditions below:

1. NPG warrants that it has, to the best of its knowledge, the rights to license reuse of this material. However, you should ensure that the material you are requesting is original to Nature Publishing Group and does not carry the copyright of another entity (as credited in the published version). If the credit line on any part of the material you have requested indicates that it was reprinted or adapted by NPG with permission from another source, then you should also seek permission from that source to reuse the material.
2. Permission granted free of charge for material in print is also usually granted for any electronic version of that work, provided that the material is incidental to the work as a whole and that the electronic version is essentially equivalent to, or substitutes for, the print version. Where print permission has been granted for a fee, separate permission must be obtained for any additional, electronic re-use (unless, as in the case of a full paper, this has already been accounted for during your initial request in the calculation of a print run). NB: In all cases, web-based use of full-text articles must be authorized separately through the 'Use on a Web Site' option when requesting permission.
3. Permission granted for a first edition does not apply to second and subsequent editions and for editions in other languages (except for signatories to the STM Permissions Guidelines, or where the first edition permission was granted for free).
4. Nature Publishing Group's permission must be acknowledged next to the figure, table or abstract in print. In electronic form, this acknowledgement must be visible at the same time as the figure/table/abstract, and must be hyperlinked to the journal's homepage.
5. The credit line should read:
Reprinted by permission from Macmillan Publishers Ltd: [JOURNAL NAME] (reference citation), copyright (year of publication)
For AOP papers, the credit line should read:
Reprinted by permission from Macmillan Publishers Ltd: [JOURNAL NAME], advance online publication, day month year (doi: 10.1038/sj.[JOURNAL ACRONYM].XXXXX)

Note: For republication from the *British Journal of Cancer*, the following credit lines apply.

Reprinted by permission from Macmillan Publishers Ltd on behalf of Cancer Research UK: [JOURNAL NAME] (reference citation), copyright (year of publication) For AOP papers, the credit line should read:
Reprinted by permission from Macmillan Publishers Ltd on behalf of Cancer Research UK: [JOURNAL NAME], advance online publication, day month year (doi: 10.1038/sj.[JOURNAL ACRONYM].XXXXX)

6. Adaptations of single figures do not require NPG approval. However, the adaptation should be credited as follows:

Adapted by permission from Macmillan Publishers Ltd: [JOURNAL NAME] (reference citation), copyright (year of publication)

Note: For adaptation from the *British Journal of Cancer*, the following credit line

applies.

Adapted by permission from Macmillan Publishers Ltd on behalf of Cancer Research UK:
[JOURNAL NAME] (reference citation), copyright (year of publication)

7. Translations of 401 words up to a whole article require NPG approval. Please visit <http://www.macmillanmedicalcommunications.com> for more information. Translations of up to a 400 words do not require NPG approval. The translation should be credited as follows:

Translated by permission from Macmillan Publishers Ltd: [JOURNAL NAME] (reference citation), copyright (year of publication).

Note: For translation from the *British Journal of Cancer*, the following credit line applies.

Translated by permission from Macmillan Publishers Ltd on behalf of Cancer Research UK:
[JOURNAL NAME] (reference citation), copyright (year of publication)

We are certain that all parties will benefit from this agreement and wish you the best in the use of this material. Thank you.

Special Terms:

v1.1

Questions? customercare@copyright.com or +1-855-239-3415 (toll free in the US) or +1-978-646-2777.

License Agreement for Reproduction of Figure 3

RightsLink Printable License	Page 1 of 3
NATURE PUBLISHING GROUP LICENSE TERMS AND CONDITIONS	
Jul 21, 2016	
<hr/> <hr/>	
This Agreement between Peter Robertson ("You") and Nature Publishing Group ("Nature Publishing Group") consists of your license details and the terms and conditions provided by Nature Publishing Group and Copyright Clearance Center.	
License Number	3913671137020
License date	Jul 21, 2016
Licensed Content Publisher	Nature Publishing Group
Licensed Content Publication	Nature Reviews Microbiology
Licensed Content Title	Molecular pathogenesis of the obligate intracellular bacterium <i>Coxiella burnetii</i>
Licensed Content Author	Erin J. van Schaik, Chen Chen, Katja Mertens, Mary M. Weber, James E. Samuel
Licensed Content Date	Jun 24, 2013
Licensed Content Volume Number	11
Licensed Content Issue Number	8
Type of Use	reuse in a dissertation / thesis
Requestor type	academic/educational
Format	print and electronic
Portion	figures/tables/illustrations
Number of figures/tables/illustrations	1
High-res required	no
Figures	Cartoon of Dot/Icm system
Author of this NPG article	no
Your reference number	
Title of your thesis / dissertation	Investigating the Secretion of HtpB, the Multifunctional Chaperonin of <i>Legionella pneumophila</i>
Expected completion date	Aug 2016
Estimated size (number of pages)	160
Requestor Location	Peter Robertson 16 Lewis Drive Bedford, NS B4B1C2 Canada Attn: Peter Robertson
Billing Type	Invoice
https://s100.copyright.com/App/PrintableLicenseFrame.jsp?publisherID=52&publisherN... 2016-07-21	

Billing Address Peter Robertson
16 Lewis Drive

Bedford, NS B4B1C2
Canada
Attn: Peter Robertson

Total 0.00 CAD

Terms and Conditions**Terms and Conditions for Permissions**

Nature Publishing Group hereby grants you a non-exclusive license to reproduce this material for this purpose, and for no other use, subject to the conditions below:

1. NPG warrants that it has, to the best of its knowledge, the rights to license reuse of this material. However, you should ensure that the material you are requesting is original to Nature Publishing Group and does not carry the copyright of another entity (as credited in the published version). If the credit line on any part of the material you have requested indicates that it was reprinted or adapted by NPG with permission from another source, then you should also seek permission from that source to reuse the material.
 2. Permission granted free of charge for material in print is also usually granted for any electronic version of that work, provided that the material is incidental to the work as a whole and that the electronic version is essentially equivalent to, or substitutes for, the print version. Where print permission has been granted for a fee, separate permission must be obtained for any additional, electronic re-use (unless, as in the case of a full paper, this has already been accounted for during your initial request in the calculation of a print run). NB: In all cases, web-based use of full-text articles must be authorized separately through the 'Use on a Web Site' option when requesting permission.
 3. Permission granted for a first edition does not apply to second and subsequent editions and for editions in other languages (except for signatories to the STM Permissions Guidelines, or where the first edition permission was granted for free).
 4. Nature Publishing Group's permission must be acknowledged next to the figure, table or abstract in print. In electronic form, this acknowledgement must be visible at the same time as the figure/table/abstract, and must be hyperlinked to the journal's homepage.
 5. The credit line should read:
Reprinted by permission from Macmillan Publishers Ltd: [JOURNAL NAME] (reference citation), copyright (year of publication)
For AOP papers, the credit line should read:
Reprinted by permission from Macmillan Publishers Ltd: [JOURNAL NAME], advance online publication, day month year (doi: 10.1038/sj.[JOURNAL ACRONYM].XXXXX)
- Note: For republication from the *British Journal of Cancer*, the following credit lines apply.**
Reprinted by permission from Macmillan Publishers Ltd on behalf of Cancer Research UK: [JOURNAL NAME] (reference citation), copyright (year of publication) For AOP papers, the credit line should read:
Reprinted by permission from Macmillan Publishers Ltd on behalf of Cancer Research UK: [JOURNAL NAME], advance online publication, day month year (doi: 10.1038/sj.[JOURNAL ACRONYM].XXXXX)
6. Adaptations of single figures do not require NPG approval. However, the adaptation should be credited as follows:

Adapted by permission from Macmillan Publishers Ltd: [JOURNAL NAME] (reference citation), copyright (year of publication)

Note: For adaptation from the *British Journal of Cancer*, the following credit line applies.

Adapted by permission from Macmillan Publishers Ltd on behalf of Cancer Research UK: [JOURNAL NAME] (reference citation), copyright (year of publication)

7. Translations of 401 words up to a whole article require NPG approval. Please visit <http://www.macmillanmedicalcommunications.com> for more information. Translations of up to a 400 words do not require NPG approval. The translation should be credited as follows:

Translated by permission from Macmillan Publishers Ltd: [JOURNAL NAME] (reference citation), copyright (year of publication).

Note: For translation from the *British Journal of Cancer*, the following credit line applies.

Translated by permission from Macmillan Publishers Ltd on behalf of Cancer Research UK: [JOURNAL NAME] (reference citation), copyright (year of publication)

We are certain that all parties will benefit from this agreement and wish you the best in the use of this material. Thank you.

Special Terms:

v1.1

Questions? customercare@copyright.com or +1-855-239-3415 (toll free in the US) or +1-978-646-2777.

Appendix B: Media Recipes

Recipe for 1L LB

- 10 g Bacto-tryptone
- 5 g Yeast Extract
- 10 g NaCl
- 15 g Agar (optional)
- Autoclave

Recipe for IL BCYE

- 6 g ACES Buffer
- 1 g α -ketoglutarate monopotassium
- 10 g Yeast Extract
- Adjust pH to 6.9 with 10M potassium hydroxide
- 1.5 g activated charcoal
- 15 g Agar (optional)
- Autoclave
- Add filter-sterilized L-cysteine (2.5mM final)
- Add filter sterilized ferric pyrophosphate (1mL of 0.1 w/v solution)

Recipe for 1L of 10x TBS

- 87.65 g sodium chloride
- 18.61 g EDTA
- 60.5 g Tris
- pH adjust to 7.4 with concentrated HCl

Recipe for 1L of 1x TTBS

- 100mL 10x TBS
- 2.5mL Tween 20
- Adjust to 1L with dH₂O

Recipe for 1L PBS

- 8 g sodium chloride
- 0.2 g potassium chloride
- 1.44 g sodium phosphate, dibasic
- 0.24 g monopotassium phosphate
- pH adjust to 7.4

Recipe for 1L PYG

- 20 g proteose peptone
- 1 g yeast extract
- 8 mL 0.05M calcium chloride
- 10 mL 0.4 M magnesium sulfate heptahydrate
- 10 mL 0.25 M sodium phosphate, dibasic
- 10 mL 0.25 M monopotassium phosphate
- 10mL 0.005 M ammonium iron(II) sulfate hexahydrate
- 1 g sodium citrate dihydrate